JANUARY 2024
ENERGINET ELTRANSMISSION A/S

INTEGRATED GEOLOGICAL MODEL FOR THE ENERGY ISLAND PROJECT

REPORT

COWI

ADDRESS COWI A/S
Parallelvej 2
2800 Kongens Lyngby
Denmark

TEL +45 56 40 00 00
FAX +45 56 40 99 99
WWW cowi.com

JANUARY 2024
ENERGINET

INTEGRATED GEOLOGICAL MODEL FOR THE ENERGY ISLAND PROJECT

REPORT

PROJECT NO.	DOCUMENT NO.
A243327	A243327-01

VERSION	DATE OF ISSUE	DESCRIPTION	PREPARED	CHECKED	APPROVED
0.1	31.10.2023	Report	CONN, SPSO, MALA, ATHN, CHLJ	KAPN, KRGE, MKOD, KAWE, AAAP	LOVG
1.0	15.12.2023	Report	CONN, SPSO, MALA, ATHN, CHLJ	OFN, KRGE, SPSO	KRGE
2.0	16.01.2024	Report	CONN, SPSO, MALA, ATHN, CHLJ	CONN, KRGE	KRGE

CONTENTS

1 Executive Summary

This report describes the work and outcome of the integrated geological model for the Energy Islands Project, Danish 3 GW offshore wind farm in the North Sea based on 2021-2023 geotechnical site investigations and reporting by Fugro and 2021-2022 geophysical investigations and reporting by Fugro and MMT.

Energinet is developing a 3 GW offshore wind farm area to be tendered out in 2024. The area of investigation is found approximately 80 km offshore the west coast of Jutland and covers around 1050 km².

The 3D integrated geological model is established using primarily 2D Multi-channel Ultra High-Resolution Seismic data (UHRS) with 1000 m between north-south lines and 210-250 m between east-west lines. Interpretation integrates geotechnical investigations at 269 locations including cone penetration testing (CPT) and boreholes (BH). Major geotechnical units are assessed and described for the combined data set. Factual reports for the North Sea Artificial Island and North Sea Offshore Wind Farm Area summarizing the results from geotechnical field tests and laboratory testing are used to evaluate the geotechnical properties for the geotechnical units.

The integrated geological model has 38 integrated model units and 19 subunits for which geological descriptions are provided. The descriptions include stratigraphic, lithological, and geotechnical characteristics and distinction is made between general lower strength deposits from Holocene, Late Weichselian and Weichselian, more consolidated deposits from Saalian, and high strength consolidated deposits from Elsterian to Miocene.

The integrated model units have been combined into seven chronostratigraphic groups based on their age for the geotechnical assessment. Each chronostratigraphic group is further divided into geotechnical units, based on the soil type, which differ between sand, clay, and mixed soil conditions. The soil properties of all geotechnical units have been evaluated and visualized in the appendices.

A geotechnical zonation encircles the geological model and structures evaluated to have a potentially significant impact on the geotechnical design and installation works from low and high strength layers. The geotechnical zonation is simplified into one single map dividing the entire OWF project site into seven geotechnical zones. For each geotechnical zone representative soil profiles are presented. One of these geotechnical zones (VII) shows presence of soft clay at great depths below the seabed. The other geotechnical zones generally comprise competent geotechnical deposits, however, some of the geotechnical zones (IV to VI) have presence of soft clay at shallow depths.

The risk related to leg penetration is assessed on a high level. The assessment is performed for each of the geotechnical survey locations considering two generic vessels. The higher leg penetration risk mainly occurs in the geotechnical zones with thick layers of normal consolidated clays, which is also expected based on the considered criteria for the leg penetration analyses and the descriptions for the geotechnical zones defined from the zonation.

Enclosures are provided presenting units and horizons of the integrated geological model with respect to depth below seabed, thickness, and lateral extent. Enclosures are further supporting the geotechnical zonation where thickness and depth of grouped units, of importance to the geological model, are presented. Furthermore 16 cross sections distributed over the OWF project site show the layering in the model together with borehole information.

All enclosures are provided digitally. The integrated geological model is delivered as a digital 3D model in a Kingdom suite project.

2 Introduction

To enable evaluation of subsurface soil conditions and related constraints for the OWF zone surrounding the area allocated for the energy island in the North Sea, Energinet has procured two geophysical 2D Multi-channel Ultra High Resolution Seismic (M-UHRS) surveys (Fugro, 2022 and MMT, 2022) each covering approximately one half of the zone, respectively. Together with two geotechnical campaigns (Fugro, 2023) these surveys have provided the basis for an integrated geological model of the OWF project site.

This report presents the results of the integrated geological modelling of the OWF project site as carried out by COWI August 2022 – December 2023.

2.1 Area of investigation

In this report the "OWF project site" covers the entire area of investigation. The OWF project site is situated approximately 80 km offshore the west coast of Jutland and covers around 1050 km².

In the survey campaign the OWF project site was further subdivided into the "Site area" covering the entire area of investigation except for an area denoted the "Island area" covering only an area formerly allocated for an intended artificial island.

For the received survey data and initial geological models, the term “East area” refers to the eastern part of the OWF project site which has been delivered by MMT and the term “West area” refers to the western part of the OWF project site which has been delivered by Fugro (Figure 2-1).

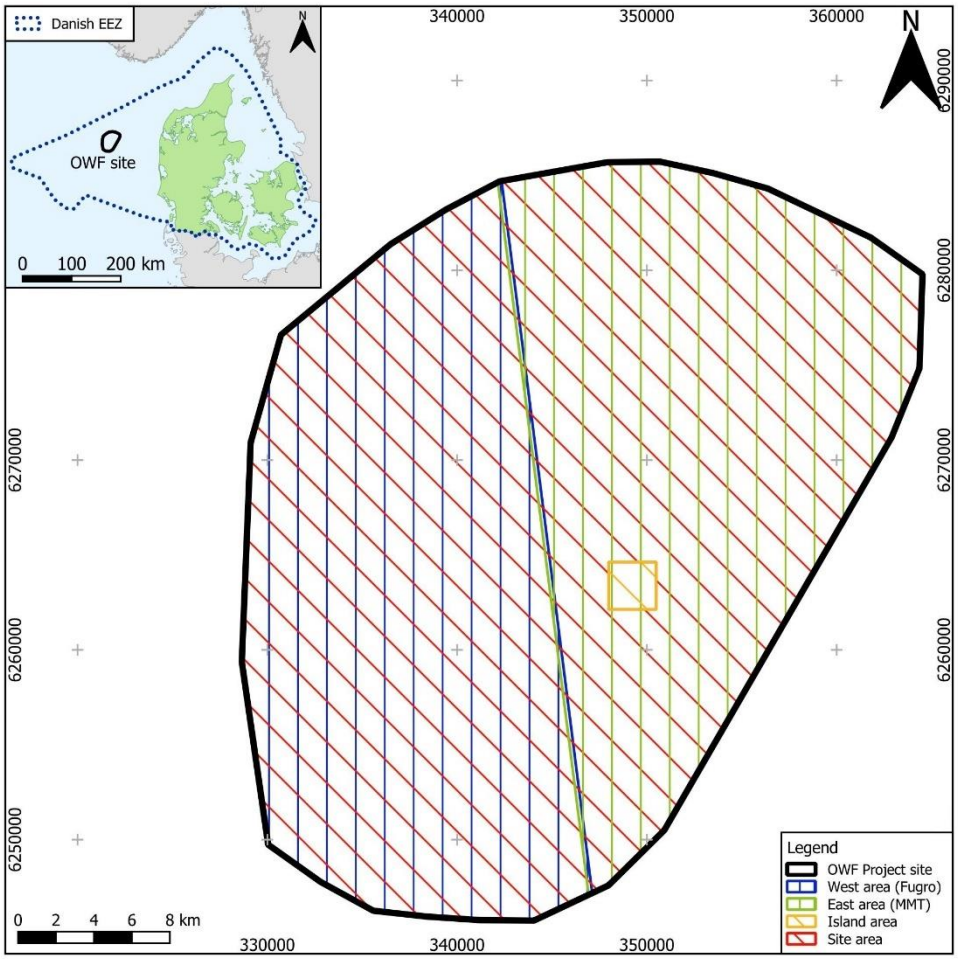

Figure 2-1 The OWF project site and the relevant subdivisions of the area.

2.2 Scope of Work

The results presented in this report will be part of the North Sea Energy Island tender process, informing development tenderers about the local geology, associated geotechnical properties and potential geohazards as well as supporting subsequent development of the OWF project site. Thus, a key objective of the present work was to ensure the applicability for sub-selection of a specific OWF site within the area of investigation.

The integrated geological model comprises a conceptual geological model, a digital, spatial geological model, and a geotechnical characterization of the geotechnical units in the model.

COWI uses the technical requirements defined by Energinet to break down the work into four WORK PACKAGES (WP), which is further detailed in the sections below and in Table 2-1. WP1 covers the work with the 3D spatial, digital geological models in Kingdom (see section 7 to 9). WP2 covers the work with the conceptual geological model, geohazards and combined soil descriptions (see section 8).

WP3 covers the work with the geotechnical characterization (see section 5 and 6) and WP4 covers the establishment of the geotechnical zones (see section 10).

Additionally, COWI has broken down the technical work into three phases. The three phases are related to the overall project schedule and the data flow into the model work. The relationship between the phases and the work packages for the technical work is illustrated in Table 2-1.

Table 2-1 Overview of the workflow and phases of the technical work

Phases	Phase 1- Geophysical data	Phase 2 – Geophysical data, CPT and boreholes	Phase 3 – Revised factual report with laboratory results
WP1 - 3D Spatial Geological Model and integrated interpretation	-Adopt the two Kingdom Models from MMT and Fugro -Test alignment of interpretations, velocity models and reflectors -Address interpreted sub-surface geohazards -Combine 2D UHRS data in one combined model	-Import CPTs and boreholes in combined model -Assess and assign major integrated model units combined from CPT and seismic data -Perform integrated interpretation -Consider geohazards in relation to geotechnical results	-Continued integrated interpretation -Final adjustments of interpretations -Produce grids and cross - sections -Prepare deliverables
WP2 - Conceptual Geological Model	-Initial geological conceptualization of the site -Regional geological setting	-Conceptualize and visualize the conceptual geological model -Continuous correlation between spatial and conceptual model -Establish a description of the geology and geotechnical units	-Final adjustments of the conceptual model and visualizations -Prepare deliverables
WP3 - Geotechnical characterization of geotechnical units	-Receive interim deliverables of the CPT and borehole data -Evaluate, prepare, and test received data for import into the Spatial Geological Model	-Geotechnical unit framework from CPT and borehole data. -Considerations of soil suitability for foundations and risk assessments -Soil descriptions and soil classification and subdivision of chronostratigraphic groups -Initial determination of soil strength/stiffness properties based on CPT data	-Receive factual geotechnical report including laboratory data -Evaluate factual geotechnical report and integrate data into the Geotechnical Characterization -Summarize geotechnical parameters for the geotechnical units -Establish and document typical values and variance -Final soil classification and strength/stiffness properties -Prepare deliverables
WP4 - Geotechnical zones		-Define initial geotechnical zones in collaboration with Energinet	-Final geotechnical zones -Establish typical soil profile for each geotechnical zone -Leg penetration risk assessment -Prepare deliverables

3 Basis

Data packages have been received from Energinet at different times. An overview of the final data received as basis from Energinet is listed below and divided into the geotechnical and geophysical data packages including reports.

Project datum is ETRS89 (EPSG: 25832) and using the GRS1980 spheroid.

The coordinate system used is the UTM projection in zone 32 N. Units are in meters. Height model is DTU21 MSL.

Geotechnical data packages	
Datatype	Year
Geotechnical Factual Report LOT 1 - V04 - Final (revised); (File: "*F191074_LOT 1_Geotechnical Factual Report_V04*") from Fugro. AGS data and Excel files providing results from offshore and onshore works of the geotechnical site investigation for LOT 1 documented in the Factual Report.	2023
Geotechnical Factual Report LOT 2 - V03 – Final; (File: "*F191074_LOT 2_Geotechnical Factual Report_V03*") from Fugro. AGS data and Excel files providing results from offshore and onshore works of the geotechnical site investigation for LOT 2 documented in the Factual Report.	2023

Geophysical data packages	
Datatype	Year
Fugro: Kingdom Project with 2D Ultra High Resolution Seismic (2D UHRS) Line spacing 250*1000m Sub Bottom profiler (SBP) Line spacing 62.5*1000m SEG-Y data was also delivered separately from the Kingdom project	2022
Fugro: GIS project with Multi Beam Echo Sounder (MBES), 0.25 m x 0.25 m bin size / 16 x pings per 1.0 m x 1.0 m Side Scan Sonar (SSS) and Magnetometer (MAG) Line spacing 62.5*1000m Tracklines, maps and results from geophysical surveys (MBES, SSS, MAG) MBES was also delivered separately in 5x5 m grid.	2022

Geophysical data packages	
Datatype	Year
MMT: Kingdom project with 2D Ultra High Resolution Seismic (2D UHRS) Line spacing 210*1000m Innomar Sub Bottom Profiler (SBP) Line spacing 70*1000m SEG-Y data was also delivered separately from the Kingdom project	2022

Reports		
Author	Title	Year
Rambøll	Geology and sea-level, desk study. November	2021
Nordjyllands Kystmuseum	Marine archaeology: archaeological analysis, desk study. November	2021
GEUS	A desk study of the geological succession below a proposed energy island, Danish North Sea	2022
RPS	Desk Study for Potential UXO Contamination Energy Island – North Sea OWF Site. February	2022
Fugro	Geophysical result report – North Sea OWF zone west (lot2) Geophysical Survey: Danish North Sea. Issue 4 June.	2022
Fugro	Energy Island North Sea Artificial Island. Investigation result. Geotechnical site investigation. June	2022
Fugro	Energy Island North Offshore Wind Farm. Investigation result. Geotechnical site investigation. July	2022
MMT	Geophysical survey report: Energy Islands – North Sea East. Revision B. August	2022
Fugro	Geophysical result report – North Sea OWF zone west (lot2) Geophysical Survey: Danish North Sea. Issue 5 August.	2022
MMT	Geophysical survey report: Energy Islands – North Sea East. Revision C. September	2022
Rambøll	Ground Conditions Risk Assessment. January	2023
Fugro	Energy Island – North Sea Artificial Island. Investigation results. Geotechnics. Issue 3. February	2023
Fugro	Energy Island – North Sea Artificial Island. Investigation results. Geotechnics. Issue 04. February	2023

Fugro	Energy Island - North Offshore Wind Farm. Investigation result. Geotechnics. Issue 2. May	2023
Marinarkæologi Jylland	North Sea OWF Zone Maritime archaeology Geo-archaeological analysis, report	2023
Fugro	Energy Island - North Offshore Wind Farm Area. Investigation result. Geotechnics. Issue 3. June	2023

3.1 Geotechnical basis

The geotechnical basis for the project can generally be divided into two categories:

- Offshore sampling and in-situ testing
- Laboratory testing and description

The site investigation work has been divided into two campaigns named LOT1 and LOT2, focusing on the Island area (area formerly planned for construction of a potential artificial island) and the Site area (North Sea Offshore Wind Farm area), respectively. This report will consider the names "*Island*" and "*Site*" to refer to the LOT1 and LOT2 campaign, respectively. The campaigns consist of in-situ testing and laboratory testing. The in-situ works for the campaigns include borehole sampling (BH), different CPT types and more. The laboratory works in the two campaigns consist of soil description and classification testing as well as a comprehensive laboratory test programme.

The geotechnical work for both campaigns has been performed by Fugro and has been summarised in a factual report for each campaign.

3.1.1 In-situ works

The offshore works consist of in-situ testing (seabed, downhole and seismic CPTs), P-S logging, and borehole drilling incl. sampling. The acquired samples are used for testing in the onshore laboratory programme.

An overview of the positions for CPT, including seabed (CPT), downhole (dCPT) and seismic (SCPT), and boreholes (with sampling) is shown Table 3-1 and on Enclosure 2.01.

Several locations across the OWF project site have multiple CPTs due to premature CPT refusal, which means that the total number of unique locations surveyed is 269 from which 109 is located within the Island area and the remaining 160 is located within the site area. Of these 269 locations, 58 locations have been surveyed with minimum one (1) CPT and one (1) borehole, while the remaining 211 have been surveyed with minimum one (1) CPT but no borehole.

For eight (8) of the survey locations the CPTs have been performed as seismic cone penetration tests, i.e., including measurement of the shear wave velocity. For boreholes a target depth of 70 m was considered, with six (6) exceptions within the Island area where a target depth of 120 m was considered. For CPTs a target depth of 55 m was considered. However, it is noted that most of the seabed CPTs have not reached the target depth due to exceedance of stop criteria, like CPT refusal or rod deviation.

The distance between CPTs and boreholes performed at the same location and the distance between extra repeated CPTs performed at the same location is maximum 9.1 m.

Table 3-1 Summary of in-situ geotechnical tests.

Test type	Campaign*	Quantity
Seabed Cone Penetration Test (CPT)	Island	112 (incl. 3 retests)
	Site	194 (incl. 42 retests)
Composite Cone Penetration Test and sampling boreholes (BH)	Island	11 (incl. 5 retests)
	Site	67 (incl. 15 retests)
Downhole Cone Penetration Test (dCPT)	Island	3
	Site	20 (4 retests)
Seismic Cone Penetration Test (SCPT)	Site	17 (incl. 9 retests)
P-S logging	Site	At 8 BHs

*Three CPT tests provided as part of the Island site investigation (SI) campaign were performed outside the Island area i.e., within the site area. These three tests are in the above table considered part of the site.

3.1.2 Laboratory works

The laboratory works consist of classification testing, advanced laboratory testing and chemical testing. The performed laboratory tests available are summarized in Table 3-2.

All laboratory works are performed using samples acquired from the geotechnical composite downhole CPT and boreholes.

Table 3-2 Summary of performed laboratory tests.

Test type	Campaign	Quantity
Water content	Island	955
	Site	3515
Bulk and dry density	Island	973
	Site	3087
Particle density	Island	159
	Site	572
Atterberg limits	Island	128
	Site	268
Particle size distribution	Island	198
	Site	693
Maximum and minimum dry density	Island	60
	Site	218
Carbonate content	Island	101
	Site	515
Acid & Water-soluble Sulphate	Island	43
	Site	239
Acid & Water-soluble Chloride	Island	43
	Site	239
Loss on ignition (Organic content)	Island	2
	Site	13
Thermal conductivity	Island	7
	Site	40
Resonant column	Site	13
Oedometer (incremental load)	Island	155
	Site	45
Laboratory hand vane test	Island	97*
	Site	377
Laboratory hand penetrometer	Island	686*
	Site	1520

Test type	Campaign	Quantity
Laboratory vane test	Island	1*
	Site	22
Unconsolidated Undrained (UU) triaxial test	Island	40
	Site	104
Unconfined compressive strength (UCS)	Island	8
	Site	11
Consolidated Isotropically Undrained (CIU) triaxial tests	Island	18
	Site	27
Consolidated Isotropically Drained (CID) triaxial tests	Island	186
	Site	144
Consolidated Anisotropically Undrained (CAU) triaxial tests	Island	44
	Site	49
Cyclic Consolidated Anisotropically Undrained (CAUcyc) triaxial tests	Island	6
Direct simple shear (DSS) tests	Island	36
	Site	55
Bender element (as part of CID)	Site	8
Bender element (as part of CU)	Site	4

**Tests not included in final revision but have been present in draft revision. Due to the tests are not included in the final revision, these have not been included in the performed assessments.*

3.2 Geophysical and hydrographical basis

The geophysical basis for this report is two geophysical surveys including 2D M-UHRS and SBP, acquired in 2021 by MMT and Fugro.

The main objectives from these surveys from MMT and Fugro were:

- Initial marine archaeological site assessment.
- Planning of environmental investigations.
- Planning of initial geotechnical investigations.
- Decision of foundation concept and preliminary foundation design.
- Assessment of subsea inter-array cable burial design.
- Assessment of installation conditions for foundations and subsea cables.
- Site information enclosed in the tender for the offshore wind farm concession.
- Acquire and interpret high quality seabed and sub-seabed data for project planning and execution. As a minimum, this includes local bathymetry, seabed sediment distribution, seabed features, seabed obstructions, wrecks, and archaeological sites, crossing cables and pipelines and evaluation of possible mobile sediments.
- Sub-bottom profiling and 2D UHRS survey along the survey lines to map shallow integrated model units.
- Mapping of magnetic targets and to identify infrastructure crossings and large metallic debris.
- Ground truthing grab samples were acquired in order to aid the surficial interpretation of seabed sediments.

The work described above and below has been performed by MMT and Fugro, and the outcome of the site investigations (SI's) has been documented in Ref. /1/ and Ref. /2/.

3.2.1 Bathymetry

MBES data were acquired individually for the East area (by MMT) and the West area (by Fugro). Together they are fully covering the OWF project site. The grids were received in 5x5 m, which is corresponding to the same cell size that COWI will deliver horizon grids in. The subsurface grids are also sharing note points with the bathymetry grids. The two separate bathymetry grids were combined and in the middle area where the two surveys overlap, the average values for the two surveys were used to accommodate for small offsets.

3.2.2 Subsurface data

The 2D UHRS data were acquired with NNW-SSE oriented survey lines with a 250 m line spacing in the West area and 210 m line spacing in the East area and ESE-WNW oriented crosslines with 1000 m line spacing (see Figure 3-1).

The SBP data were acquired with NNW-SSE oriented survey lines with a 1000 m line spacing and ESE-WNW oriented crosslines with 62 m line spacing in the West area and 70 m line spacing in the East area (see Figure 3-2).

The combined integrated geological model only uses the 2D UHRS data sets as basis. The layer boundaries identified in the SBP data were either less clear to interpret as compared to the 2D UHRS data or the boundaries were placed between layers interpreted to be insignificantly different when considering geological and geotechnical properties. Hence, the use of SBP data was discontinued in the updated model.

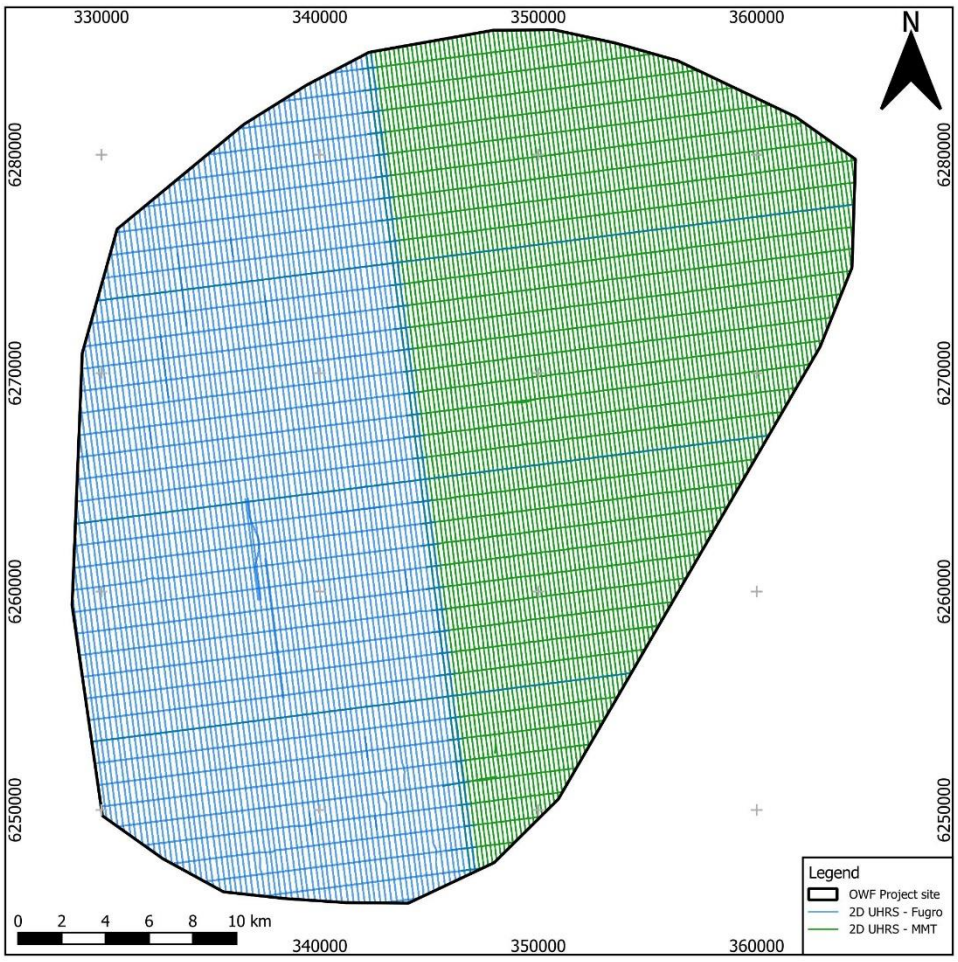

Figure 3-1: 2D UHRS survey lines from the West area (Fugro) and East area (MMT).

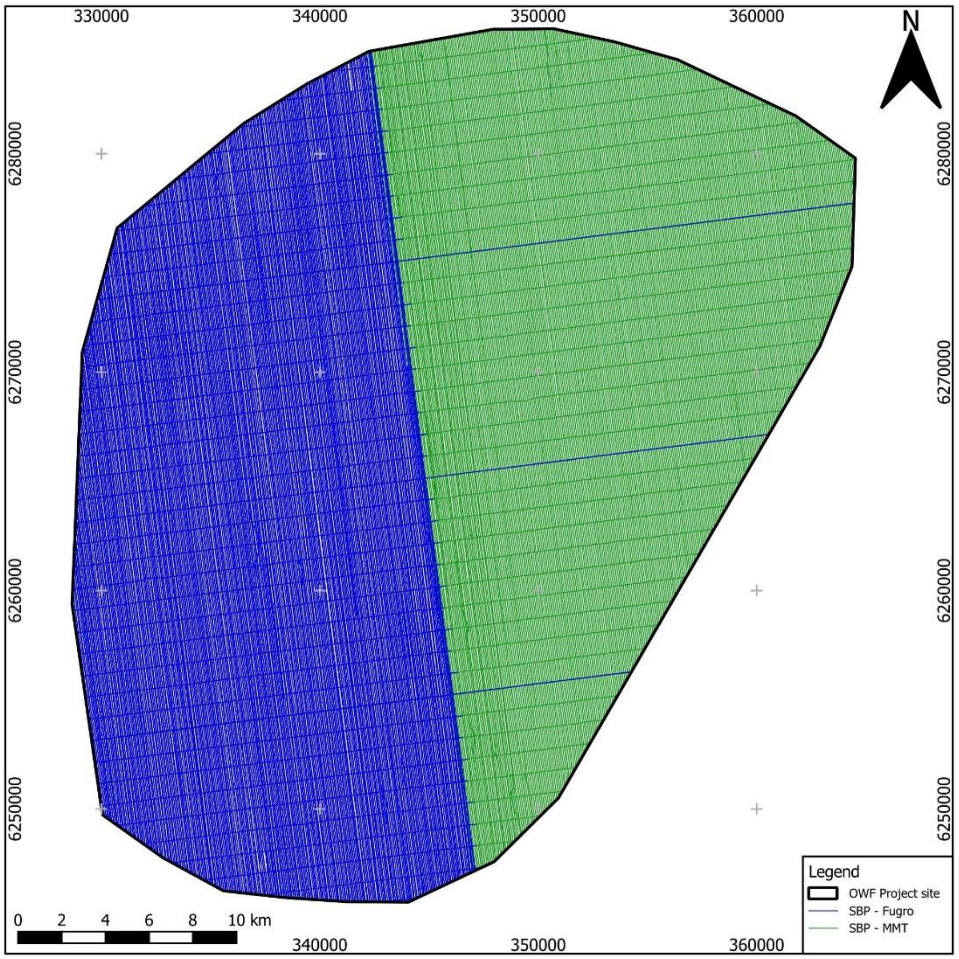

Figure 3-2 SBP survey lines from the West area (Fugro) and East area (MMT).

4 Methodology for integration of geotechnical/geophysical data

The methodology used for the performed work with interface between geophysics and geotechnics is an iterative process, from which the geophysical and geotechnical findings support each other to obtain an integrated geological model representing the site conditions.

The steps in the iterative work process between geophysics and geotechnics for the work covered in this report are the following:

1 The geophysical and geotechnical work is initially assessed in each discipline for establishing a basis to work from.

   1a) The geophysical model was received as two separate models for East and West areas of the OWF project site. The initial work included merging and reinterpretation of the two models for having the basis for one consistent model for the entire site.

   1b) The geotechnical basis is established by generating a stratigraphy for each available test location across the OWF project site. In addition, classification parameters are determined to support this selection. The soil behaviour type index, I_c, (cf. section 5.2.1) with depth is shared with the geophysical team as basis for merging the two models and initial interpretation.

2 The geophysical and geotechnical disciplines share horizons and stratigraphy at the test locations across the OWF project site.

3 Each discipline reviews the received information from the other discipline for re-evaluation and update the models for alignment. This is supported through meetings between the disciplines.

4 Steps 2 and 3 are repeated until an alignment between the geophysical and geotechnical interpretation is made. When the work for updating the model is finalised, the documentation and post processing of the result is completed within each discipline.

5 In parallel with the individual work for each discipline, the zonation is ongoing between the disciplines, where input from both parties is considered.

The iterative process used for the project is visualised by a flowchart in Figure 4-1.

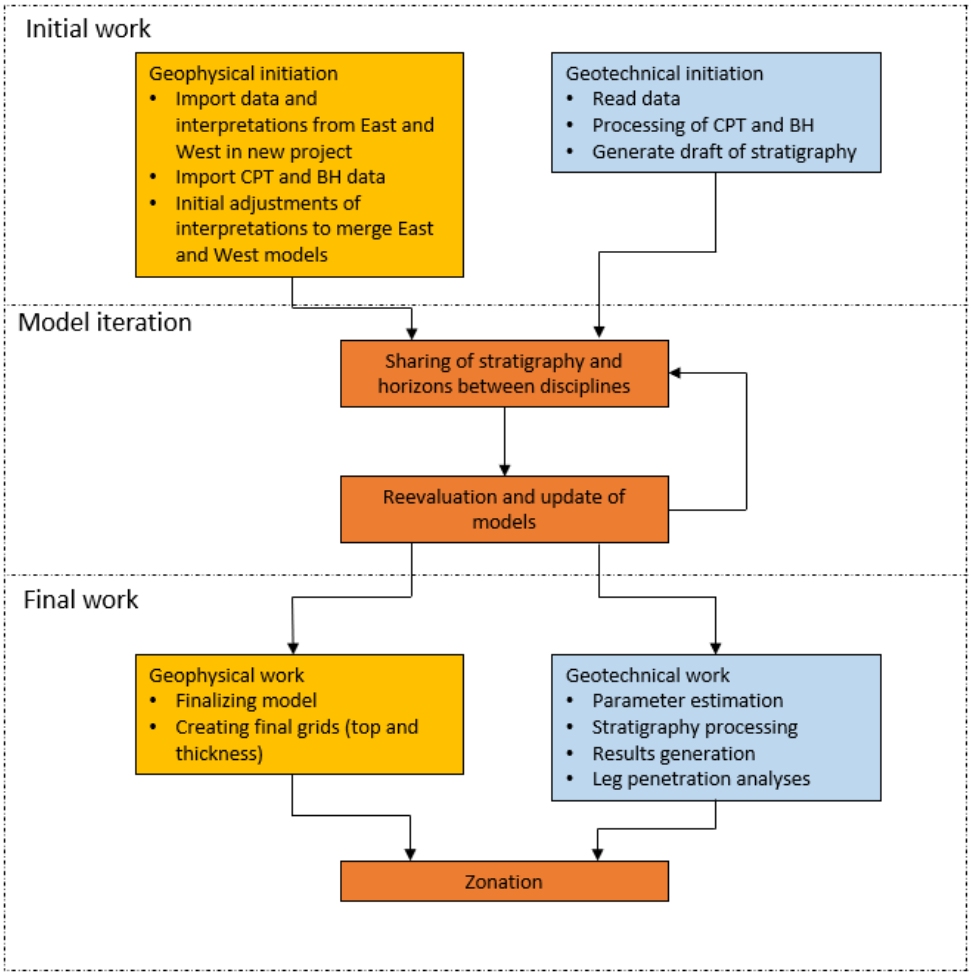

Figure 4-1 Flowchart for visualising the work iteration between disciplines.

5 Geotechnical interpretation

In this section it is described how the geotechnical data have been evaluated to characterize the soils at the OWF project site and the layering of geotechnical units at each geotechnical survey location. The layering and soil characterization interpreted at survey locations has served as input to the integrated geological model, cf. section 9.

For each geotechnical survey location, a geotechnical interpretation of the stratigraphy has been carried out. This interpretation has considered input from borehole logs, CPT logs (using CPT correlations as presented in section 5.2) and geophysical data (to link geotechnical units across the OWF project site). One geotechnical interpretation of the stratigraphy has been prepared for each geotechnical survey location. This also implies that at geotechnical survey locations where borehole and CPT data are available, or CPT data from multiple tests are available, the information from these tests has been combined into one interpreted stratigraphy. A total of 269 unique geotechnical interpretations of stratigraphy have been developed, cf. Appendix A, where geophysical data has been included for the stratigraphy estimation. All these interpretations have been applied as input to the integrated geological model.

The following sections describe the procedure for the geotechnical stratigraphic interpretation in further detail.

5.1 Geotechnical unit overview

The development of the soil stratigraphy can generally be divided into two parts:

- based on borehole log descriptions,
- based on CPT classification and correlation.

The work documented in Ref. /3/ and Ref. /4/ can be considered the basis. The soil descriptions provided in the borehole logs provide descriptions of soil type/class as well as estimates of soil age and depositional environment. In addition, the seismic horizons interpreted from the geophysical data also serves as input into the definition of geotechnical units.

Due to the high number of integrated model units established for the OWF project site, groupings of the integrated model units into chronostratigraphic groups have been performed for establishing the relevant geotechnical units. The chronostratigraphic groups are based on the geological age of the integrated model units as similar geotechnical behaviour within the same chronostratigraphic group has been observed. Each chronostratigraphic group is used to establish three geotechnical units as the units are differentiated between the soil material types of sand, clay, and mix. The mix materials consist of silt material, and rapidly switching sand and clay.

An overview of the defined chronostratigraphic groups and geotechnical units is presented in Table 5-1 from which it can be seen which integrated model units are grouped together, and the amount of available CPT data for each geotechnical unit. The integrated model unit ID refers to the presented integrated model units in section 9.8.

Figures for verifying a similar behaviour for the established geotechnical units are presented in Appendix B. For each geotechnical unit, a figure presenting all grouped integrated model units are presented. An additional figure is illustrating what data is from the Island campaign and site campaign respectively.

The following is noted with regards to the defined chronostratigraphic groups:

- *The Holocene group* mostly consist of sand, with few layers of normally consolidated clay. The group is found at shallow depths (up to approximately 25 m below seabed).

- *The Late Weichselian group* consist of sand, clay and mixed soil conditions, where the clay material is slightly over-consolidated. The group is found mainly at shallow depths, but at a few locations extending to approximately 45 m below seabed.

- *The Weichselian group* consist of sand, clay and mixed soil conditions. The clays found within the group are found to be higher strength and more consolidated compared to the Late Weichselian group.

- *The Saalian group* is consisting of sand, clay and mixed soil conditions, where sand is the dominating soil type. The clay in the Saalian group is over-consolidated.

- *The Elsterian group* consist of channel deposits differentiated between sand, clay and mixed soil conditions, with clay being the most predominant soil behaviour type in the group. The clay has a high strength and is over-consolidated.

- *The Elsterian & older group* is interpreted as a sand dominated group with partly mixed sediments of high strength. The group is found at great depths for most of the site, but also found at relative shallow depth for smaller areas of the site. Since the group is normally present at great depth, a limited number of in-situ and laboratory tests are present for the Geotechnical unit.

- *The Miocene group* is found at great depths for most of the site, but also found at relative shallow depth for smaller areas of the site. The group consists of both sand, clay and mixed sediments. Since the group is normally present at great depth, a limited number of in-situ and laboratory tests are present for the unit.

Table 5-1 Overview of identified chronostratigraphic groups, integrated model units, and geotechnical units.

Chronostratigraphic group	Integrated model unit	Geotechnical unit	Total length of CPT measurement [m]	Percent of total CPT length in chronostratigraphic group [%]
Holocene	U10, U11, U12, U13, U14, U15	Holocene Sand	1903.3	92.0
		Holocene Clay	105.3	5.1
		Holocene Mix	59.7	2.9
Late Weichselian	U16, U17, U18, U19, U20, U21, U22	Late Weichselian Sand	304.5	55.7
		Late Weichselian Clay	187.4	34.3
		Late Weichselian Mix	54.5	10.0
Weichselian	U23, U24, U25, U30, U35	Weichselian Sand	1616.1	48.7
		Weichselian Clay	927.1	28.0
		Weichselian Mix	771.9	23.3
Saalian	U37, U38, U40-01, U40-02, U40-03, U41, U42, U45-01, U45-02, U50-01, U50-02, U56, U57, U58, U59	Saalian Sand	595.0	64.6
		Saalian Clay	144.7	15.7
		Saalian Mix	181.8	19.7
Elsterian	U65, U70-01, U70-02, U70-03, U70-04, U70-05, U70-06, U70-07, U70-08, U70-09, U70-10, U70-11, U70-12, U73	Elsterian Sand	169.1	25.1
		Elsterian Clay	389.4	57.7
		Elsterian Mix	116.3	17.2
Elsterian & older	U75, U85	Elsterian & older Sand	500.7	94.1
		Elsterian & older Mix	31.4	5.9
Miocene	U89, U90, U95, U96	Miocene Sand	149.4	36.2
		Miocene Clay	101.4	24.6
		Miocene Mix	162.2	39.3

5.2 Stratigraphic interpretation based on CPT

The process of determining the stratigraphy for all survey locations based on the CPT data is described in the following steps:

1 Load raw CPT data from AGS-file.

2 Calculate additional parameters for soil interpretation and classification.

3 Calculate soil behaviour type for each depth with available CPT data.

4 Select stratigraphy based on calculated parameters and soil behaviour type related to depth.

5 Define geotechnical unit for all defined layers.

Initially, the raw CPT data is loaded into a script designed to classify the soils (Step 1). Some postprocessing of the raw data is performed to derive additional parameters required for classifying the soil using the Robertson-method (Step 2). These parameters are shown below, cf. Ref. /6/.

Corrected cone resistance: $q_t = q_c + u_2 \cdot (1 - a)$

Friction ratio: $R_f = \frac{f_s}{q_t}$

Normalised cone resistance: $Q_{tn} = \left(\frac{q_t - \sigma_{v0}}{P_a}\right) \cdot \left(\frac{P_a}{\sigma'_{v0}}\right)^n$

Stress exponent: $n = 0.381 I_c + 0.05 \left(\frac{\sigma'_{v0}}{P_a}\right) - 0.15 \leq 1.0$

Normalised pore pressure ratio: $B_q = \frac{u_2 - u_0}{q_t - \sigma_{v0}}$

Normalised friction ratio: $F_r = \left(\frac{f_s}{q_t - \sigma_{v0}}\right)$

Soil behaviour type index: $I_c = [(3.47 - \log Q_{tn})^2 + (\log F_r + 1.22)^2]^{0.5}$

Where:

f_s is the measured CPT sleeve friction

q_c is the measured CPT cone tip resistance

u_2 is the measured pore pressure immediately behind cone tip

u_0 is the hydrostatic pore pressure

σ_{v0} is the total vertical in-situ stress

σ'_{v0} is the effective vertical in-situ stress

a is the area ratio of the adopted CPT cone

P_a is the atmospheric pressure

From the available parameters, an initial estimation of the soil behaviour type for each layer is made based on different classification methods (Step 3). Three different classification methods are used for evaluating the variation in the soil behaviour type (SBT):

- Using soil behaviour type index.
- Using normalised cone resistance and friction ratio.
- Using normalised cone resistance and pore pressure ratio.

The three considered classification methods are described in section 5.2.1, 5.2.2 and 5.2.3, respectively.

Based on the measurements in the CPT (cone resistance, sleeve friction and pore pressure) and the estimated SBT, the soil layering can be determined, and the geotechnical units can be defined (Step 4 and 5).

Once the soil stratigraphy and the associated geotechnical units have been defined, layer specific information can be determined in the postprocessing. For each soil layer, the associated CPT data can be used to estimate the strength and stiffness parameters for that specific soil layer. The methods adopted for defining strength and stiffness properties can be found in section 6.

5.2.1 Soil behaviour type index

The estimation of the SBT is based on the soil behaviour type index I_c value using Table 5-2 as seen below. It shall be noted that the correlation between the soil behaviour type index and SBT only applies for SBT zones 2-7, i.e., zones 1, 8 and 9 are not considered here.

This method considers both the normalised cone resistance and the normalised friction ratio, whilst pore pressure is not accounted for.

Table 5-2 Soil behaviour types (SBT) based on I_c, cf. Ref. /6/.

Zone	Soil Behaviour type	I_c
1	Sensitive, fine grained	N/A
2	Organic soils – clay	> 3.6
3	Clays – silty clay to clay	2.95 - 3.6
4	Silt mixtures – clayey silt to silty clay	2.6 - 2.95
5	Sand mixtures – silty sand to sandy silt	2.05 - 2.60
6	Sands – clean sand to silty sand	1.31 - 2.05
7	Gravelly sand to dense sand	< 1.31
8	Very stiff sand to clayey sand	N/A
9	Very stiff, fine grained	N/A

5.2.2 Normalised cone resistance and friction ratio

SBT is estimated based on Ref. /6/ where normalised cone penetration resistance, Q_{tn}, and normalised friction ratio, F_r, are used as basis, cf. Figure 5-1.

As seen from Figure 5-1, information about OCR/age and sensitivity can also be deduced from the plot. However, this type of information shall be treated with some caution, and it has not been used actively to establish geological age or degree of pre-consolidation for the soils.

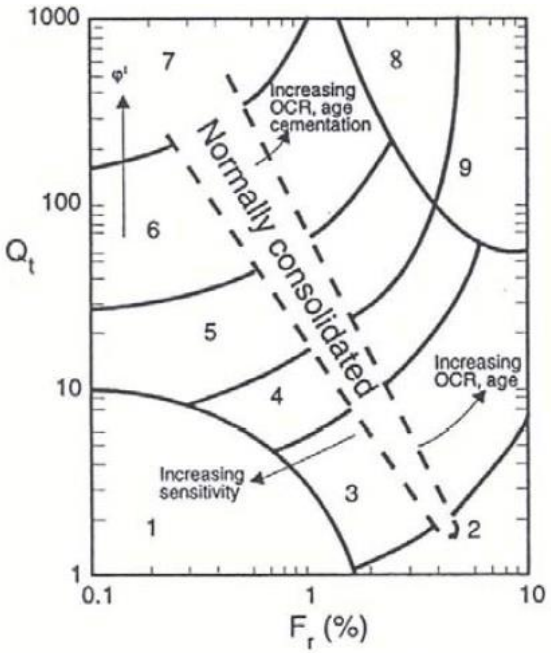

Figure 5-1 Robertson Q_t – F_r classification chart for soil behaviour type, cf. Ref. /6/. As recommended in Ref. /6/ the normalised cone resistance (Q_{tn}) is considered instead of Q_t when evaluating the soil behaviour type.

5.2.3 Normalised cone resistance and pore pressure ratio

SBT is estimated based on Ref. /6/ were normalised cone penetration resistance, Q_{tn}, and normalised pore pressure ratio, B_q, are used as basis, cf. Figure 5-2.

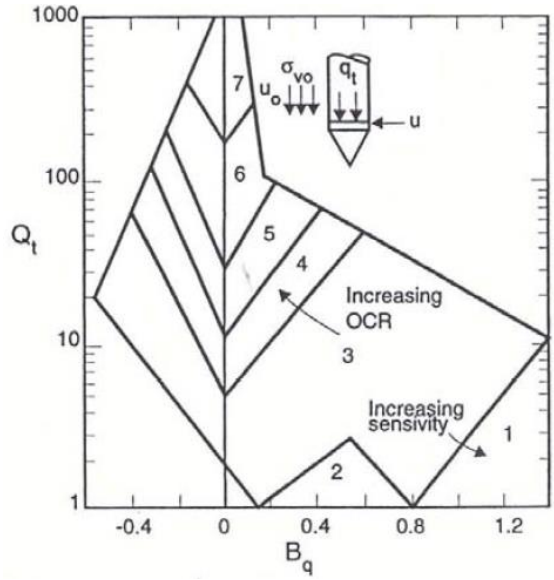

Figure 5-2 *Robertson $Q_t - B_q$ classification chart for soil behaviour type, cf. Ref. /6/. As recommended in Ref. /6/ the normalised cone resistance (Q_{tn}) is considered instead of Q_t when evaluating the soil behaviour type.*

5.3 Classification of soils using CPT, borehole logs and geophysical horizons

For the classification of soils used for the definition of the stratigraphy and the geotechnical units, the following is noted:

- In the borehole logs, the soil types given are evaluated based on classification tests (particle size distribution, Atterberg limits, etc.) and based on geological evaluation.

- Classification based on CPT interpretation, cf. section 5.2, generally takes into consideration the mechanical behaviour of the soil.

Hence, the source of the interpreted stratigraphy from borehole log and CPT is different and each geotechnical investigation type is valuable for a detailed understanding of the soil characteristics and behaviour.

At the survey locations the maximum distance between the performed tests is found as 9.1 m. Some lateral variation of the stratigraphy may be present between the locations for borehole and CPT. However, given the short distance between borehole and CPT, such lateral variation is expected to be insignificant.

The variation in soil behaviour type (based on normalised cone resistance together with normalised friction ratio or normalised pore pressure, cf. section 5.2.2 and 5.2.3) interpreted from CPT of selected geotechnical units are presented in Figure 5-3 to Figure 5-6 as an example for Weichselian sand and clay. It is observed that Weichselian clay plot in soil behaviour type zone 3 and 4 representing "Clay – silty clay to clay" and "Silt mixtures – clayey silt to silty clay", respectively, cf. Figure 5-5 and Figure 5-6. The concentrated area in the soil behaviour type plot covered by these clay units, considering the large amount of data, highlights the similarity in behaviour of this grouped clay unit.

Weichselian sand generally fall within the soil behaviour zone 6 representing "Sands – clean sand to silty sand", cf. Figure 5-3 and Figure 5-4.

Further, it is noted from the normalised friction ratio plot that the soil behaviour type plots shows a tendency to have experienced some over consolidation.

The same Robertson charts for all other geotechnical units are presented in Appendix B.2.

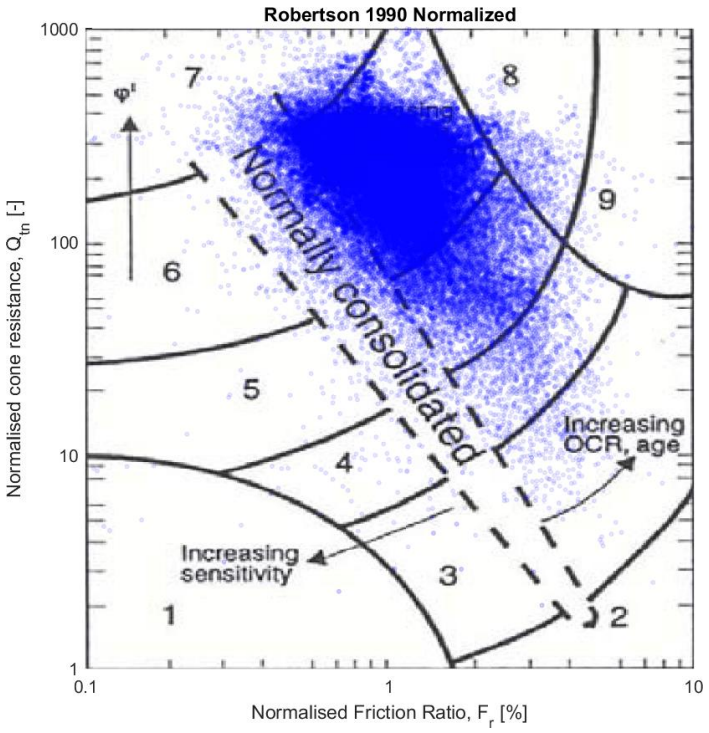

Figure 5-3 Robertson Q_{tn} – F_r classification chart for soil behaviour type plotted for all CPT survey locations for the geotechnical unit Weichselian sand.

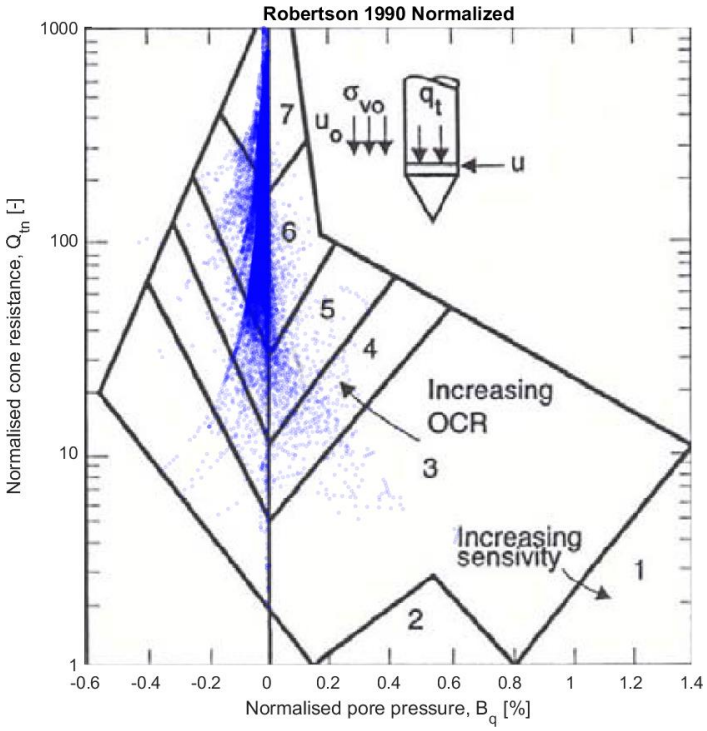

Figure 5-4 *Robertson Q_{tn} – B_q classification chart for soil behaviour type plotted for all CPT survey locations for the geotechnical unit Weichselian sand.*

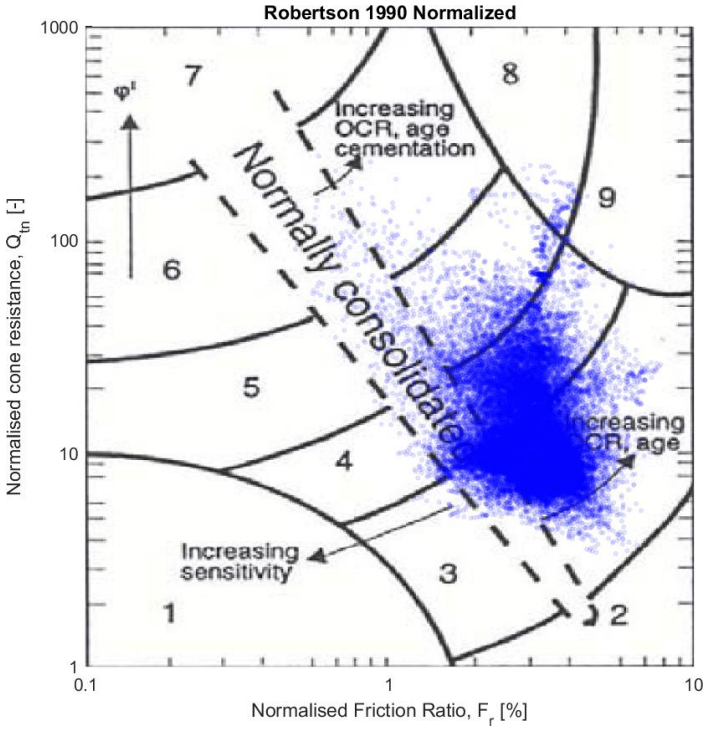

Figure 5-5 *Robertson Q_{tn} – F_r classification chart for soil behaviour type plotted for all CPT survey locations for the geotechnical unit Weichselian clay.*

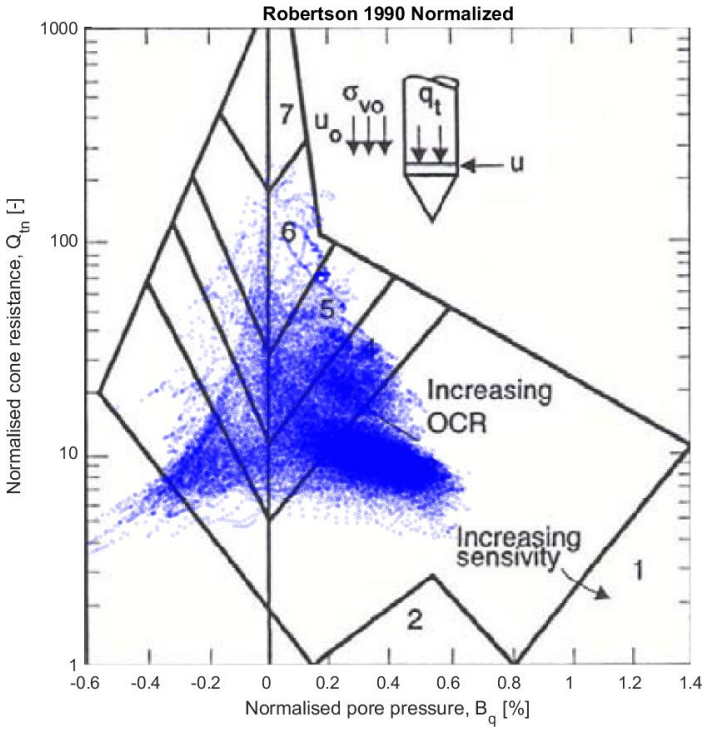

Figure 5-6 *Robertson Q_{tn} – B_q classification chart for soil behaviour type plotted for all CPT survey locations for the geotechnical unit Weichselian clay.*

6 Geotechnical properties and variation

Following the definition of soil layers and stratigraphy based on CPT and borehole data outlined in section 5.3, this section addresses the methodologies considered for determination of geotechnical properties and associated variation including the assignment of these properties to the geotechnical units. For geotechnical units considered as mix materials the properties are calculated with formulas based on both sand and clay material behaviour. The results for all geotechnical units are presented in Appendix D.

The determination of geotechnical properties is based on both selected CPT correlations and the available laboratory test data from the two performed campaigns, cf. Ref. /3/ and Ref. /4/. For the CPT data, the geotechnical properties are determined based on selected correlations, while the properties derived on the basis of onshore laboratory testing are generally taken as-is from the outcome of the testing. The only performed processing of the data are:

- The undrained shear strength from UU tests have been calibrated by multiplying with a factor of 1.2, cf. Ref. /5/. The lack of consolidation of the sample before shear result in lack of radial stresses which exist in the in-situ conditions. This means it will most likely show a false low strength as the sample is not brought to the actual in-situ condition, hence the applied factor is used for considering this.

- The friction angle determined from the laboratory campaign for the Island area has been reevaluated for the effective cohesion to be zero. This has been done for the estimated friction angles at the Island area to be comparable to the values estimated from the site campaign.

- The G_{max} results from the seismic CPTs are provided for the x-, y- and z-direction from the test. Overall, the validity of the results from the z-direction can be questioned due to the unrealistic values, hence these have been disregarded. For estimating one value per depth, the average of the results from x- and y-directions have been used if the difference between these is less than 50 MPa. For larger differences, the test from this depth has been disregarded.

- The G_{max} results from the P-S logging have been determined from the two shear wave velocities received in digital format per test depth. The small strain stiffness has been calculated with the average of the wave velocity by the equation:

$$G_{max} = \rho \left(\frac{s1_{wave} + s2_{wave}}{2} \right)^2$$

Beside the above points, no additional interpretation has been imposed on the laboratory testing.

The use of CPT correlations to derive soil parameters is an efficient way of assessing the soil characteristics reducing the need for soil sampling and subsequent onshore laboratory testing. It must, however, be emphasized that these correlations shall ideally be benchmarked using results from testing of soil specimens under controlled laboratory conditions. The assessed soil properties based on the CPT correlations are shown for all CPT survey locations in Appendix C.

The relevant geotechnical properties assessed in the following are divided into three categories:

- State properties
- Strength properties
- Stiffness properties

Table 6-1 provides an overview of the parameters that will be determined including the data sources considered for each of these. The abbreviation presented in the brackets represent the naming in the plots. The focus is to provide estimates for traditional soil parameters including the expected ranges of variation for the different geotechnical units. These parameters provide an estimate of the soils' ability to withstand loads and a general understanding of the deformation characteristics of the soil. The laboratory test results included in the plots through this section can be differentiated between the Island campaign and Site campaign by the legend name, as laboratory results from the Island campaign is marked with "*I*" and laboratory results from the site campaign are marked with "*S*". Results from the CPT correlations are made with a 90% transparent scatter for being able to determine the concentrated areas in the plots.

In addition, an overview of the ranges of classification, strength, and stiffness properties per geotechnical unit are presented in section 6.4.

Table 6-1 Overview of data sources adopted for assessing geotechnical properties.

Category	Soil property	Data source
State	Over-consolidation ratio	CPT correlation
	Relative density	CPT correlation
Strength	Undrained shear strength	CPT correlation Triaxial testing (CAU, CIU, UU) Direct Simple Shear (DSS) Unconfined compressive strength (UCS) Pocket penetrometer (PP) Laboratory hand vane test (Hand vane) Laboratory vane test (Vane)
	Friction angle	CPT correlation Triaxial testing (CID)
Stiffness	Small-strain shear modulus	CPT correlation Seismic CPT (SCPT) P-S logging (PS) Bender element test (BE) Resonant column test (RC)

6.1 Presentation of CPT properties

As outlined in section 6, the soil parameters are derived partly using CPT correlations and partly using results from the laboratory testing when available.

This section presents the data from the CPTs across the OWF project site. The results are presented per geotechnical unit.

Figure 6-1 and Figure 6-2 show an example of range of basic CPT measurements for Holocene sand which include cone tip resistance, cone shaft resistance, friction ratio, pore water pressure and soil behaviour type index. Figure 6-1 shows the variation of the different integrated model units grouped for the geotechnical unit, while the second figure is only included for geotechnical units where measurements are available from both performed site investigation campaigns. The presented example shows that the CPT measurements in these fine-grained layers generally plots within a consistent trend. It is also noted that the measurements from the Island area and Site area show a consistent trend, although the depth, at which the geotechnical unit is encountered, differs.

In Appendix B.1 the variation of measured CPT parameters is presented for the considered geotechnical units.

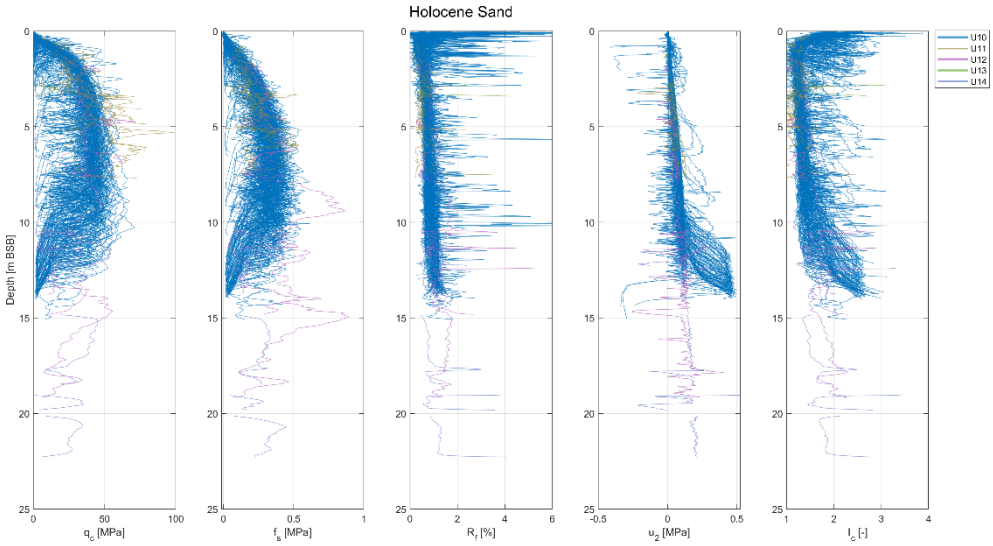

Figure 6-1 *Range of CPT parameters for geotechnical unit Holocene sand when differing between the integrated model units (5 units, see legend).*

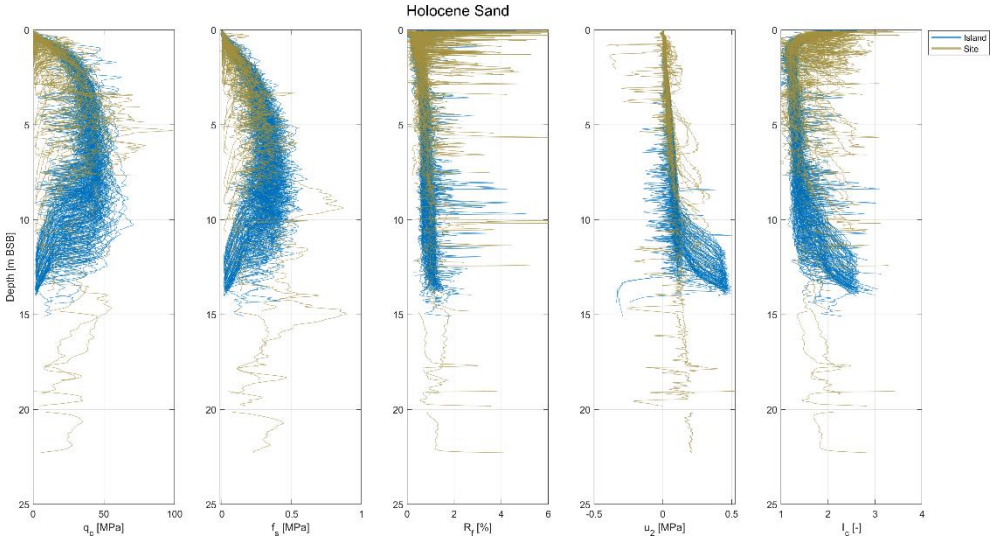

Figure 6-2 *Range of CPT parameters for geotechnical unit Holocene sand when differing between data from the Island campaign (blue) and the site campaign (dusty green).*

6.2 Presentation of state properties

As outlined in section 6, state parameters such as over-consolidation ratio (for cohesive soils) and relative density (for non-cohesive soils) have been determined from CPT correlations.

The assessment of these parameters serves as input to the overall understanding of the in-situ soil state, which is crucial for assessing the general soil behaviour. This section presents the methods adopted for the analyses of these parameters as well as the outcome.

6.2.1 Over-consolidation ratio

The over-consolidation ratio, OCR, is determined by a CPT correlation commonly used in the industry. The method considered for the parameter estimation is the Mayne (2019) methodology which is representative for both sand, clay, and mixed soil conditions due to the correction from the *m'* exponent.

The Mayne methodology adopts the following formula, cf. Ref. /8/:

$$OCR = k\left(\frac{(q_t - \sigma_{v0})^{m'} * \left(\frac{p_a}{100}\right)^{1-m'}}{\sigma'_{v0}}\right)$$

where q_t is the corrected cone resistance, σ_{v0} is the total in-situ vertical stress, σ'_{v0} is the effective in-situ vertical stress, p_a is the atmospheric pressure, *k* is a dimensionless constant which is set to 0.33, and *m'* is an exponent which can be calculated from below formula, where I_c is the soil behaviour type index, cf. Ref. /8/.

$$m' = 1 - \frac{0.28}{1 + (I_c/2.65)^{25}}$$

Figure 6-3 presents the variation of OCR (interpreted based on CPT) with depth for the geotechnical unit Saalian mix which shows a variation of the interpreted material based on the considered material type. It is observed that if the material is interpreted as sand, the OCR generally indicate normal- to slightly over-consolidated state with higher values near the top. It should be kept in mind the OCR value is sensitive in the depths near seabed due to the low overburden pressure. If the material is interpreted as clay, a high over-consolidation is noticed.

In Appendix D.1, the variation of OCR with depth is presented for the individual geotechnical units.

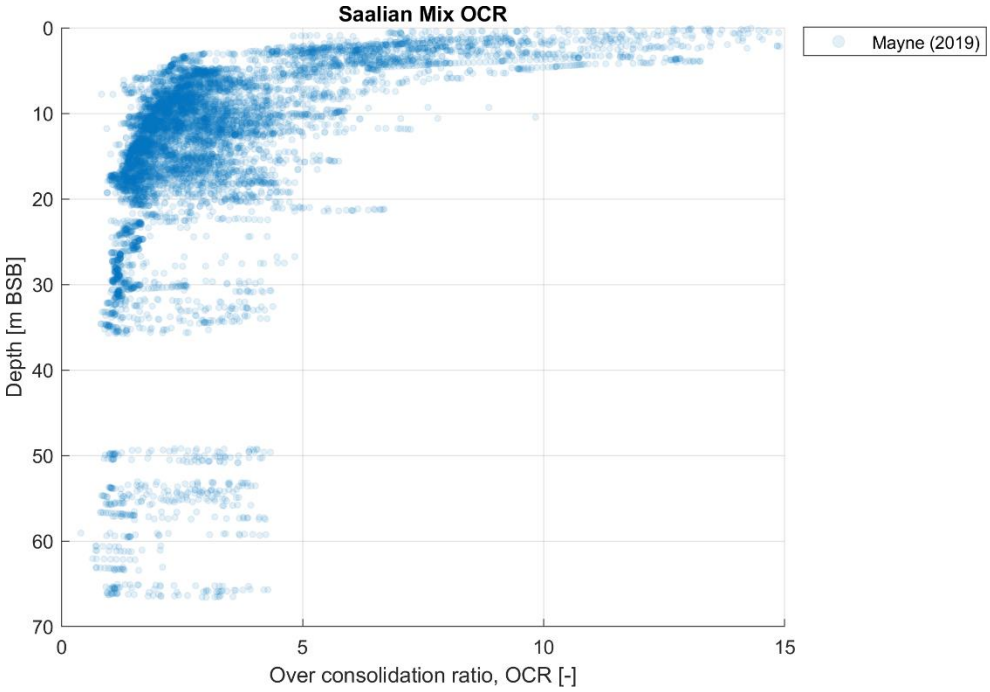

Figure 6-3 Range of OCR for geotechnical unit Saalian mix.

6.2.2 Relative density

The relative density, I_D, is determined for the non-cohesive soils by two different CPT correlations commonly used in the industry as no laboratory testing is used for calibration of the parameter. The different methods considered for the CPT correlations are listed below:

- Baldi (1986)
- Jamiolkowski (2003)

From Baldi (1986) the relative density correlation is calculated by the below expression, cf. Ref. /7/:

$$I_D = \frac{100}{2.41} \ln\left(\frac{q_t}{157\ (\sigma'_{v0})^{0.55}}\right)$$

where q_t is the corrected cone resistance and σ'_{v0} is the effective in-situ vertical stress.

The Jamiolkowski (2003) correlation is determined from the below formulas, cf. Ref. /9/:

$$I_{D,sat} = I_{D,dry} * \frac{-1.87 + 2.32\ \ln\left(\frac{q_t}{(p_a\ *\ \sigma'_{v0})^{0.5}}\right)}{100} + I_{D,dry}$$

$$I_{D,dry} = \frac{100}{2.96} \ln\left(\frac{q_t/p_a}{24.94\ (\sigma'_m/p_a)^{0.46}}\right)$$

where q_t is the corrected cone resistance, σ'_m is the in-situ mean effective stress, σ'_{v0} is the effective in-situ vertical stress and p_a is the atmospheric pressure. By assuming a value for $K0$ of 1.0, which means the material is considered as slightly over-consolidated, the in-situ mean effective stress σ'_m is set equal to the effective in-situ vertical stress σ'_{v0}.

In Figure 6-4, an example of the variation of relative density (interpreted based on CPT) with depth is presented for Weichselian sand. It is observed that the relative density of the geotechnical unit is in the range 60% to 120% with the highest concentration of scatter located around 100%. It should be noted the values above 100% is due to the formula from the CPT correlation. In Appendix D.2, the variation of relative density with depth is presented for the further geotechnical units.

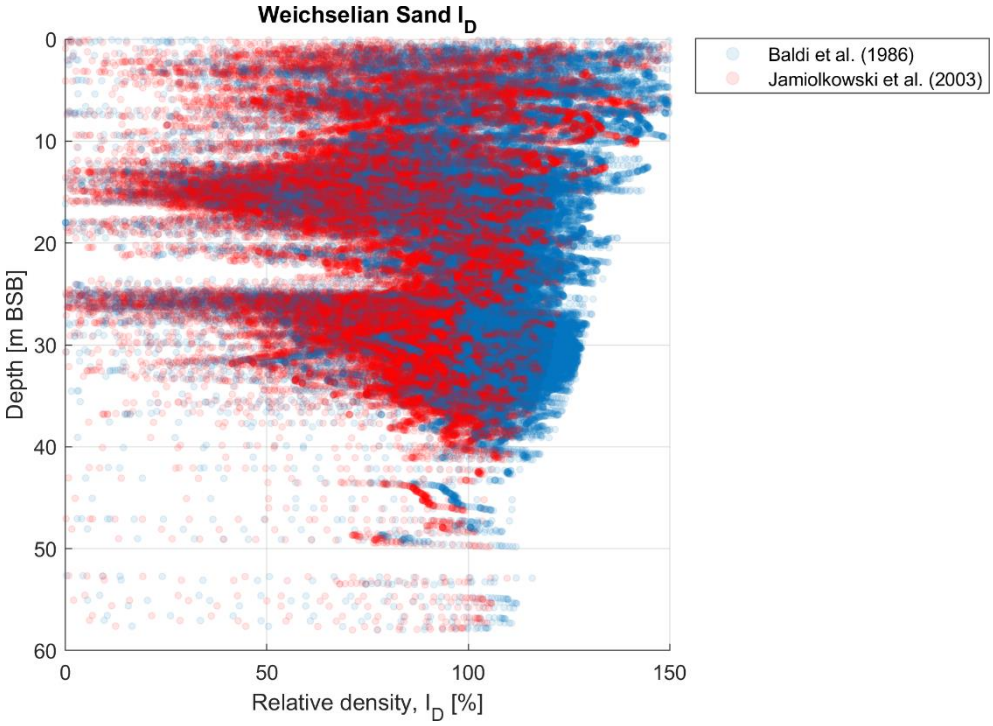

Figure 6-4 Range of estimated I_D using CPT correlations for geotechnical unit Weichselian sand.

6.3 Presentation of strength and stiffness properties

Following the state parameters described in section 6.2, strength and stiffness parameters such as undrained shear strength (for cohesive soils), friction angle (for non-cohesive soils) and small-strain shear modulus (all soils) have been determined from CPT correlations, supplemented by laboratory testing, cf. Ref. /1/. In addition, the small-strain shear modulus has also been evaluated based on SCPT and P-S logging. The CPT correlations have been selected based on which of the considered literature correlations match the laboratory testing best.

The assessment of these parameters serves as input to the overall understanding of the soil behaviour during loading, e.g., in relation to placement of wind turbine foundations or jack-up operations on the OWF project site. This section presents the method adopted for the analyses of these parameters as well as the outcome.

To determine just one representative value (soil strength/stiffness) per geotechnical unit per survey location, the average value for each geotechnical unit is determined. When deriving the average value for the sand and clay layers, the peaks and troughs in the CPT trace (usually found close to the layer boundaries) are removed to reduce the impact of this data on the average value, i.e., to obtain the most representative value.

6.3.1 Friction angle

The peak friction angle, φ'_p, is calculated for non-cohesive soils according to the method of Schmertmann (1978) assuming that the sand is "uniform fine sand", cf. Ref. /7/. The Schmertmann correlation have been selected as representative for the OWF project site based on visual inspections of the comparison between CPT correlated values and the laboratory test results from the same positions and depths.

$$\varphi'_p = 28.0 + 0.14\, I_D$$

where I_D is the relative density determined from Baldi (1986).

As the relative density calculated from CPT correlation is regularly found above 100%, and values larger than 100% is considered for the correlation, a line representing the friction angle for a relative density of 100% is added to the figures.

Further to the CPT correlation, the friction angle is obtained through triaxial testing, CID. The CID triaxial tests have been performed as single tests for the site campaign, i.e., tests have not been performed at varying confining pressure, while the CID triaxial tests from the Island campaign have been performed as three tests where an associated effective cohesion has been determined. The peak friction angle, φ'_p, has been derived from the CID tests from the Island campaign through the following equations to make comparable values between the two geotechnical campaigns:

$$M = \frac{q}{p'}$$

$$\varphi'_p = \text{asin}\left(\frac{3M}{6+M}\right)$$

where q is the deviatoric stress at failure and p' is the effective mean stress at failure. Hereby it is assumed that the effective cohesion is zero.

Using CPT data for all survey locations as well as the available laboratory test data, the range of friction angle for geotechnical unit Holocene sand is shown in Figure 6-5. It is observed that the friction angle interpreted based on CPT generally estimates larger values than those measured in the CID tests. In regard to the laboratory tests for the sand material it is noted that uncertainties are present in regard to the restitution of the specimens and hence to how well the reconstituted specimen represents in-situ conditions.

In Appendix D.3, the variation of friction angle with depth is presented for the remaining geotechnical units.

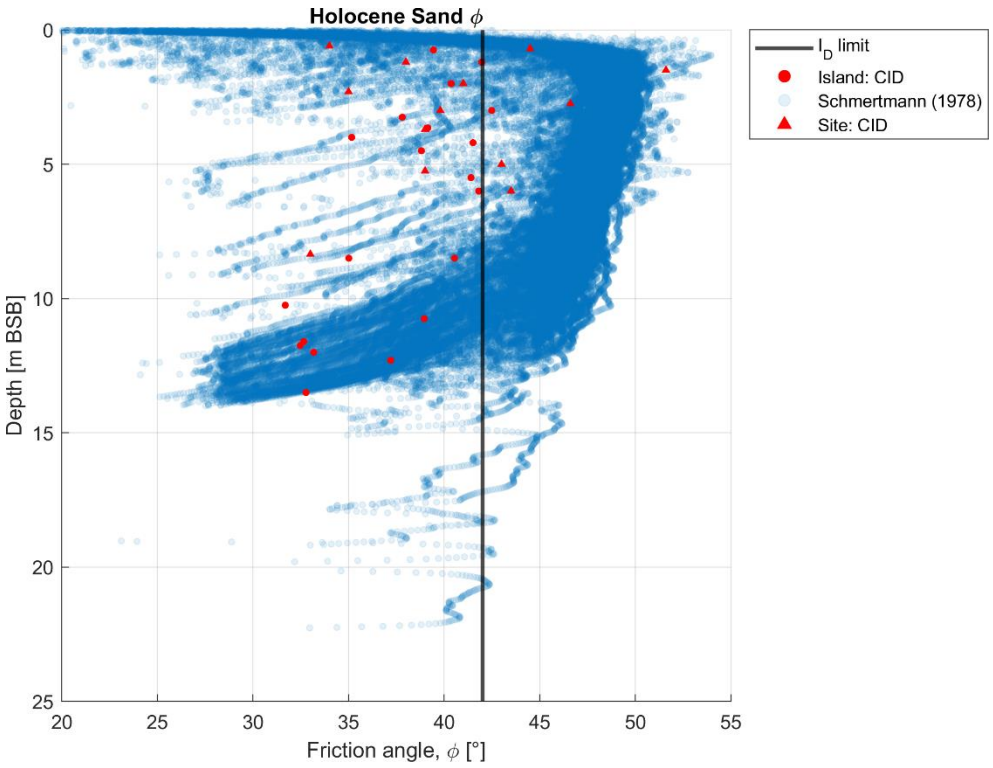

Figure 6-5 Range of φ for geotechnical unit Holocene sand using CPT correlation and laboratory test results (CID – Consolidated Drained triaxial test).

6.3.2 Undrained shear strength

The undrained shear strength, c_u, is determined for cohesive soils according to Ref. /6/ as:

$$c_u = \frac{q_t - \sigma'_{v0}}{N_{kt}} = \frac{q_{net}}{N_{kt}}$$

For determination of undrained shear strength in fine grained materials, a cone factor has been determined for each chronostratigraphic group, which is presented in Table 6-2. These values are determined from visual inspections of CPT vs laboratory data, and they are found to ensure a proper match between the undrained shear strength determined based on CPT, and the undrained shear strength from the consolidated undrained triaxial tests (CIU and CAU).

In addition to the consolidated undrained triaxial tests, the correlations have also been established partly from the unconsolidated undrained triaxial tests (UU) and direct simple shear tests (DSS), where a multiplication factor of 1.2 have been used on the UU tests, cf. section 6. In the borehole logs some of the clay layers in Saalian and Elsterian chronostratigraphic groups are classified as fissured. This may partly explain the high estimated cone factors for these geotechnical units, but it is recommended that this is investigated further during foundation design.

Table 6-2 Cone factors used for undrained shear strength of clay material per chronostratigraphic group.

Chronostratigraphic group	Cone factor, N_{kt}
Holocene	14
Late Weichselian	17
Weichselian	20
Saalian	24
Elsterian	26
Elsterian & older	26
Miocene	26

Further to the CPT correlation, the undrained shear strength is obtained through triaxial testing, namely consolidated anisotropically undrained (CAU) tests, consolidated isotropically undrained tests (CIU) and unconsolidated undrained triaxial tests (UU), from direct simple shear tests (DSS), and from Torvane tests and Pocket penetrometer (PP) tests.

Using CPT data for all survey locations as well as the available laboratory test data, the range of undrained shear strength is shown in Figure 6-6 for the geotechnical unit Elsterian clay. It is observed that the grouping shows increasing strength with depth but with strength variations for minor parts of the data being present at certain depths. Further, it is observed that the CPT predicted strength matches generally well the strength derived from consolidated triaxial tests and DSS tests. In contrast pocket penetrometer tests and unconsolidated undrained triaxial tests generally yield higher strength than the CPT predictions. In this regard it is emphasized that consolidated triaxial tests and DSS tests are considerably more reliable than the other laboratory tests.

In Appendix D.4, the variation of undrained shear strength with depth is presented for the individual geotechnical units.

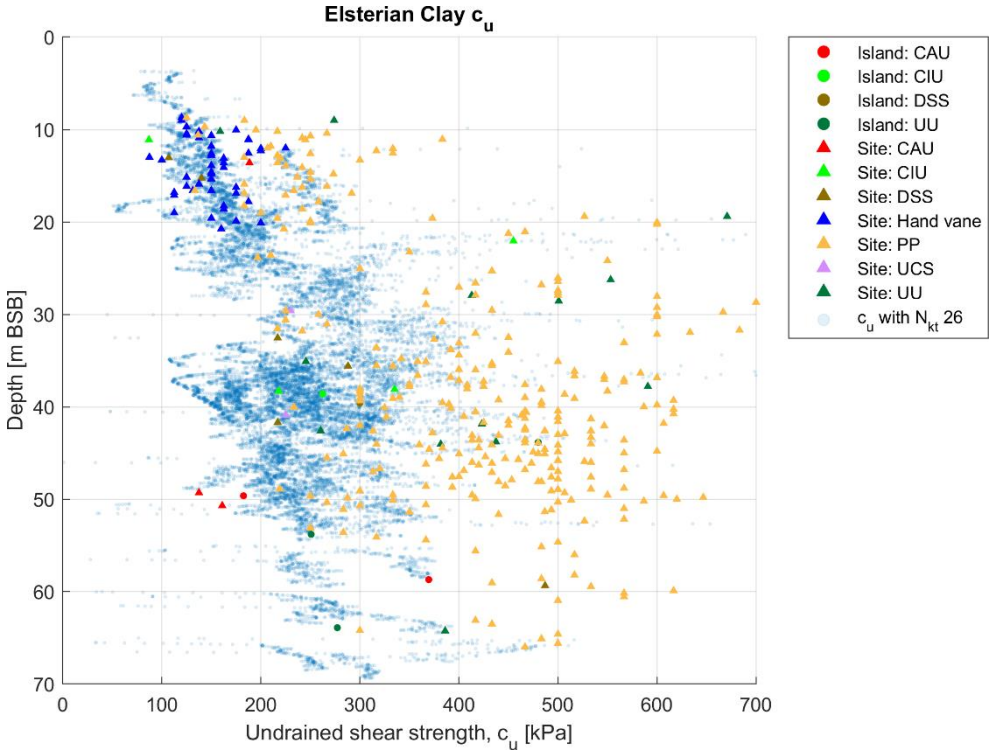

Figure 6-6 *Range of c_u for the geotechnical unit Elsterian clay using CPT correlation (blue dots) and laboratory test results.*

6.3.3 Small-strain shear modulus

The small-strain shear modulus, G_{max}, is determined in all soils from the Rix & Stokoe (1991) correlation, cf. Ref. /10/:

$$G_{max} = 1634 \left(\frac{q_c}{\sqrt{\sigma'_{v0}}} \right)^{-0.75}$$

where q_c is the measured CPT cone tip resistance and σ'_{v0} is the effective in-situ vertical stress.

Further to the CPT correlation, the small-strain shear modulus is obtained mainly through seismic CPT (SCPT) and P-S logging, but also from few available bender element and resonant column tests.

Using CPT data for all survey locations as well as the available SCPT data and P-S logging data, the range of small-strain shear modulus for Saalian mix is shown in Figure 6-7. It is noted that the small-strain shear modulus from PS logging and SCPT generally fits well with the values interpreted from the CPT correlation, with a bit more differentiation of the SCPT values. In Appendix D.5, the variation of small-strain shear modulus with depth is presented for all the individual geotechnical units.

Figure 6-7 *Range of G_{max} for the geotechnical unit Saalian mix using CPT correlation, SCPT and P-S logging.*

6.4 Range of soil parameters per geotechnical unit

In Appendix E the range, average and standard deviation values from the laboratory results (including both performed campaigns) of classification, strength and stiffness parameters are presented for the geotechnical units.

7 Geological Setting

In this section the geological setting for the OWF project site is presented.

7.1 Pre-Quaternary Geology

The OWF-project site is located off the west coast of mainland Denmark in the Danish sector of the North Sea basin. The major structural features in the near area are the WNW-ESE striking Sorgenfrei-Tornquist fault zone and the Ringkøbing-Fyn High to the south. The North German Basin is located south of the Ringkøbing-Fyn High (Ref. /11/). The main faults, salt structures, structural highs and the top of Pre Zechstein are illustrated on Figure 7-1.

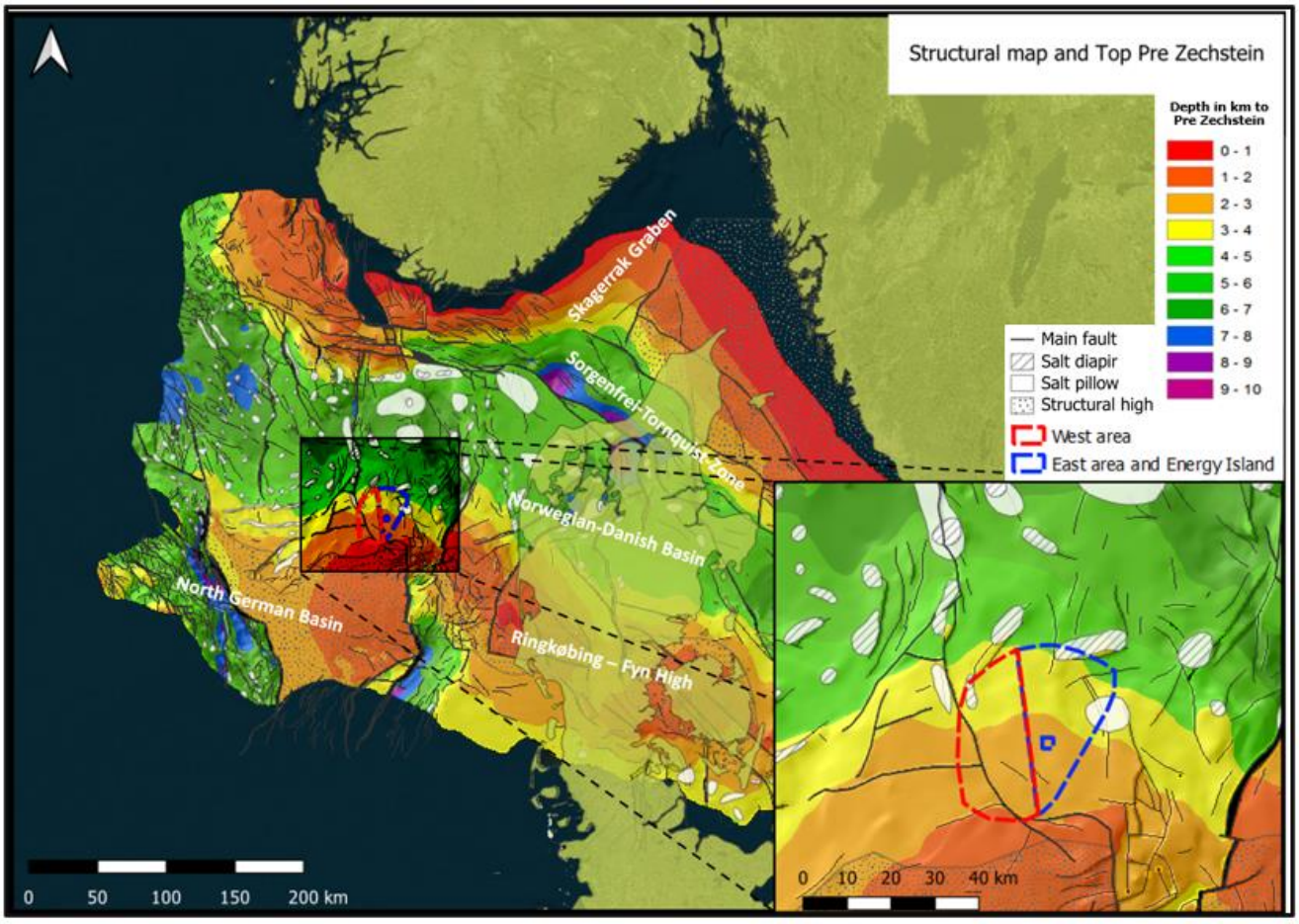

Figure 7-1: Map of the top Pre Zechstein along with the major structural elements. Salt structures are seen as white/hatched areas and structural highs are marked by dots. Copyright GEUS WMS.

The North Sea is a failed arm of the Arctic-North Atlantic rift system occurring in the Carboniferous to the Triassic along with the formation and breakup of Pangea (Ref. /12/, Ref. /13/).

In early Permian volcanic activity induced by the lithospheric thinning ended and thermal subsidence created space for Permian evaporites (Ref. /14/; Ref. /15/). During the Zechstein (Late Permian) 4-5 cycles of evaporites were deposited, creating the "Zechstein salts" (Ref. /16/;Ref. /17/).

The evaporite deposits were up to a 1000 m in thickness and after being covered by thick layers of Mesozoic sediments, an activation of the salts (halokinesis) and following diapirism was onset. The creation of salt pillows and diapirs altered the younger sediments deposited on top. After a period of no movement the halokinesis was reactivated during the Quaternary when massive ice sheets spread over the Danish area (Ref. /18/, Ref. /14/).

From the Cenozoic to middle Pleistocene the Danish sector of the North Sea was heavily influenced by the Eridanos river system that flowed into the North Sea, from what is now the Baltic Sea, in the south and west through what is today Denmark. The Cenozoic deposits are expected to come from deltaic successions of clay and sand which are coarsening upwards. This, however, changed over time when the Eridanos river system shifted westwards and mostly fluvial sediments were deposited instead of deltaic (Ref. /19/). The pre-Quaternary sediments expected to underly the Quaternary sediments are Miocene, potentially with a thin cover of Pliocene sediments (see Figure 7-2).

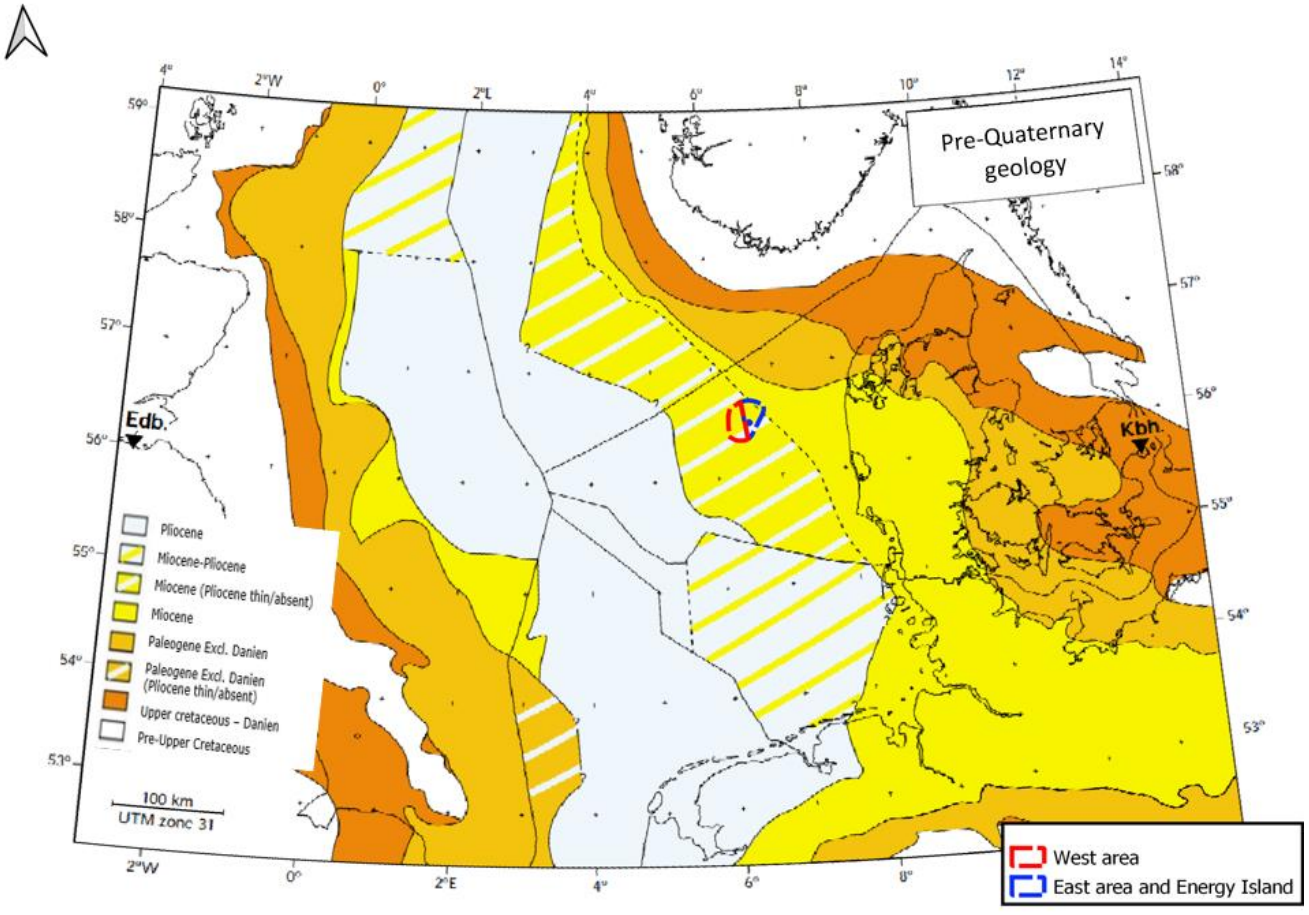

Figure 7-2: Map of pre-Quaternary deposits in the North Sea. The OWF project site is marked by a red shape for the West area and a blue shape for the East area. Modified from Ref. /20/.

7.2 Quaternary Geology

The Pleistocene is a complex period of interchangeable ice ages and interglacial periods, with different glacial-tectonic, erosional, and depositional features seen in the geology. The early and pre-Pleistocene sediments have also been influenced through glacio-tectonic deformation during the glaciations (Ref. /21/; Ref. /22/). Three major glaciations have been recorded in the Pleistocene: the Saalian, the Elsterian and the Weichselian ice advance.

The Elsterian and Saalian ice advances covered the entire OWF project site, see Figure 7-3, and has created tunnel valleys running several tens of kilometres long and cutting as deep as 350 m into older deposits. The valleys have complex infills of sand, clay and locally till (Ref. /21/). The remnants of the Saalian ice advance can also be seen as large moraine plateaus, "Bakkeøer", which correlates to onshore structures observed on the Danish west coast (Ref. /22/). After the Saalian glaciation a warmer period followed, the Eemian interglacial, where a transgression and a change to a marine environment occurred. The Eemian deposits consist of marine sand and clay and in the near shore deposits a high content of organic material are found (Ref. /23/).

The Weichselian ice advance had a maximum extent (LGM) just north of the OWF project site and southward through the middle of Jutland (Main stationary line) see Figure 7-3 (Ref. /21/). In the northern part of the OWF project site where the ice sheet has laid on top, glaciotectonic deformations and other subglacial formations can be expected. Further south proglacial formations such as riverplains with deposited glaciofluvial sand and gravel are found Ref. /23/. After the retreat of the ice sheet subglacial tunnel valleys emerged and clay, silt, and fine sands were deposited in the unaccommodated space Ref. /24/.

The LGM occurred about 18,000 years BP and approximately at 16,000 BP the deglaciation of the Danish area began. The large amount of meltwater from the ice sheets created a rise in global sea-levels simultaneously with an uplift of the land masses that was previously covered by an ice sheet. This caused a regression until 11,000 BP because the uplift was larger than the sea-level rise.

In Figure 7-4 the deglaciation is illustrated in two different phases. The left map in the figure illustrates the Yoldia Sea covering the northern part of what is Denmark today. Except for the Yoldia Sea the entire area was dry land which can be seen in the stratigraphy as peat deposits. The right map in the figure illustrates a further deglaciation with approximately the same extend of the Yoldia Sea but with a large freshwater lake formed in the Baltic Sea area (Ref. /23/, Ref. /25/, Ref. /26/, Ref. /27/, Ref. /28/).

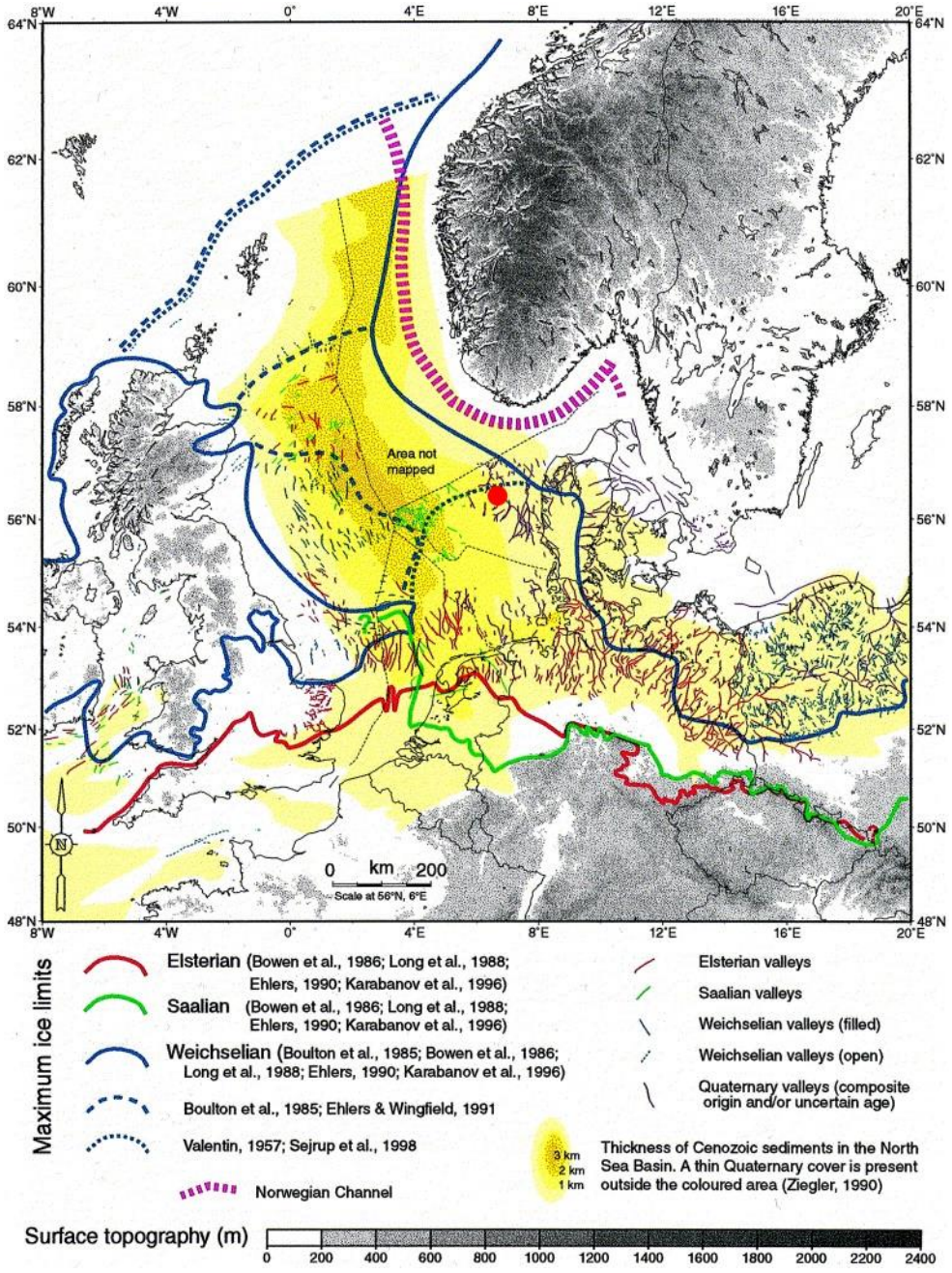

Figure 7-3: Extent of the 3 major ice advances in the Pleistocene. The OWF project site is marked by a red dot. (Ref. /21/)

From 11,000 to 6,000 BP a global transgression changed the area from dry land to marine conditions, and the glacial landscape was thereby eroded and later covered by marine sand, which is the youngest deposits found in this area. From then until present times the area around the OWF project site has been influenced by Holocene sea-level fluctuations (Ref. /23/).

The integrated geological model presented in in this report focuses on the upper 100 m of the stratigraphy and therefore only includes deposits of ages ranging from Miocene to present.

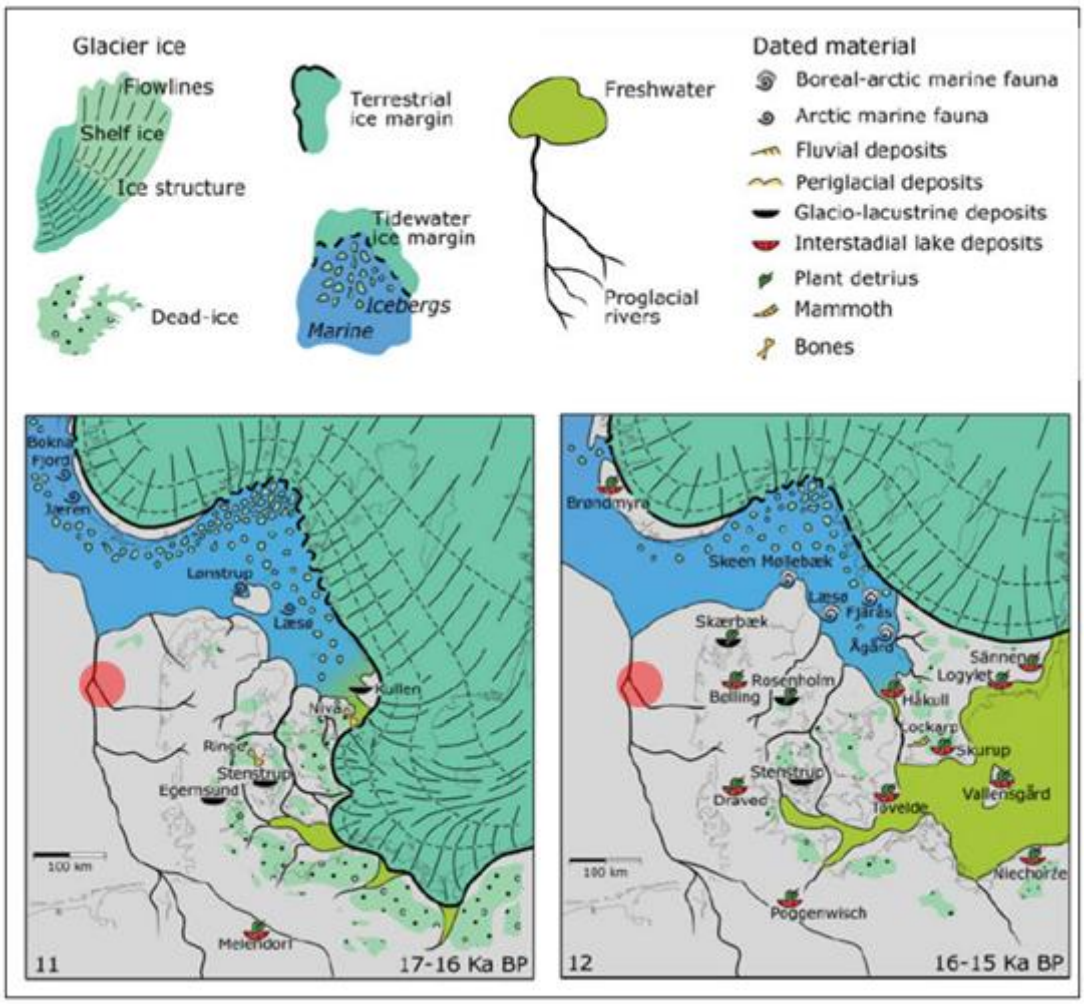

Figure 7-4: Paleogeographic map showing two stages of deglaciation. The left map is 17-16 Ka BP and the right map is 16-15 Ka BP. The blue is the Yoldia Sea, the turquoise is the retreating ice sheet, and the green is freshwater lakes. The red dots represent approximate location of the OWF project site. Ref. /29/

8 Conceptual Geological Model

8.1 Presentation of Conceptual Geological Model

The Conceptual Geological Model is compiled as hand-drawn geological profiles that summarize the geology across the entire OWF project site. It is based on units from the Integrated Geological Model, geological cross sections, and layer thickness maps extracted from the 3D digital model.

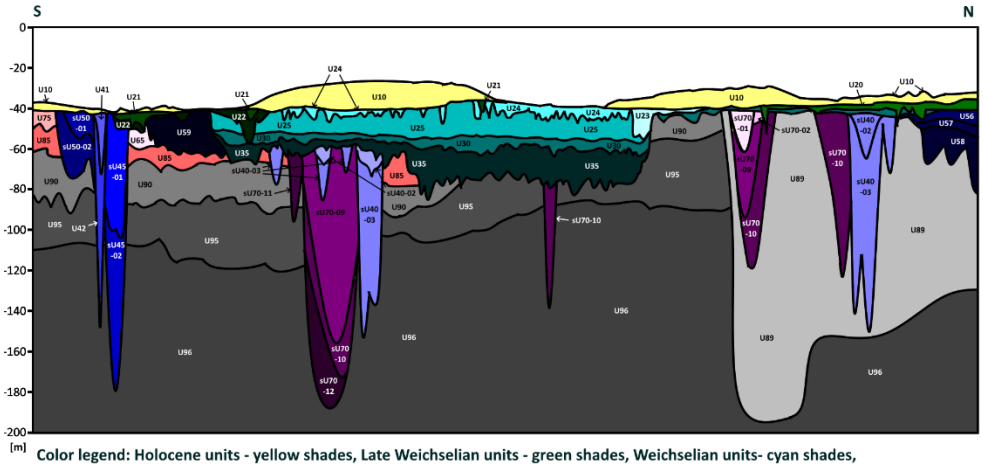

Figure 8-1 *Conceptual model cross section oriented from south to north through the central part of the OWF project site.*

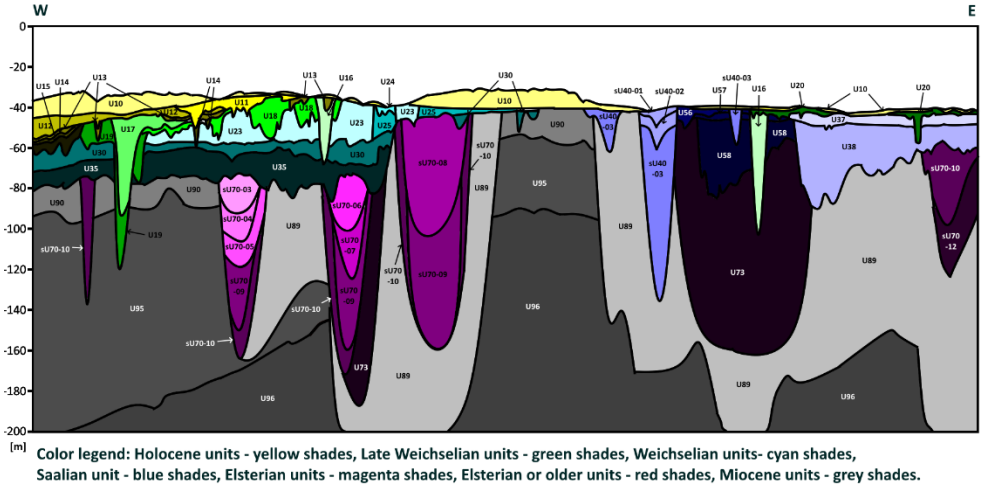

Figure 8-2 *Conceptual model cross section oriented from west to east through the central to northern part of the OWF project site.*

The conceptual geological model presents all the interpreted and integrated model units. Thickness, depth and location are only indicative for the individual units.

The deposits are characterized by many channel/valley systems belonging to different stratigraphic ages and largely all related to glacial periods through the Pleistocene. In the following the term unit refers to integrated model unit. Further description of the different integrated model units can be found in section 9.8. Please refer to Table 5-1 for an overview of which unit numbers that have been utilized.

Units 10 to 15 have been deposited in Holocene (postglacial) and have not been impacted by glacial overriding.

Units 16 to 20 have been deposited in Late Weichselian (when the Weichselian ice sheet reached its maximum extent) and may partly or entirely have been exposed to glacial compaction by the Weichselian ice sheet. However, the Weichselian ice sheet is considered to have had a relatively small thickness in the marginal region which the northwestern part of the OWF project site is part of. Therefore, the applied compaction force is interpreted not to have been significant.

Unit2 21 to 22 have also been deposited in Late Weichselian but in an area that was not overridden by the Weichselian ice sheet.

Units 23 to 35 have been deposited in the Weichselian prior to the greatest advance in Late Weichselian. The units have partly been overridden by the ice sheet, in particular Unit 23 which constitutes a glaciotectonite consisting primarily of a mixture of the other units (Unit 24 to Unit 35). For the same reason as the superimposed units (Unit 16 to Unit 20) the applied compaction by the Weichselian ice sheet is considered insignificant.

The interpreted maximum extent of the Weichselian ice sheet, is illustrated in Figure 8-3. The ice sheet extent has mainly been interpreted by the extent of the partly subglacial units between Unit 16 to Unit 20 and the glaciotectonic Unit 23. Unit 22, which is interpreted to have been deposited in an extramarginal meltwater channel, limits the extent from the ice-free side.

Units 37 to 59 are interpreted to have been deposited during the Saalian Glaciation. The soil strength of the units indicate that the layers have been exposed to glacial compaction.

Units 65 to 73 are interpreted to have been deposited during the Elsterian Glaciation (could also be attributed to Early Saalian or another earlier glacial event). Soil strength of samples from these units indicate varying degrees of compaction.

Units 75 and 85 are interpreted to have been deposited during the Elsterian Glaciation and/or earlier in Pleistocene. The depositional environment within the units is interpreted to be glaciofluvial to inter-/pre-glacial fluvial and lacustrine. Like the superimposed units, samples indicate varying degrees of compaction.

Units 89 to 96 have been attributed to the Miocene and consist of fluvial to marine deposits. Like the superimposed units, samples indicate varying degrees of compaction.

The integrated model units will be described in more detail in section 9.8.

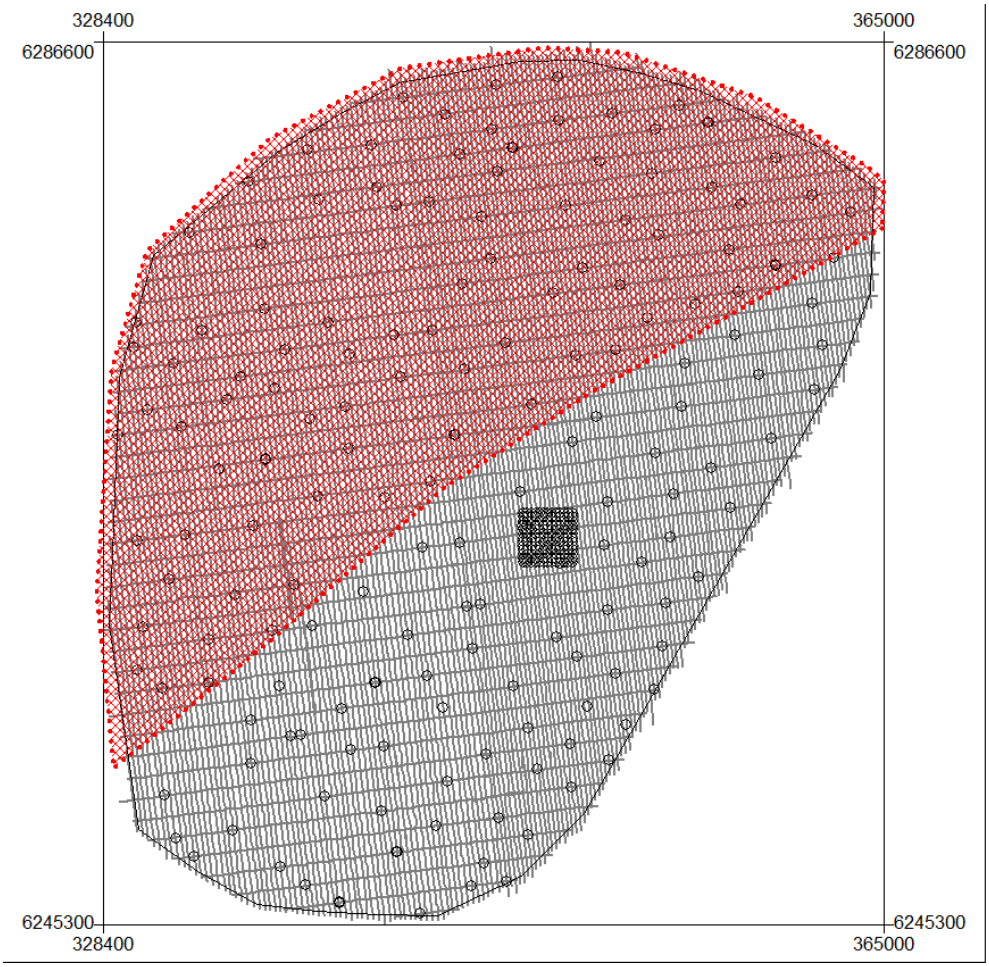

Figure 8-3 Interpreted maximum extent of the Weichselian ice sheet within the OWF project site (red hatching).

9 Integrated Geological Model

In this section it is described how the integrated geological model has been developed using the geotechnical results from (Fugro, 2023) and (Fugro, 2022a), and geotechnical interpretations in the present report along with the geophysical results from (Fugro, 2022b), (MMT, 2022) and geophysical interpretations in the present report.

9.1 Datum, coordinate system and software

The model has been comprised of the two separate kingdom models received from the East area and the West area and is set up with the datum ETRS89 (EPSG: 25832) and the GRS1980 spheroid.

The coordinate system used is the UTM projection in zone 32 N. Units are in meters. The height model is DTU21 MSL.

The data were delivered in separate packages for the two survey areas West area (Fugro) and East area (MMT). A Kingdom project for each survey area was received from the respective survey companies. Both 2D UHRS and SBP data were loaded into the Kingdom projects. The 2D UHRS seismic data were delivered both in time and depth domain accompanied by velocity models with RMS velocities in time domain (the East area model also included interval velocities in time domain). The SBP data were delivered in both time and depth and the data set from the East area included a velocity model.

A combined Kingdom project has been setup using the 2D UHRS seismic data and their velocity models. Horizons from each project have been imported and used as a basis for the integrated geological model. Geotechnical data and borehole information have been imported into the Kingdom project from the delivered AGS files and incorporated into the integrated model.

Existing horizons have been modified and new horizons have been interpreted along clear reflectors in the seismic data. Finally, results have been exported as grids for visualization. The grids include layer boundaries as well as grid calculations such as depth below seabed and vertical thickness (isochore) of the layers.

The 2D UHRS survey of the East area covers approximately 526 km² with a 210 m interval between main lines and 1000 m interval between crosslines. The East survey has a total of 3197.5 km UHRS lines surveyed.

The 2D UHRS survey of the West area covers approximately 534 km² with 250 m between lines and 1000 m between cross lines. The West survey has a total of 2872.5 km UHRS lines surveyed (measured from track lines in GIS project).

In total this sums up to 6070 km UHRS lines surveyed.

9.2 Assessment of existing geophysical models

The two geophysical data sets and geological models from East area and West area form the base of the integrated geological model together with the UCPT and borehole data from Fugro (Ref. /1/ and Ref. /4/) for entire OWF project site. Each geophysical model was based on the two seismic datasets, 2D-UHRS and SBP data. The upper most units have only been identified on the SBP data, while the units below the resolution of the SBP could only be recognised on the 2D-UHRS data. In Appendix H a table overview of the received units from each of the model areas (East and West) is presented. The tables in Appendix H also illustrate the relationship between the mapped horizons and the units. Although the two models use the same names/numbers for many layers/surfaces they do not necessarily map the exact same layers/surfaces. In most cases it is not possible to form consistent layers/surfaces across both survey areas using the surfaces mapped in each model.

The existing interpreted units have been based on clear and continuous reflectors identified in the datasets. Horizons has then been drawn on these, as unit boundaries. However, especially in areas interpreted as having been glacially overridden, the impact of glacial deformation made it necessary to make the interpretation more detailed. This, in particular, relates to areas that includes incised valleys, where a further subdivision of units was deemed necessary. In some cases, a specific layer was identified by one of the models but not on the other. In these cases, additional units were added to maintain a consistent model across the East and West area. The exception would be local units with limited extent.

9.3 Setup of the integrated geological model

After a geological and geotechnical assessment of received data sets it has been determined that there was no significant need to keep the shallowest part of the models mapped in the SBP data in the integrated geological model. The SBP part of the models primarily includes internal boundaries to the most superficial unit mapped along discontinuous reflectors and these boundaries were generally not considered lithological or geotechnical important. In the model from the West side the base of the most superficial unit was also mapped in the SBP data, but since it didn’t match what could be interpreted from the 2D UHRS it was decided to reinterpret this boundary in the 2D UHRS data.

The 2D UHRS data sets were then imported into a new Kingdom project including the corresponding velocity models to form the data basis for the integrated geological model.

The initial seismo-stratigraphic interpretation resulted in mapping of 53 horizons. The mapped horizons correspond to the base of the seismic units of geological significance. Some horizons are continuous in extensive areas whereas others are very local seismic units.

Seismic reflectors were selected based on their geological and geotechnical significance and spatial continuity across the site.

The individual horizons were picked using a combination of the physical characteristics of the seismic reflectors, seismic facies analysis and reflector terminations.

Of key importance was to create a logical stratigraphy across the two surveyed areas. It was also valued not to end up with horizons consisting of many different geological events and geotechnical properties, but with more consistent and homogeneous units in term of formation or geotechnical parameters. This is one of the main reasons for the increase in interpreted seismic horizons compared to the original interpretations by Fugro and MMT.

All interpretations are included in a Kingdom Suite project together with processed seismic profiles in time and depth domain. Some of the 53 horizons (including the seabed horizon, H00) have been grouped together to reduce the number of layers to present in grids and section plots. Grouping of layers have only been created where it made sense geologically and did not cross any primary geotechnical boundaries. The number of horizons used for creating grids and section plots are 38 (seabed horizon + 37 base of unit horizons) and 38 integrated model units are presented.

9.4 Interpolation and adjustment of surfaces

An overview of the resulting integrated model units in the integrated geological model and its relation to the previous model is presented in Table 9-1. To the extent it was possible the unit numbers used in the previous West and East models have been kept in the updated integrated geological model to allow easier comparison to the previous works by Fugro and MMT. However, for many new integrated model units it was not possible, and numbers have been added.

Table 9-1 Summary of updates to the horizon based geological model. Previous Units refer to the two previous models – suffix W indicate model from West area by Fugro and suffix E indicate model from East area by MMT.

Primary Previous Units	Updated integrated model units	Base Horizons	Comments to updates	Chrono-stratigraphic group
U10E, U10W	U10	H10	No changes to H10 in the east, reinterpretation in the west.	Holocene
U10W, U10W, U20W	U11	H11	Sand layer found beneath the most recent Holocene sand.	Holocene
U10W, U10E, U20W	U12	H12	Internal layer in H20	Holocene
U20W	U13	H13	Internal clay layer in H20	Holocene
U20W	U14	H14	Internal sand layer in H20	Holocene
U20W	U15	H15	Internal clay layer in H20	Holocene

Primary Previous Units	Updated integrated model units	Base Horizons	Comments to updates	Chrono-stratigraphic group
U20W, U40E	U16	H16	Internal channel in H20	Late Weichselian
U20W, U20E, U40E	U17	H17	Internal clay infilled incision in H20	Late Weichselian
U20W, U24W	U18	H18	Internal transparent layer in H20	Late Weichselian
U20W	U19	H19	Internal channel in H20	Late Weichselian
U20W	U20	H20	Segments of H20 has been kept, mostly in the northeast survey area.	Late Weichselian
U20W, U20E, U25E	U21	H21	Clay infill in incision	Late Weichselian
U10E, U25E, U20E, U20W, U30W, U35W, U90W	U22	H22	Base of incision	Late Weichselian
U20W, U24W, U25E	U23	H23	Tectoglacially deformation of unit U25. Added in the east.	Weichselian
U25E, U30W	U24	H24	Sand lenses in the upper part of U25	Weichselian
U25E, U30W	U25	H25	Main infill of a large incision complex. Added in the west	Weichselian
U30E, U30W	U30	H30	Remain to some extent as it originally was interpreted with some adjustments and part taken out become part of other units.	Weichselian
U35E, U35W	U35	H35	Base of wide valley kept in I this unit with some adjustments. Other parts have been moved to other units.	Weichselian
U50E	U37	H37	U50E was split into two different units due to lithology	Saalian
U60E	U38	H38	Part of U60E that has been isolated	Saalian
	U40	H40_all	(see subunits below)	

Primary Previous Units	Updated integrated model units	Base Horizons	Comments to updates	Chrono-stratigraphic group
U25E	sU40-01	H40-01	Changed from U25E due to different facies. Infill unit for incision	Saalian
U30E, U31W, U40E,	sU40-02	H40-02	Base for U40-01 infill	Saalian
U70E, U60E, U40E, U31W	sU40-03	H40-03	Deepest U40 incision. Some parts of the U70E incisions have been included in this.	Saalian
U69W, U40E, U35E	U41	H41	Added interpretation of upper fine-material infill.	Saalian
U40E, H69W, U70W, U90W	U42	H42	A part of a U40E incision and in the West an added interpretation inside the U69W and U70W	Saalian
	U45	H45_all	(see subunits below)	
U70E, U69W, U35W	sU45-01	H45-01	Internal unit of the U45 incision complex	Saalian
U70E, U70W	sU45-02	H45-02	Bottom of the U45 complex in the south. Changed from the older incisions interpreted as U70E and U70W	Saalian
	U50	H50_all	(see subunits below)	
U70W, U69W, U40E	sU50-01	H50-01	Internal unit of U50 incision. Generally added as an internal unit for U70W and U40E	Saalian
U85E, U70W, U40E,	sU50-02	H50-02	Base unit of U50 incision. Has been changed occasionally from U70W and U70E but also extended unto uninterpreted reflectors previously included in U85E.	Saalian
U40E, H30W	U56	H56	Subdivision of U40E and H30W	Saalian
U50E, U35W	U57	H57	Subdivision of U50E into two parts, the other is U37. In the west it is U35W	Saalian
U60E	U58	H58	Subdivision of U60E	Saalian
U35W, U60E	U59	H59	Subdivision of U60E in the East, includes the southern part. Subdivision of U35W.	Saalian

Primary Previous Units	Updated integrated model units	Base Horizons	Comments to updates	Chrono-stratigraphic group
U90W, U35W	U65	H65	Subdivision of U35W in the most Western part of the unit, otherwise an additional unit inside U90W	Elsterian
	U70	H70_all	(see subunits below)	
U70W, U40E, U35W	U70-01	H70-01	Additional internal unit of U40E. Subdivision of U35W and rarely an internal unit of U70W.	Elsterian
U40E, U60E, U69W, U35W	sU70-02	H70-02	Reassignment of several units into a smaller internal H70 infill unit.	Elsterian
U69W	sU70-03	H70-03	Internal unit of U69W	Elsterian
U69W, U70W	sU70-04	H70-04	Either a subdivision or an internal unit of U69W, or an internal unit of U70W	Elsterian
U69W, U70W	sU70-05	H70-05	Internal unit of U69W or U70W	Elsterian
U69W, U70W	sU70-06	H70-06	Internal unit of U69W or U70W	Elsterian
U69W, U70W	sU70-07	H70-07	Internal unit of U69W or U70W	Elsterian
U69W, U70E, U70W	sU70-08	H70-08	Internal unit of U69W, U70W or U70E	Elsterian
U70W, U70E, U69E, U69W, U60E, U40E	sU70-09	H70-09	A reinterpretation of different incisions and internal incision units – to some extent H70-09 follows base of U69W. In the north it is primarily either a reinterpretation of U70W/E or an internal unit of them, or a reinterpretation of U40E. In the south it is primarily a subunit of U70W	Elsterian
U70E, U70W, U31W	sU70-10	H70-10	Mainly an internal unit or reinterpretation of U70E/W. In the south-west a small part of U31W has been reinterpreted	Elsterian

Primary Previous Units	Updated integrated model units	Base Horizons	Comments to updates	Chrono-stratigraphic group
U-KSA-E, U90W, U70E, U70W, U40E	sU70-11	H70-11	Reinterpretation of U70E/W and U40E. Occasionally also an internal unit	Elsterian
U70W U90W U-KSA-E	sU70-12	H70-12	A deeper unit of the U70E/W incisions occasionally a reinterpretation of them	Elsterian
U-KSA-E, U70W	U73	H73	An even deeper unit of the U70E/W incisions. Occasionally included in U70W.	Elsterian
U75W, U90W	U75	H75	Addition to the unit towards the south	Elsterian or older
U90W, U90E, U85E, U40E	U85	H85	Addition of U85E across the survey site to the west. New interpretation most places.	Elsterian or older
UKSA-E, UKSB-E, U70W	U89	H89	Subdivision and adding of new areas to U-KSA-E. Also, interpretation across the survey area to the western side.	Miocene
U90E, U90W,	U90	H90	Most of the original interpretations has been kept but some as been reassigned to other units.	Miocene
UBase	U95	H95	New interpretated unit.	Miocene
UBase	U96	-	New interpretated unit.	Miocene

9.5 Uncertainty in the grid

The grid cell size of 5x5 m is chosen to accommodate file size, accuracy of the data and lateral resolution of the seismic data. For grids to be continuous across gaps between survey lines, interpolation was needed. Normally an interpolation/extrapolation distance a little larger than the half of survey line spacing would have been chosen and a trim of the grids afterward by the overlying grids. However, since the interpreted base of unit horizons (new and received) were not terminated with crossing of the overlying horizons, unacceptable horizontal “wings” were seen everywhere in the model. Especially at edges of the abundant steep-sided buried valleys in model this did not look realistic.

Instead, math-on-two-maps tools in Kingdom have been applied to create continuous combined horizons present within the entire OWF project site for each unit. Math-on-two-maps tools have after gridding been applied to trim the grids again to make the final grids present only where the unit is present. Grids for top of units and thickness (isochore) of units are delivered.

The cell size of the grids fit well along the seismic lines where the uncertainty is low. However, in areas far from the closest seismic line (maximum distance is up to approximately 125 meters) the cell size is small and may indicate a higher certainty than the actual seismic data density provides. The uncertainty becomes larger as the distance to the seismic lines increases independent of cell size and it is therefore important to note the location of the seismic lines when working with the grids in detail.

For channel structures which are smaller than the grid distance between two lines i.e., only visible on only one line, their true nature will not be visible on the grid. The interpolation of the data results in small "islands" of the deeper incisions, and they are not connected across the lines. This is not factual compared to what is expected for a channel and is an artefact in the interpolation which should be noted. An example of this is illustrated in Figure 9-1.

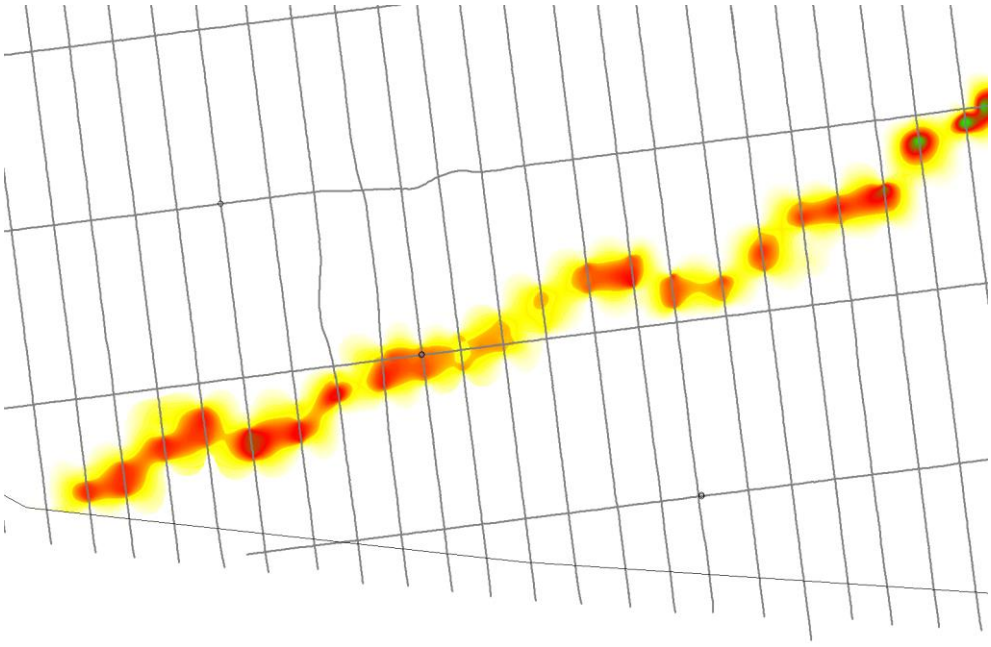

Figure 9-1: Example of gridding problems for smaller structures, where the interpolation does not connect all the deeper areas but instead creates small "islands". The example is from Base Unit 42.

9.6 Depth conversion

The 2D UHRS data was converted from two-way-time (TWT) to depth in the processing and interpretation process. RMS velocities were calculated and delivered with the segy-files.

All interpretation carried out on the data after the delivery, was performed in time domain. RMS velocities were then extracted for the given seismic layer, which was then converted to depth in the extended math calculator in the Kingdom software, using time and RMS velocity. This was done in order to ensure that interpretations were available both in time and depth domain, should any further work be needed. For the shallow interpretations on the SBP data, no new horizons were interpreted. For converting interpretations from SBP a simple two-layer model was applied (constant velocity below seabed).

Velocity models from the East area and the West area were created by two different companies and are slightly different, which gives some minor vertical offset effects on horizons when converting from two-way-time to depth. Another issue which can be difficult to assess the impact of, is that the velocity model is based on the initial interpretations, which has now been modified. E.g., newly interpreted deep buried valley may have a slightly too high velocity.

9.7 Potential geohazards; shallow gas, organic-rich deposits, faults, and sub-surface boulders

From the Geotechnical Factual Report delivered by Fugro (Ref. /1/ and Ref. /4/), the geotechnical log indicates that organic-rich deposits are found in some units. There are also a few instances of peat layers located in some units, which it is important to highlight due to the potential geohazard it presents. It is noted that these instances are found to not generally represent the characteristics of the soil units, but merely local occurrences.

There are a few instances of peat deposits found in the borehole investigation including younger deposits and deposits in Unit 75, Unit 85, Unit 90, and Unit 95. The younger deposits are more scattered and is found in the bottom of Unit 13, Unit 21, and Unit 22. The occurrences of peat in these units are isolated and not found in other boreholes. Peat in Unit 13 is found in BH-1035, the deposits in Unit 21 is found in BH-1006, and the peat in Unit 22 is found in BH-1011. The peat found in Unit 75 is identified in BH-1005 and is marked by a strong seismic reflector, as is seen in Figure 9-2 where the extent of the bright seismic reflector is also displayed. There is only one borehole penetrating the shown extent of Unit 75 and it can therefore not be verified if the peat layer is present in the entire area.

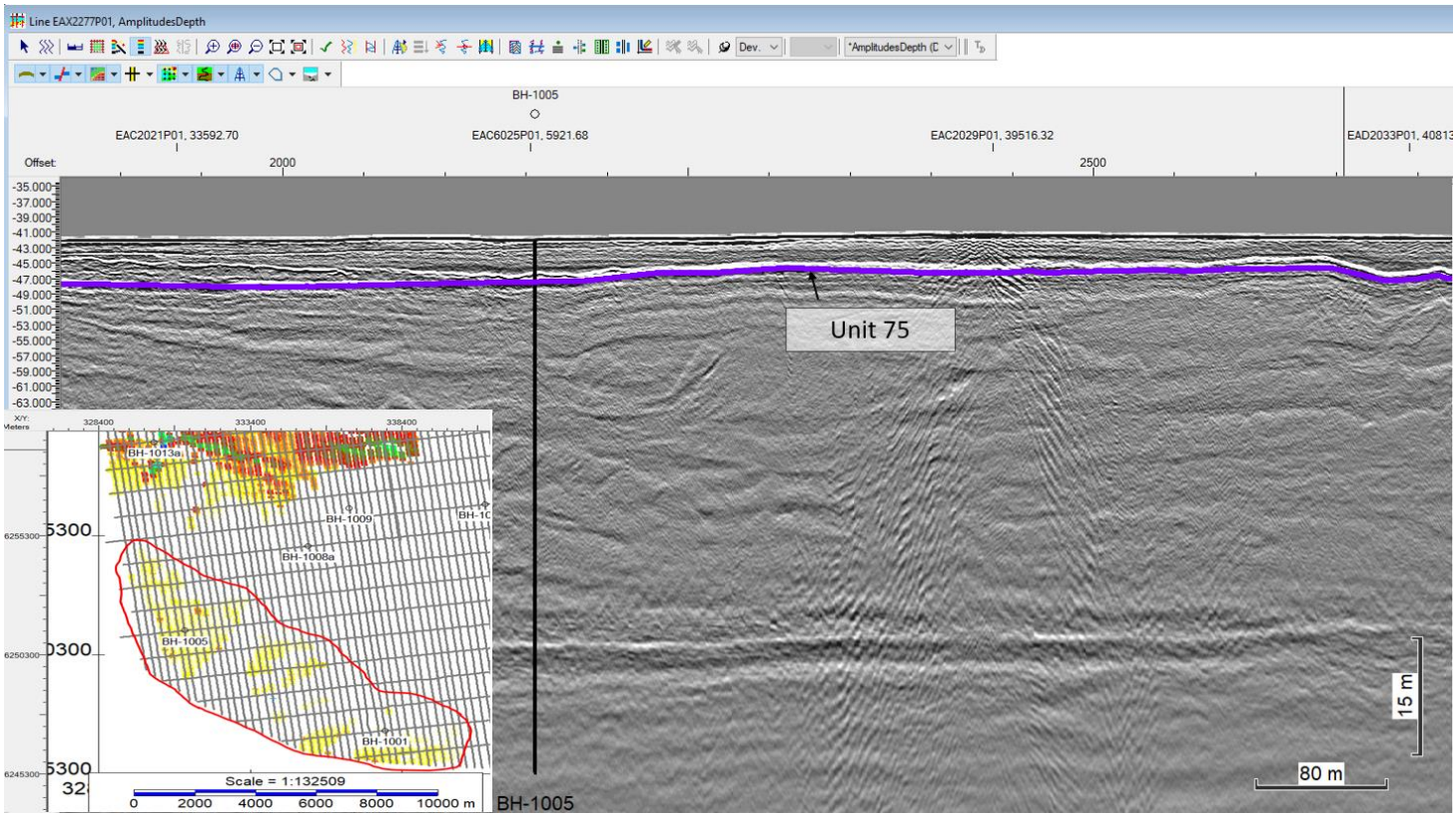

Figure 9-2: Line: EAX2277P01. Example of the bright seismic reflector indicating a possible peat layer as identified in BH-1005.

A very strong reflector is identified as a peat layer at the base of Unit 85 in several boreholes. The peat base is found in BH-1002, BH-1005, BH-1015, BH-1007, and BH-1019. An example of the seismic reflector at the base can be found in Figure 9-3. Peat was also found internally in Unit 85 at BH-1026.

A peat observation is made in Unit 90 in BH-1016. Ref. /4/ describes findings of wood fragments within the different peat layers found in the area.
The last peat observation is made in Unit 95 in BH1016 in 67 m depth.

In Unit 38 a high amount of seismic bright spots/soft kicks has been observed which indicate a change from harder to softer material. These spots could indicate organic material or old bottoms of river channels where softer sediments such as clay has been deposited. An example of the bright spots can be seen in Figure 9-4 where they are marked by black arrows. In the same figure, examples of hard kicks which could be smaller boulders are seen marked by orange arrows.

Since most of the layers in the model are interpreted to be related to glacial environments (Units 16 to 85) there is a potential for encountering boulders in large parts the stratigraphy. Generally, hard kick bright spots which potentially indicate boulders are not abundant anywhere in the model but have been observed in different units. Potential boulders are not considered to constitute a significant hazard within the OWF project site. However, a detailed study of boulders and boulder picking is outside the scope of this report.

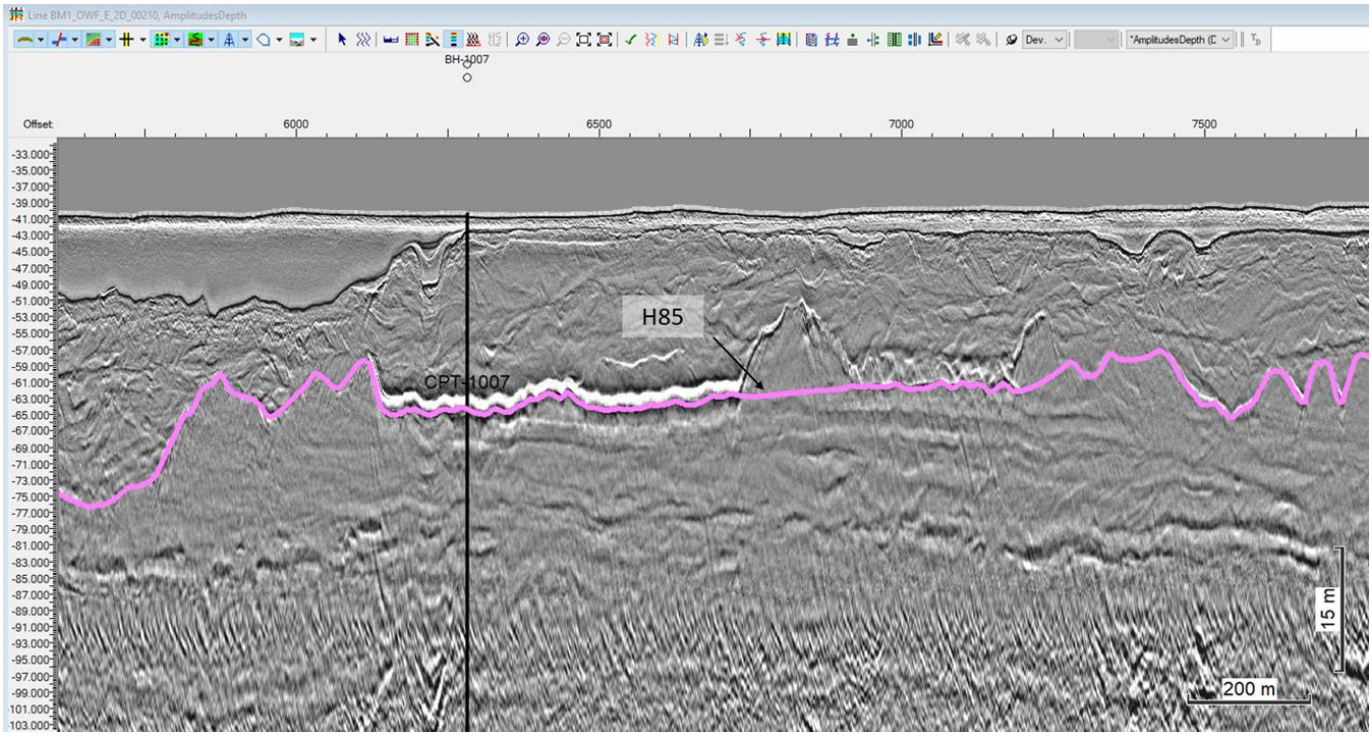

Figure 9-3: Line BM1_OWF_E_2D_00210. Bright seismic reflector identified as peat in several boreholes at the base of U85.

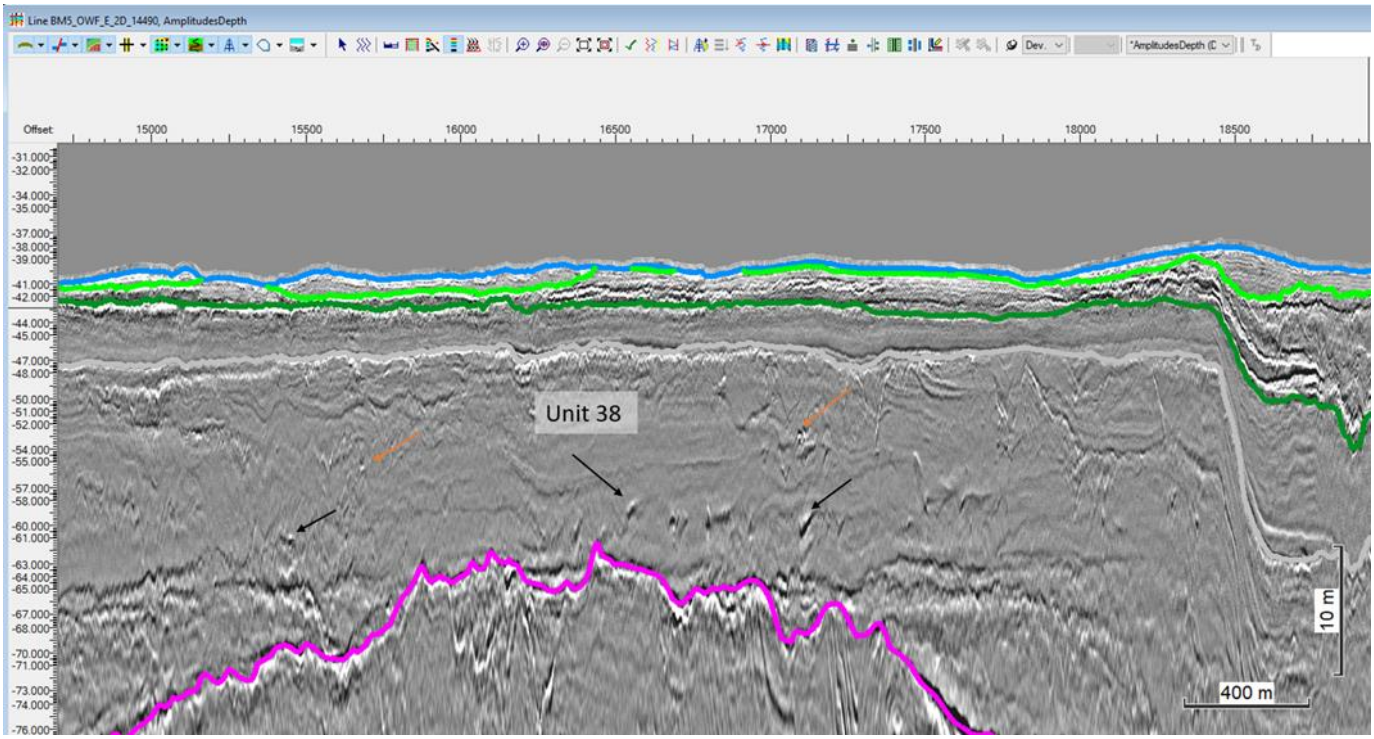

Figure 9-4: Line BM5_OWF_E_2D_14490. Examples of seismic soft kicks (soft sediments) (black arrow) and hard kicks (boulders) (orange arrow) in Unit 38.

Gas in the sediment and fluids moving upwards can be seen as disturbance and blanking of the seismic signal. A few instances of disturbances have been recorded but gas has not been deemed a common occurrence within the OWF project site. Throughout the site areas affected by gas disturbance only constitute local areas of very limited extent mostly related to infill of younger channels (see Figure 9-5). Examples of fluid migrations and gas disturbance can be seen in Figure 9-6 and Figure 9-7.

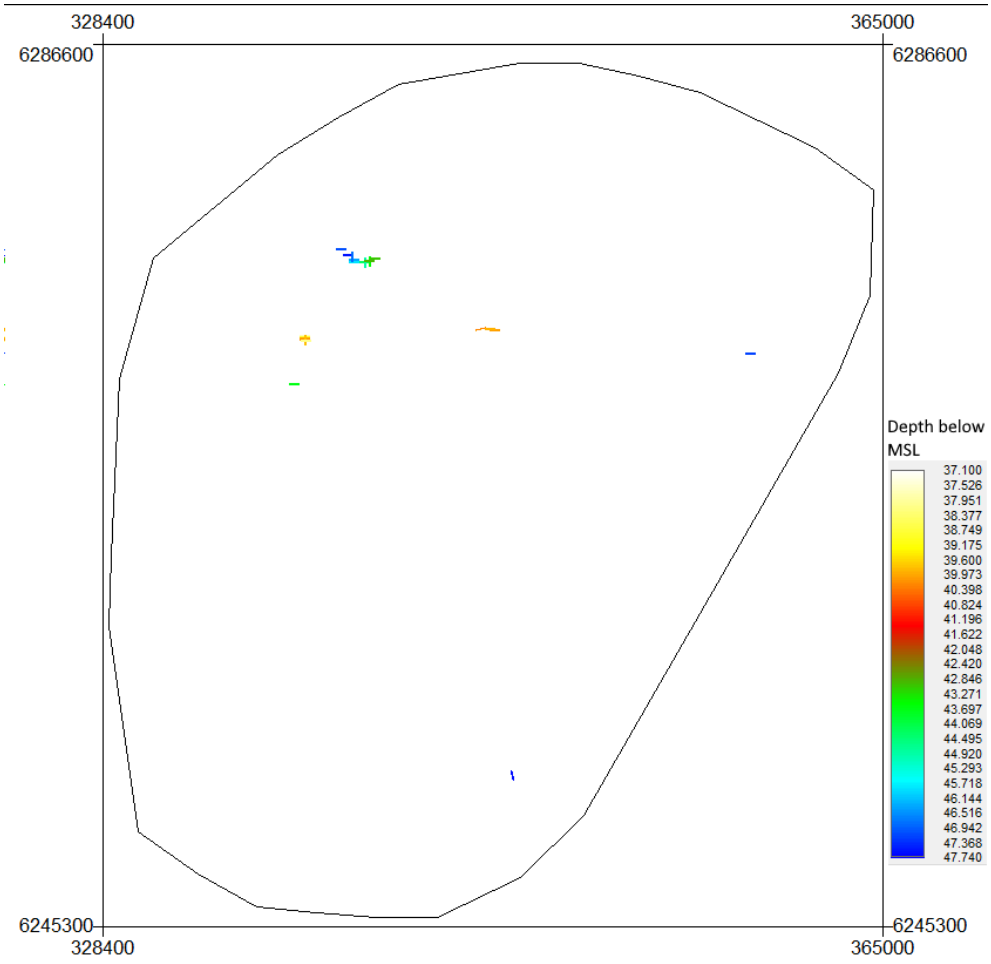

Figure 9-5: Overview of locations where local gas disturbance have been identified.

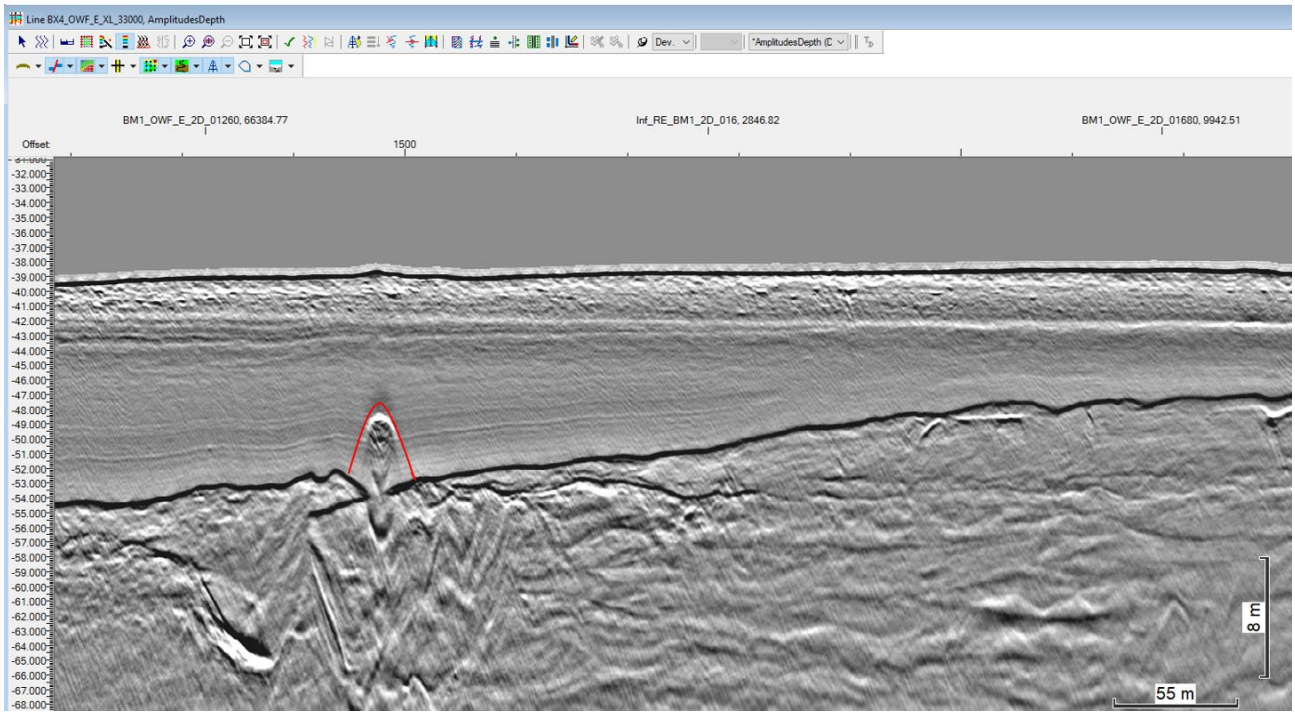

Figure 9-6: Line BX4_OWF_E_XL_33000. Possible upward migrating fluids in the sediment.

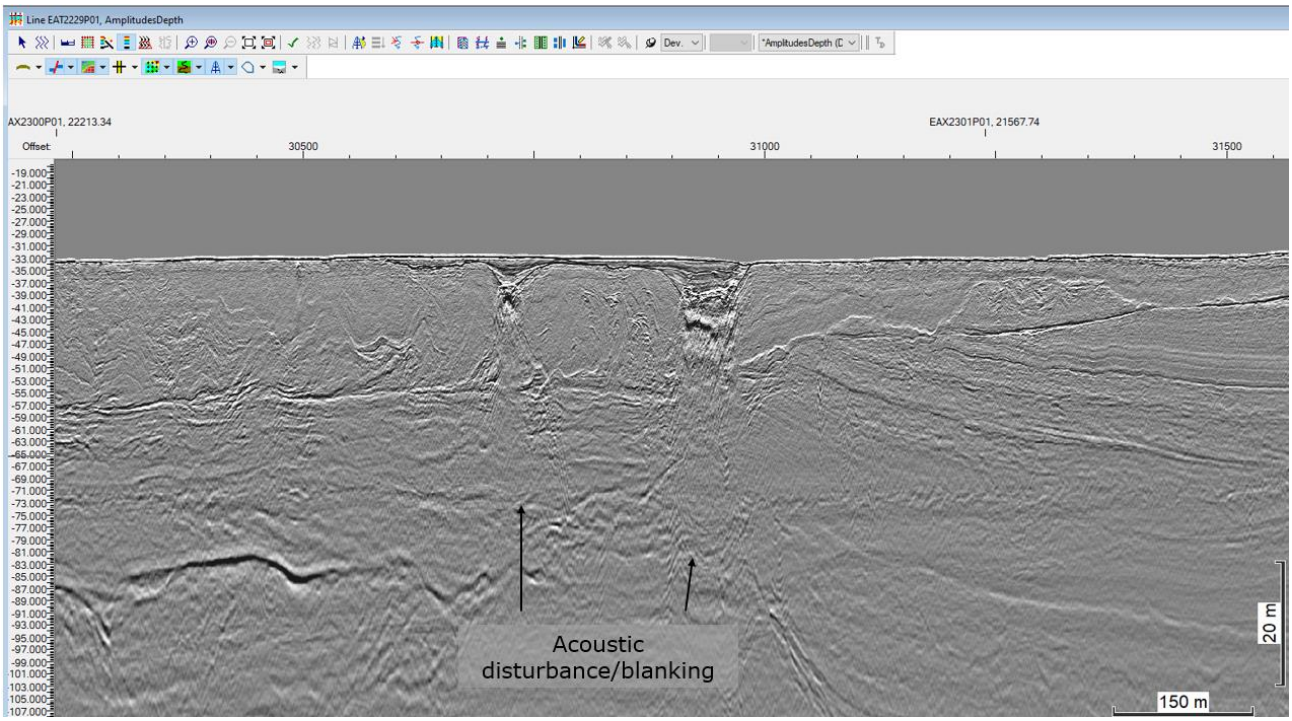

Figure 9-7: Line EAT2229P01. Examples of acoustic disturbance/blanking the seismic signal caused by gas content.

Active faults have not been observed within the OWF project site. Glacial thrust faults have been observed in many parts of glacial and pre-glacial stratigraphy especially within Unit 89 which is defined by these thrust faults. The thrust faults are inactive and have not been active in post glacial time.

Faults have also been observed in areas affected by salt tectonics (e.g. within Unit 20, Unit 37, Unit 38 and Unit 89). The effect of the salt tectonics appears to cease in the Holocene, but it is difficult to determine for certain. However, the impact of the slow development of salt tectonics is expected to be small in relation to the OWF project lifetime.

The different potential geohazards have been evaluated at high level for the OWF project site and the primary geohazard is considered to be related to the presence of peat. The risk of encountering boulders is considered low, but not unlikely.

9.8 Model stratigraphy

The stratigraphy of the North Sea Energy Island OWF site has been divided into 38 integrated model units with a further subdivision of Unit 40, 45, 50 and 70. That gives the model a total of 38 units and 19 subunits. A summarized description of the different units can be found in Table 9-2 whereas a detailed version can be found the table in Appendix I. Cross sections through the model are presented in enclosures 5.01 to 5.16.

The stratigraphy interpreted in the data collected for the North Sea Energy Island OWF has been guided by scientific papers and reports, amongst others from the desktop studies conducted by Rambøll and GEUS (Ref. /23/, Ref. /30/). The units have been appointed an age based on the seismic characteristics, the lithology and the general behaviour of the unit.

The 38 units have been divided into seven chronostratigraphic groups named as the following: Holocene, Late Weichselian, Weichselian, Saalian, Elsterian, Elsterian or older, and Miocene. The ages indicated for the five oldest groups are based on interpretations. E.g., the units assigned to Elsterian age could in fact represent the same glaciation as the above lying units but related to an earlier glacial advance during the same glaciation. Assignment to the different glaciations should therefore be regarded with some uncertainty.

None of the units found in the OWF project site have been interpreted as belonging to the interglacial periods Eem and Holstein. However, there is a possibility that they are present in the OWF area, but do not stand out clear enough to be separated from the glacial units.

Where the Weichselian ice sheet has been overlying, the substratum has in many areas been tectonically deformed by glacial advances. This causes a disorder in the chronostratigraphy where older units are overlaying younger units. An example of this have been illustrated in Figure 9-8 where the shear zones and the deformation of the individual units can be seen. The faults seen are reverse faults and indicate the push of the moving ice sheet. Shear zones are marked where there is a possibility that older sediments are smeared upwards in a mix with other units.

In the following the term unit refers to integrated model unit.

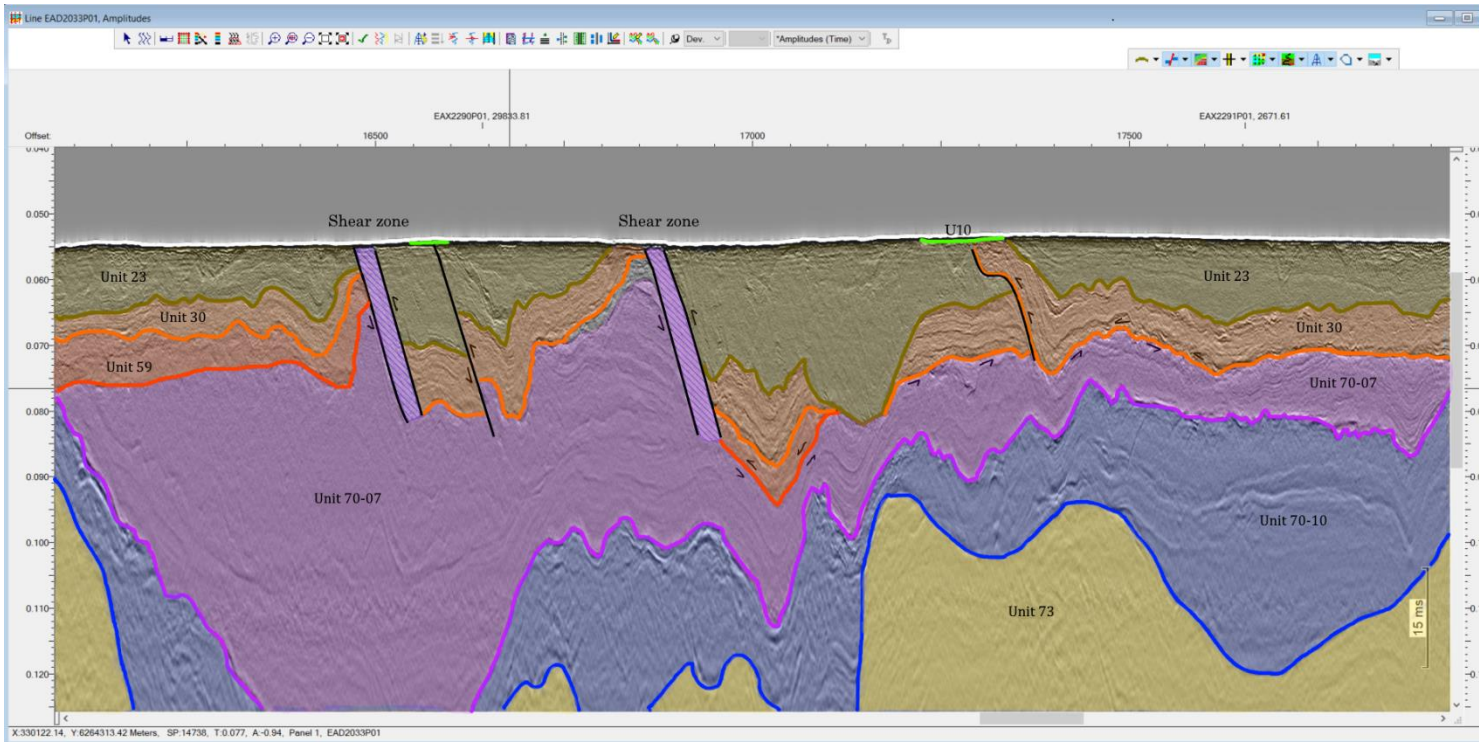

Figure 9-8: Line EAD2033P01. Glaciotectonic deformation of Pleistocene units resulting in altering of the stratigraphic sequence.

Table 9-2 Summary of units in the integrated geological model.

Unit	Base Horizon	Seismic Character	Soil Type according to the borehole descriptions. (Ordered by frequency) Ref. /1/	Chronostratigraphic group	Depositional Environment
Unit 10	H10	Acoustically semi-transparent in the thickest deposits of the sand dunes. In the shallower deposits semi-parallel to parallel reflector of medium amplitude.	SAND, Silty SAND, Gravelly SAND, Sandy CLAY, Silty Gravelly SAND	Holocene	Marine
Unit 11	H11	Transparent to chaotic reflectors. Mostly low amplitude but includes positive high amplitude reflectors.	SAND		Coastal marine
Unit 12	H12	Facies is partly transparent and with parallel reflectors. Some areas are semi-chaotic with high amplitude reflectors.	SAND, Silty SAND, SILT, Clayey SILT, Sandy CLAY		Lagoonal marine
Unit 13	H13	Low amplitude parallel reflectors. Strong basal reflector.	Sandy CLAY, CLAY		Transition from fluvial to lagoonal.

Unit	Base Horizon	Seismic Character	Soil Type according to the borehole descriptions. (Ordered by frequency) Ref. /1/	Chronostratigraphic group	Depositional Environment
Unit 14	H14	In the western area transparent to slightly laminated facies. Low amplitude reflectors. In the more eastern area slightly undulating reflectors with low to high amplitude reflectors.	SAND, CLAY		Fluvial
Unit 15	H15	Semi chaotic to parallel reflectors with low to high amplitude. Reflectors are slightly undulating.	CLAY		Lacustrine depression infill
Unit 16	H16	Parallel to undulating to chaotic reflectors. Low to medium amplitude reflectors. Some infill shows deformation structures and slight transparency. Most chaotic towards the bottom.	SAND, Silty SAND, Clayey SILT, Silty CLAY (CPT Only)	Late Weichselian	Mainly Subglacial fluvial /proglacial lacustrine
Unit 17	H17	Semi parallel medium to low amplitude reflectors. Some deformed blank and undulating areas.	CLAY, Silty SAND, Gravelly SAND		Periglacial or Proglacial lacustrine channel infill.
Unit 18	H18	Mostly transparent facies. Occasionally high amplitude chaotic reflectors and semi parallel facies.	Silty CLAY, Sandy CLAY, Silty gravelly SAND,		Proglacial lacustrine
Unit 19	H19	Chaotic low to medium amplitude reflectors. Some instances of deformed facies and some parallel to undulated facies.	SAND, Sandy GRAVEL, Silty gravelly SAND		Subglacial and proglacial fluvial
Unit 20	H20	In the East transparent facies with occasional medium amplitude reflectors and some deformed areas. In the west parallel reflectors with strong amplitude and some low amplitude semi-transparent reflectors.	Sandy Gravelly CLAY, Silty SAND, Silty CLAY, Gravelly SAND, CLAY, SAND		Subglacial to proglacial fluvial and lacustrine
Unit 21	H21	Mainly transparent facies. Instances of parallel medium to high amplitude reflectors.	CLAY, Sandy CLAY, Silty CLAY, Clayey PEAT		Periglacial fluvial to lacustrine channel infill
Unit 22	H22	Semi-chaotic medium amplitude reflectors. Some areas with low amplitude to transparent reflectors.	SAND, Silty SAND, Silty gravelly SAND		Glaciofluvial in extramarginal channel
Unit 23	H23	Deformed reflectors heavily undulated.	Silty CLAY, CLAY, Silty SAND, Clayey SILT	Weichselian	Primarily periglacial lacustrine and fluvial

Unit	Base Hori-zon	Seismic Character	Soil Type according to the borehole descriptions. (Ordered by frequency) Ref. /1/	Chronostrati-graphic group	Depositional Environment
Unit 24	H24	Semi-transparent facies. Some parallel reflectors.	SAND, Silty SAND, Clayey SILT, SILT		Periglacial fluvial
Unit 25	H25	Parallel reflectors of low amplitude.	CLAY, Silty CLAY, Silty SAND, SILT		Periglacial lacustrine
Unit 30	H30	Parallel medium to low amplitude reflectors.	SAND, Silty SAND		Periglacial fluvial
Unit 35	H35	Semi-chaotic to semi-parallel reflectors. Many internal structures. The top of the unit is occasionally semi-transparent.	Gravelly SAND, SAND, Silty SAND		Peroglacial fluvial
Unit 37	H37	Chaotic to undulating reflectors with low to high amplitude, occasionally transparent.	Sandy CLAY, CLAY	Saalian	Periglacial lacustrine
Unit 38	H38	Both transparent facies with point diffraction hyperbolas and areas with semi-undulating reflectors of medium amplitude.	Silty SAND, Silty gravelly SAND, SAND		Periglacial fluvial
Unit 40	H40 _all	Divided into three subunits. For details about their seismic character see Appendix I.	Silty CLAY, Silty SAND, SAND, Sandy CLAY, SILT, Sandy SILT, Sandy GRAVEL		Sub-proglacial fluvial and proglacial to periglacial lacustrine channel infill
Unit 41	H41	Semi-parallel undulating reflectors of low to medium amplitude. More chaotic reflectors towards the bottom. Occasional high amplitude areas.	CLAY		Periglacial lacustrine
Unit 42	H42	Parallel reflections occasionally in the top, chaotic to undulating in the rest of the unit.	Silty SAND, Gravelly SAND, Sandy SILT, Silty CLAY		Subglacial fluvial and proglacial to periglacial fluvial and lacustrine

Unit	Base Horizon	Seismic Character	Soil Type according to the borehole descriptions. (Ordered by frequency) Ref. /1/	Chronostratigraphic group	Depositional Environment
Unit 45	H45_all	Divided into two subunits. For details about their seismic character see Appendix I.	Silty SAND, Sandy SILT, SAND, Gravelly SAND, GRAVEL (Based only on CPT)		Subglacial and proglacial glaciofluvial and proglacial to periglacial lacustrine
Unit 50	H50_all	Divided into two subunits. For details about their seismic character see Appendix I.	SAND, Silty SAND, Clayey SILT, Silty CLAY (Based only on CPT)		Subglacial fluvial and pro- or periglacial lacustrine infill of channel.
Unit 56	H56	Transparent facies and semi-chaotic low to medium amplitude reflectors	Silty SAND, CLAY,		Periglacial lacustrine to fluvial
Unit 57	H57	Mostly transparent facies with some areas of semi parallel reflectors of low amplitude.	Silty SAND, Sandy SILT, Silty gravelly SAND		periglacial fluvial or fluvial
Unit 58	H58	Parallel to semi parallel reflectors in the top. Overlapping structures of low to medium amplitude reflectors towards the bottom.	Silty gravelly SAND, Silty SAND		Periglacial fluvial
Unit 59	H59	Semi chaotic reflectors of low to medium amplitude	SAND, Silty SAND,		Periglacial fluvial
Unit 65	H65	Mostly transparent facies occasionally with some deformed structures.	SAND, Silty SAND, Gravelly SAND, Silty SAND, Sandy SILT (Based only on CPT)	Elsterian	Subglacial fluvial
Unit 70	H70_all	Divided into twelve subunits. For details about their seismic character see Appendix I.	Silty SAND, Silty CLAY, Sandy gravelly CLAY, CLAY, SILT, gravelly CLAY, SAND, GRAVEL, Silty gravelly SAND, GRAVEL, Silty sandy GRAVEL		Proglacial lacustrine to fluvial channel infill, and subglacial fluvial and till
Unit 73	H73	Chaotic reflectors with signs of deformation. The facies is more transparent with deformation structures at the top of the unit.	GRAVEL, Silty SAND, Silty CLAY, Silty gravelly SAND, SILT, Gravelly SAND, Sandy GRAVEL		Subglacial fluvial and till mixed with Miocene deposits

Unit	Base Horizon	Seismic Character	Soil Type according to the borehole descriptions. (Ordered by frequency) Ref. /1/	Chronostratigraphic group	Depositional Environment
Unit 75	H75	Transparent to chaotic reflectors with some higher amplitude structures.	Silty gravelly SAND, SAND, Sandy GRAVEL	Elsterian and older	Periglacial fluvial and lacustrine
Unit 85	H85	Chaotic reflectors with low to high amplitude. Often has a bright negative amplitude reflector at the bottom.	SAND, Silty SAND, Gravelly SAND, Clayey PEAT,		Glaciofluvial and pre-glacial fluvial
Unit 89	H89	Chaotic low to medium amplitude reflectors. More transparent with deformed structures towards the top.	Silty CLAY, Sandy CLAY, Silty SAND, CLAY	Miocene	Mostly marine
Unit 90	H90	Semi-transparent to chaotic low amplitude reflectors. Large scale gently sloping reflectors.	Silty SAND, Clayey SAND, SAND, Silty Gravelly SAND, Gravelly SAND, Silty SAND,		Fluvial to Deltaic
Unit 95	H95	Different facies including chaotic with low amplitude reflectors and sub-parallel with low amplitude reflectors	Silty SAND, SAND, Sandy CLAY, CLAY, Sandy SILT, Clayey SILT, Silty CLAY		Marine
Unit 96	(not map-ped)	Sub-parallel to parallel low to medium amplitude reflectors	Silty CLAY, CLAY, Silty SAND, Sandy CLAY, Sandy SILT		Marine

9.8.1 Holocene (Unit 10 to Unit 15)

The units assigned to the chronostratigraphic group Holocene represent an environmental transition from terrestrial to marine. Most of the units (Unit 11 to Unit 15) are only present in the northwestern part of the OWF project site and represent different steps from lacustrine and fluvial environments over lagoonal and coastal to offshore marine conditions in Unit 10, which covers most of the site.

Unit 10

Unit 10 (see Figure 9-9) is the shallowest unit in the model and represents the Holocene to recent marine sediment. Consists mainly of sand. Present ongoing morphological seabed changes is expected only to have effect on this layer. Unit 10 is many places less than a meter thick and the largest thicknesses are where it constitutes sandbanks. The largest thickness of the unit is seen around the proposed Energy Island location where the entire layer constitutes a large cross-bedded sandbank. Unit 10 has an erosional contact to all the below lying units.

Internal erosional contacts are also present – e.g., where interpreted migrating sand banks override remains of eroded older sandbanks.

Enclosure 3.01 shows the depth below seabed of the top of Unit 10 and enclosure 4.01 shows the thickness (isochore) of Unit 10.

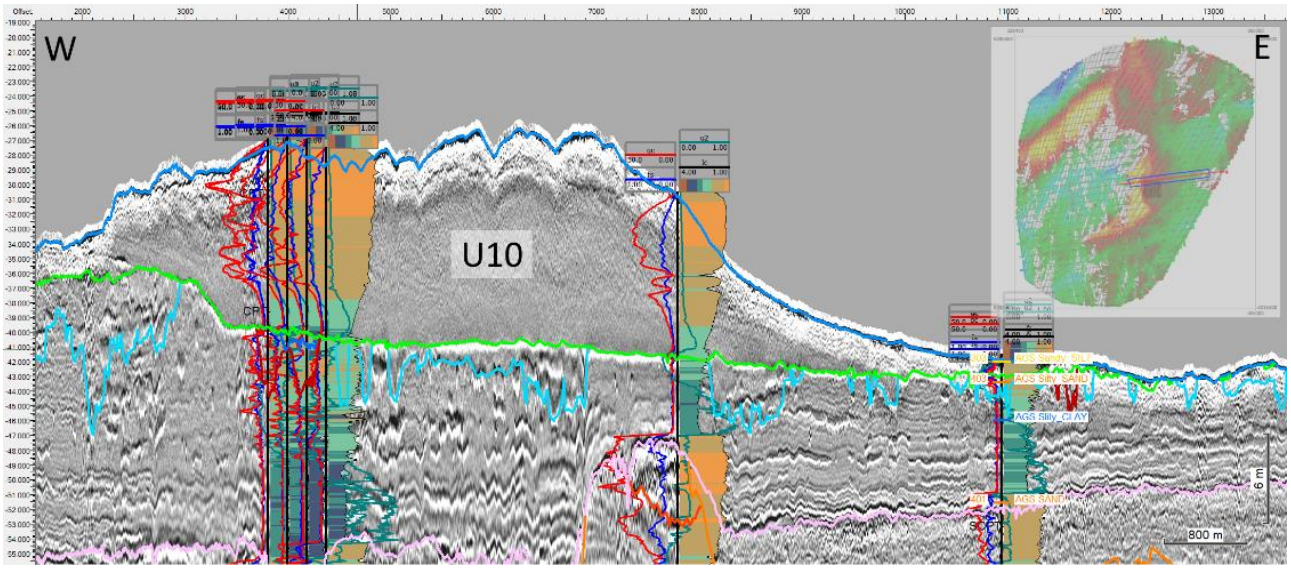

Figure 9-9: Unit 10 (U10) as interpreted in section BX3_OWF_E_XL_21000 (MMT) with geotechnical logs from LOC-0020, LOC-0022, LOC-0023, LOC-1105, and LOC-1022.

Unit 11

Unit 11 (see Figure 9-10) is only present in the north-western part of the site and consists of Holocene coastal marine sand. The sand is expected to have been deposited in a coastal bar complex. Underlying sand filled channel deposits has been included into the unit mainly to reduce the number of units.

Enclosure 3.02 shows the depth below seabed of the top of Unit 11 and enclosure 4.02 shows the thickness (isochore) of Unit 11.

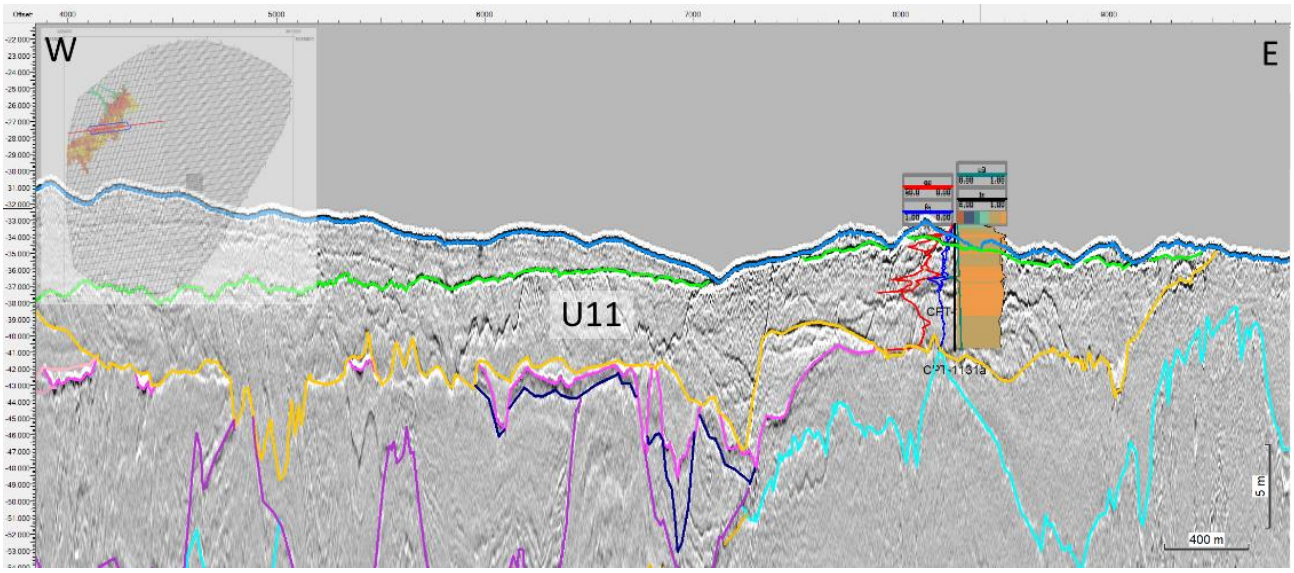

Figure 9-10: Unit 11 (U11) as interpreted in section EAX2297P01 (Fugro) with geotechnical logs from LOC-1131.

Unit 12

Unit 12 (see Figure 9-11) is only present in the north-western part of the site and consists of Holocene lagoonal marine sand. There is a gradual change from the base of the layer where it constitutes the sandy upper part of channel fill. In the upper and main part of the layer it consists of laminated deposits. Numerous layers of soft kick bright spots indicate presence of organic matter in large parts of the unit (confirmed by borehole samples from LOC-1034).

Enclosure 3.03 shows the depth below seabed of the top of Unit 12 and enclosure 4.03 shows the thickness (isochore) of Unit 12.

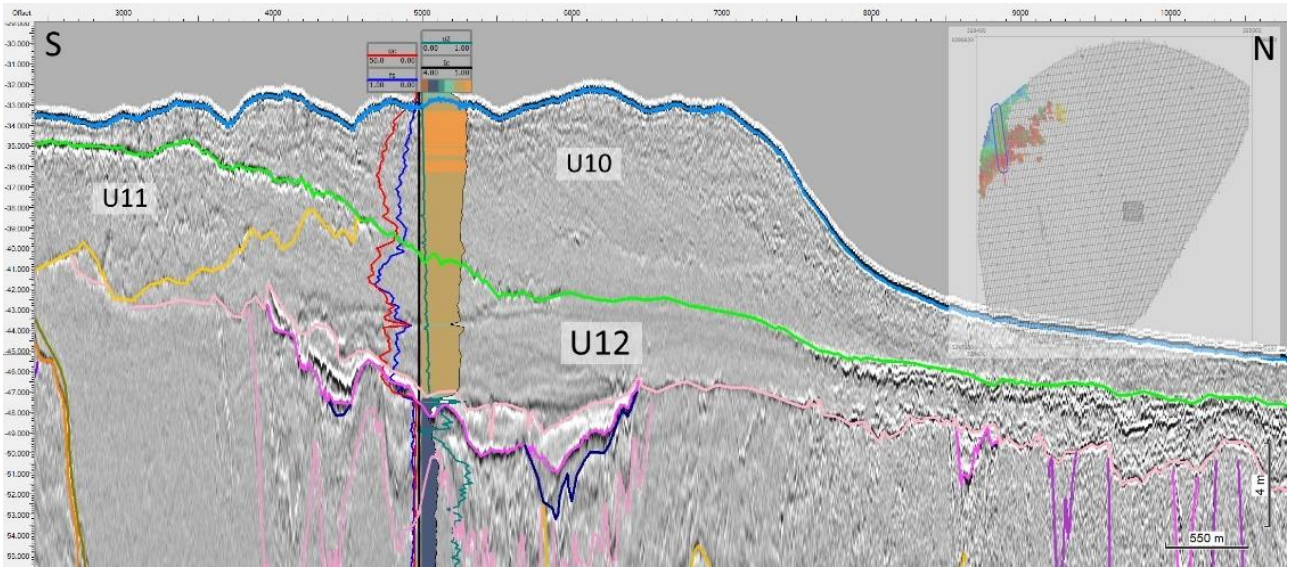

Figure 9-11: Unit 12 (U12) as interpreted in section EAF6073P02 (Fugro) with geotechnical logs from LOC-1127.

Unit 13

Unit 13 (see Figure 9-12) is only present in the north-western part of the site and consists of Holocene silt/clay deposits deposited in a transitional environment from fluvial to lagoonal. The fluvial channels appear to have been submerged and filled with silty clay in a low energy environment before it was superseded by the overlying Unit 12.

Enclosure 3.04 shows the depth below seabed of the top of Unit 13 and enclosure 4.04 shows the thickness (isochore) of Unit 13.

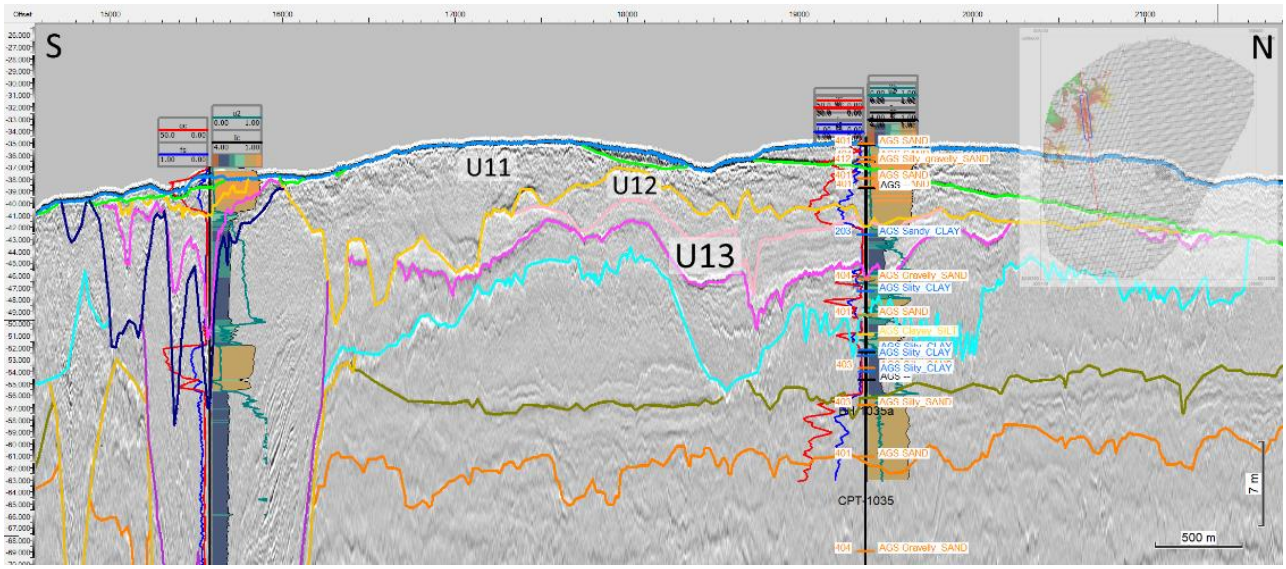

Figure 9-12: Unit 13 (U13) as interpreted in section EAM6145P02 (Fugro) with geotechnical logs from LOC-1122 and LOC-1035.

Unit 14

Unit 14 (see Figure 9-13) is only present in the north-western part of the site and consists of Holocene fluvial sand mostly restricted to narrow channels. The channels are likely to have carried meltwater from stagnant ice.

Enclosure 3.05 shows the depth below seabed of the top of Unit 14 and enclosure 4.05 shows the thickness (isochore) of Unit 14.

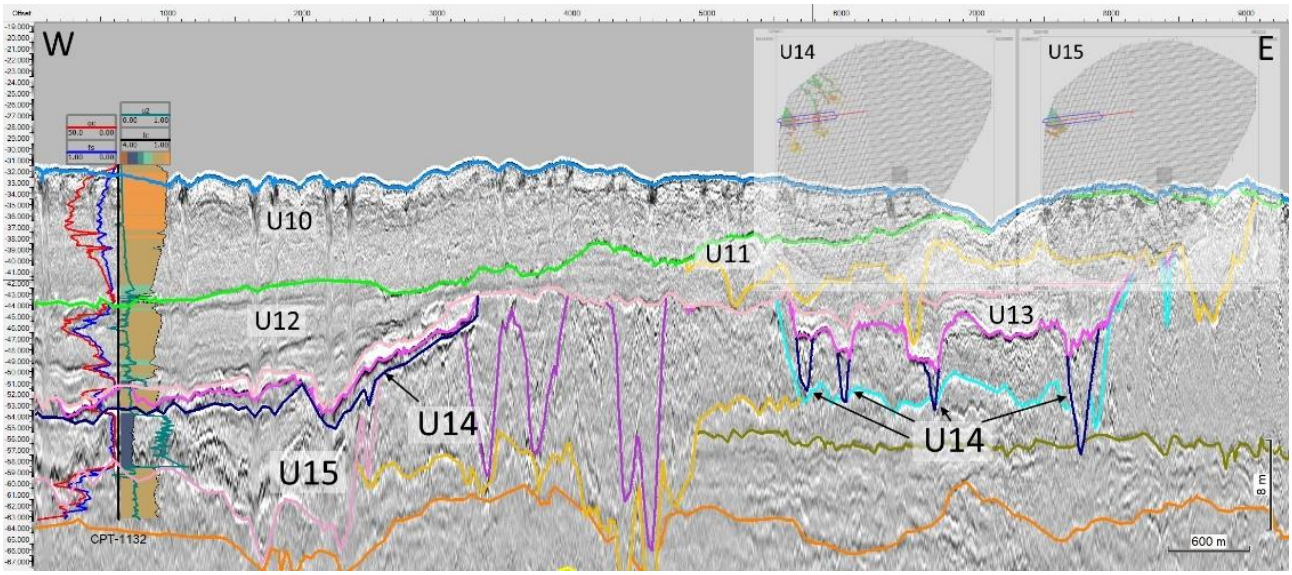

Figure 9-13: Unit 14 (U14) and Unit 15 (U15) as interpreted in section EAX2298P01 (Fugro) with geotechnical logs from LOC-1132.

Unit 15

Unit 15 (see Figure 9-13) is only present in the north-western part of the site and consist of Holocene clay. Unit 15 is interpreted to consist of lacustrine deposits that fills a depression formed by a late glacial readvance.

Enclosure 3.06 shows the depth below seabed of the top of Unit 15 and enclosure 4.06 shows the thickness (isochore) of Unit 15.

9.8.2 Late Weichselian (Unit 16 to Unit 22)

The units assigned to the chronostratigraphic group Late Weichselian group are related to last glacial maximum, which occurred in last phase of the Weichselian around 20,000 years ago. Some of the units represent proglacial fluvial and lacustrine deposits which fill in depressions formed by subglacial meltwater erosion (Unit 16 to Unit 20). Many of these depressions form typical tunnel valleys. Some of the infilled layers show impact of heavy deformation by glacial readvances. Also, the clayey layers from the underlying group of Weichselian units show clear evidence of glaciotectonic deformation. The extent of the Last Glacial Maximum is partly estimated based on clear evidence of deformation, which the ice sheet has exerted onto the top of the underlying group. The southeastern extent of the subglacially formed Late Weichselian tunnel valleys (Unit 16, Unit 19, and partly Unit 20) indicate a similar ice sheet extent.

The Late Weichselian group also include layers which have been interpreted to fill in extramarginal meltwater channels (Unit 21 and Unit 22). These channels have led meltwater away from the ice margin. The extent of these units also guides the interpretation of the location of the Last Glacial Maximum.

Unit 16

Unit 16 (see Figure 9-14) is only present in the north-western part of the site and consists of Late Weichselian channel fill sand. The channels have been carved by subglacial meltwater erosion. The primary part of the fill has been deposited in a proglacial lacustrine environment. Melting of stagnant glacier ice placed at the base of the channels is likely to have affected the deposits during and after deposition. Some of the channels in Unit 16 are to some degree influenced by irregular subsidence structures, which may be caused by melting of stagnant ice. The Stagnant ice can both be blocks of glacier ice or meltwater frozen in subglacial meltwater tunnels.

Enclosure 3.07 shows the depth below seabed of the top of Unit 16 and enclosure 4.07 shows the thickness (isochore) of Unit 16.

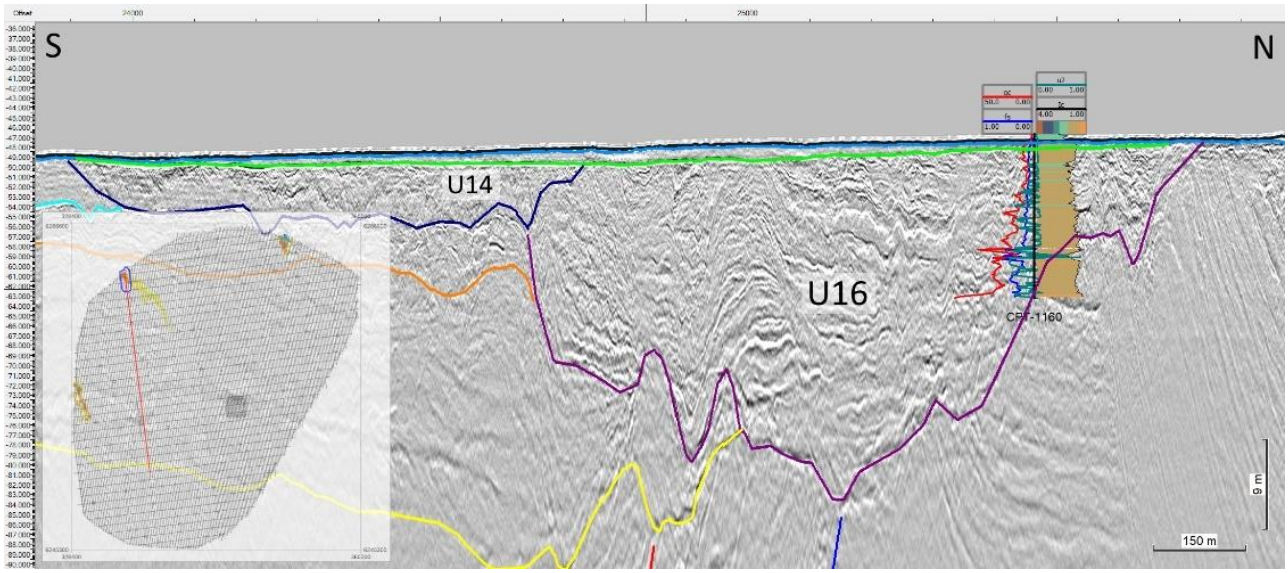

Figure 9-14: Unit 16 (U16) as interpreted in section EAM6145P02 (Fugro) with geotechnical logs from LOC-1160.

Unit 17

Unit 17 (see Figure 9-15) is only present in the north-western part of the site and consists of Late Weichselian proglacial or periglacial glaciolacustrine channel fill silt/clay. It follows the contours of the underlying channel of Unit 19. Late melting of stagnant ice placed in or below Unit 19 is likely to have formed part of the depression that Unit 17 fills up. The irregular geometry of Unit 17 may partly be a result of the displacement caused by melting of the of stagnant ice below Unit 17. Irregular subsidence structures within Unit 17 indicate that the melting process has continued during the deposition of the unit.

Enclosure 3.08 shows the depth below seabed of the top of Unit 17 and enclosure 4.08 shows the thickness (isochore) of Unit 17.

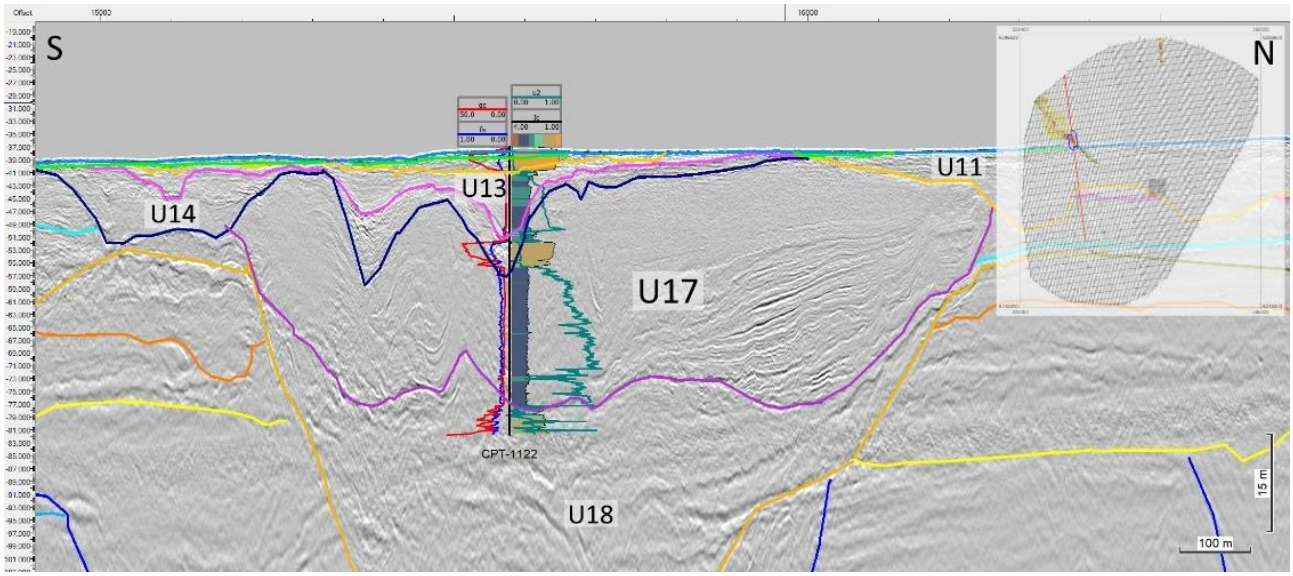

Figure 9-15: Unit 17 (U17) as interpreted in section EAM6145P02 (Fugro) with geotechnical logs from LOC-1122.

Unit 18

Unit 18 (see Figure 9-16) is only present in the north-western part of the site and consists of Late Weichselian glaciolacustrine silt/clay. Unit 18 is interpreted to constitute mainly redeposited sediments of Unit 23. Unit 18 itself has also been heavily affected by glacial deformation from a subsequent glacial advance.

Enclosure 3.09 shows the depth below seabed of the top of Unit 18 and enclosure 4.09 shows the thickness (isochore) of Unit 18.

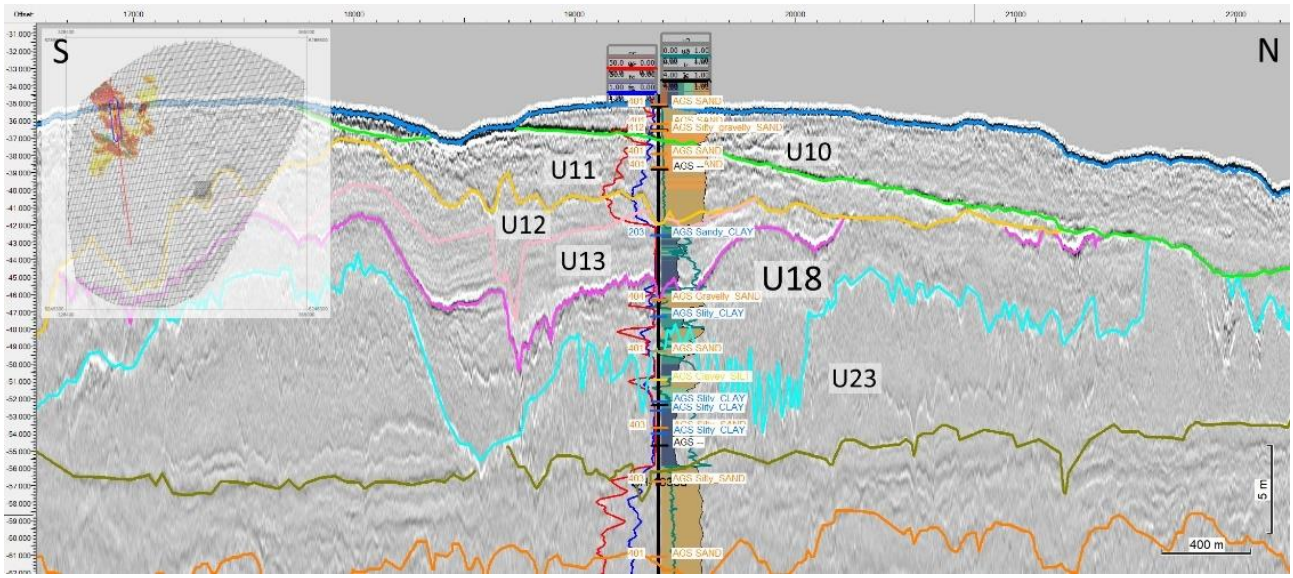

Figure 9-16: Unit 18 (U18) as interpreted in section EAM6145P02 (Fugro) with geotechnical logs from LOC-1035.

Unit 19

Unit 19 (see Figure 9-17) is only present in the north-western part of the site and consists of Late Weichselian channel fill sand. The channel depression that Unit 19 partly fills up has in some areas a steep and very pronounced V-shape. In Figure 9-10 the depth of the depression is around 110 m and the width is around 400 m when measuring across the valley in map view at the same location. The channels have been carved by subglacial meltwater erosion during the time when the Weichselian ice sheet reached its maximum extent in the area. The fill deposits in the channel probably both consist of subglacial and proglacial glaciofluvial deposits. Deep and irregular subsidence structures within and above Unit 19 is interpreted to indicate that melting of stagnant ice has taken place.

Enclosure 3.10 shows the depth below seabed of the top of Unit 19 and enclosure 4.10 shows the thickness (isochore) of Unit 19.

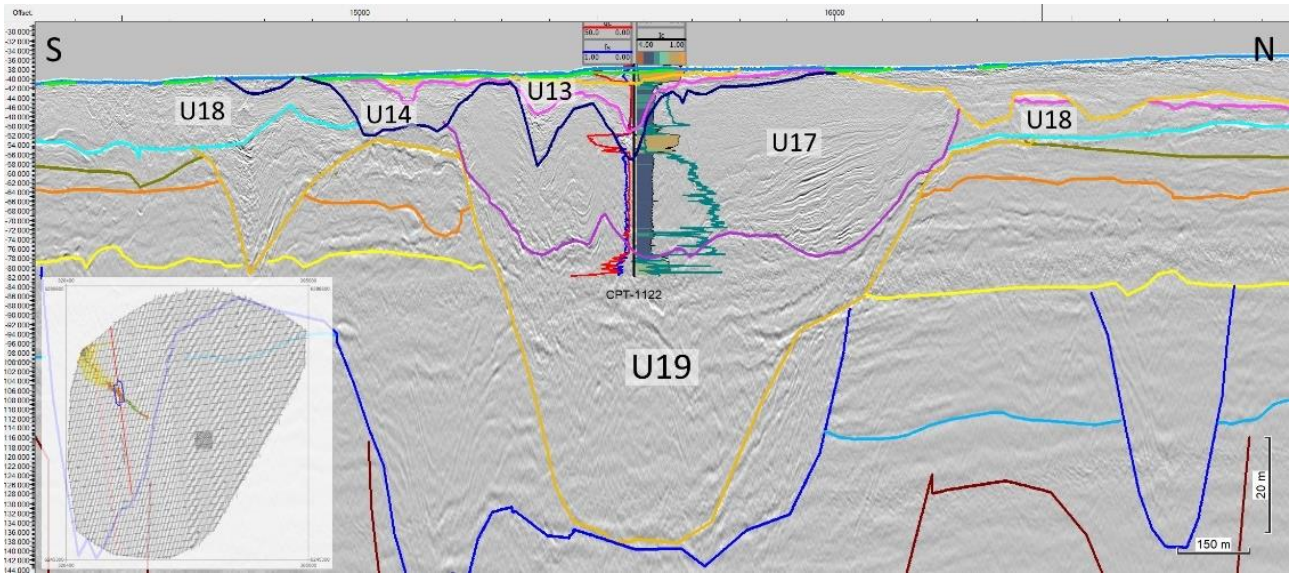

Figure 9-17: Unit 19 (U19) as interpreted in section EAM6145P02 (Fugro) with geotechnical logs from LOC-1122.

Unit 20

Unit 20 (see Figure 9-18) is present in a large part of the site and consists of Late Weichselian channel deposits. The deposit is expected to be dominated by proglacial and subglacial fluvial sand but silt/clay may also be found in some channels. Unit 20 channels are most likely related to the events described for Unit 15 to Unit 19. However, the size of the channels and the survey grid makes it difficult to relate the different parts of Unit 20 to the other units.

Around LOC-1051 Unit 20 is significantly thicker than in the surrounding areas which is interpreted to be caused by salt tectonics which can also be observed in the underlying units Unit 37, Unit 38, and Unit 89.

Enclosure 3.11 shows the depth below seabed of the top of Unit 20 and enclosure 4.11 shows the thickness (isochore) of Unit 20.

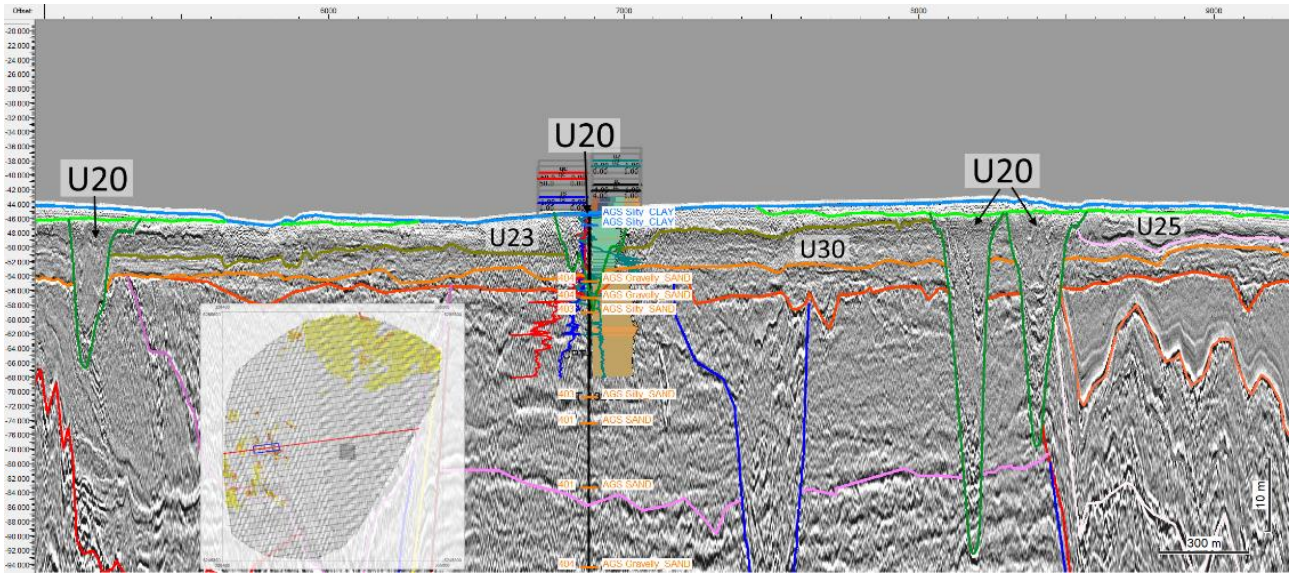

Figure 9-18: Unit 20 (U20) as interpreted in section BX3_OWF_2D_Baseline_2 (MMT) with geotechnical logs from LOC-1020.

Unit 21

Unit 21 (Figure 9-19) is present in the southern part of the site and consists of glaciofluvial or fluvial channel fill deposits consisting of silt/clay. Unit 21 represents the last infilling sequence in the channel system that Unit 22 overwise occupies. During the deposition of Unit 21 the channel is interpreted to have become completely waterfilled in a process where the flow speed drops from the previous conditions. The unit is interpreted to mainly be of Late Weichselian age, however, deposition of these layers could potentially have continued into the beginning of Holocene since environmental conditions changed gradually. The primary change in environmental conditions happened around 7000 years ago when the marine transgression occurred. The interpreted base of Unit 21 can be seen in Figure 9-20.

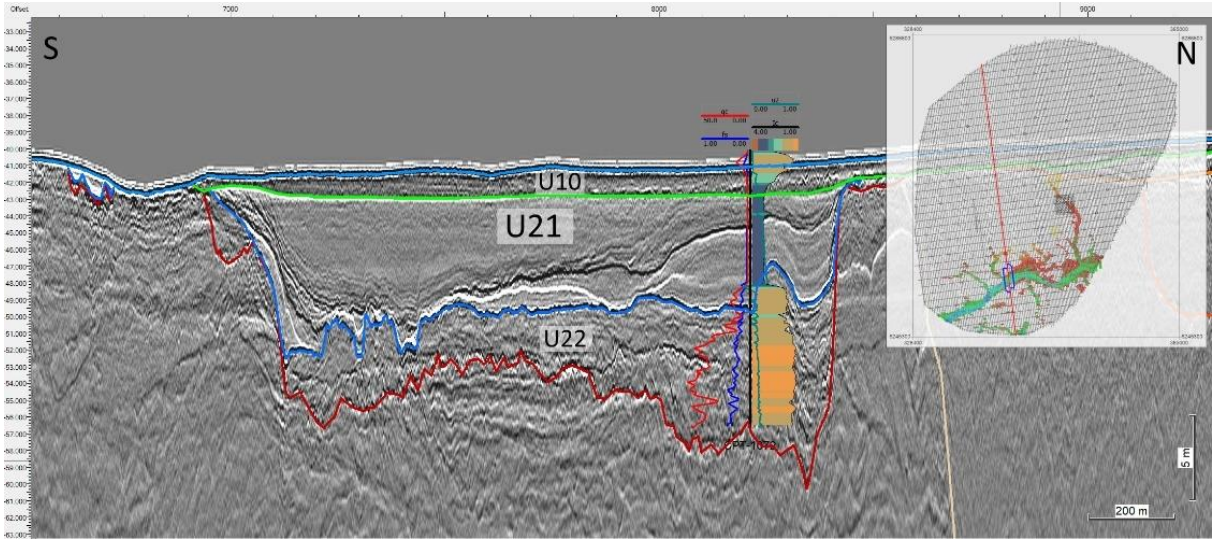

Figure 9-19: Unit 21 (U21) as interpreted in section EAQ6193P01 (Fugro) with geotechnical logs from LOC-1072.

Enclosure 3.12 shows the depth below seabed of the top of Unit 21 and enclosure 4.12 shows the thickness (isochore) of Unit 21.

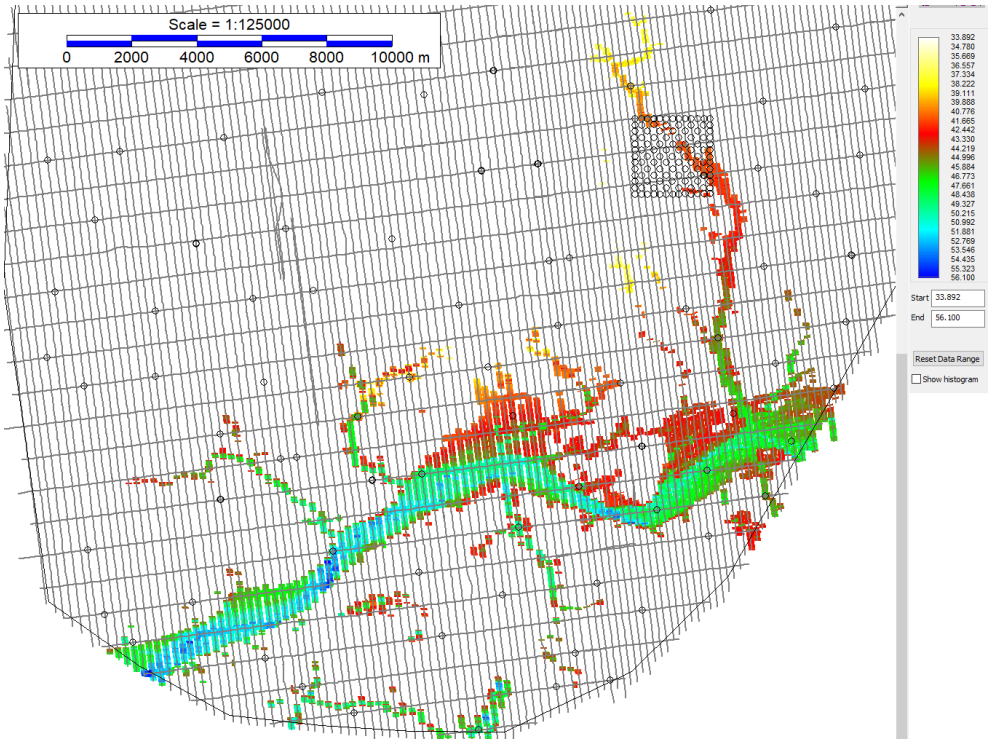

Figure 9-20: Depth map of the base horizon of Unit 21.

Unit 22

Unit 22 (see Figure 9-21) is present in the southern part of the site and consists of Late Weichselian glaciofluvial channel fill deposits consisting of sand. The channels of Unit 22 form a many-branched channel system which is interpreted to have been a main meltwater river system for the area during Late Weichselian when the northern opening of the North Sea area to the Atlantic was blocked by the ice sheet. The river system has fed into to a larger channel system which led water from Northern Europe to the Atlantic through a connection over the English Channel area. At a later stage the channel may have connected to the sea in the in the northern part of the North Sea when the ice sheet eventually melted away in this area. The channel systems presented in Figure 7-4 could potentially represent the channel system of Unit 22.

Enclosure 3.13 shows the depth below seabed of the top of Unit 22 and enclosure 4.13 shows the thickness (isochore) of Unit 22.

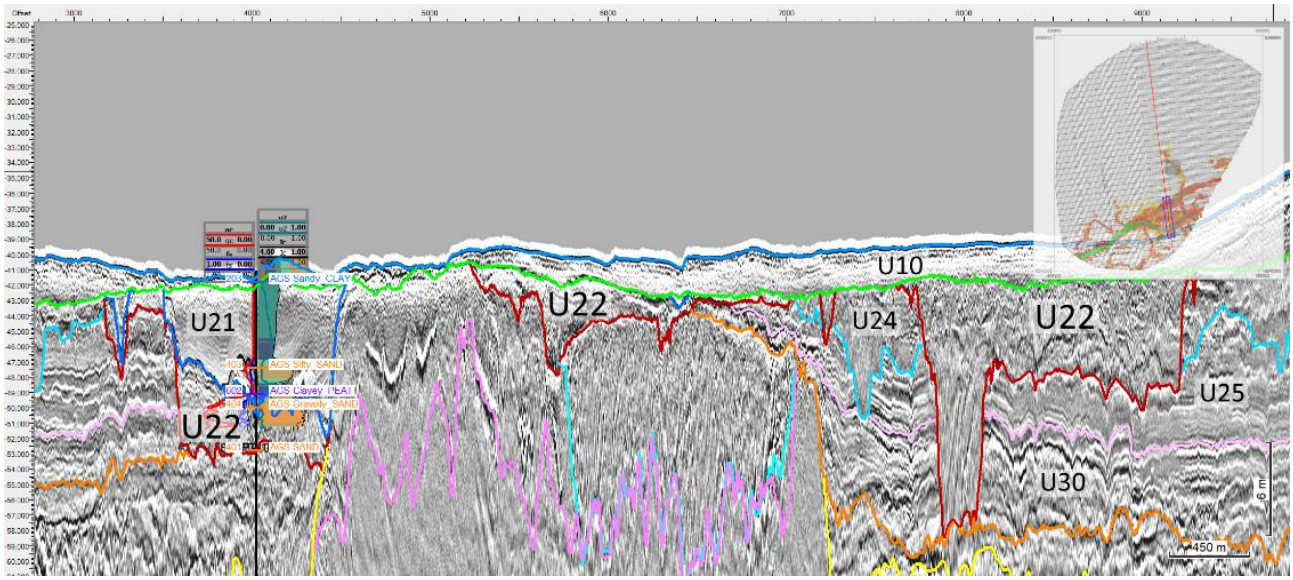

Figure 9-21: Unit 22 (U22) as interpreted in section BM1_OWF_E_2D_02520 (MMT) with geotechnical logs from LOC-1006.

A more detailed model could be interpreted in the channel system of Unit 22 and Unit 21 including many more units, but for the purpose of the report two units primarily dividing between sand and clay is sufficient. Figure 9-22 shows an example of how the channel system which has been divided into Unit 21 and Unit 22 in another study has been subdivided into several units which can be identified in the seismic section. Figure 9-22 is the same seismic sections as displayed in Figure 9-19.

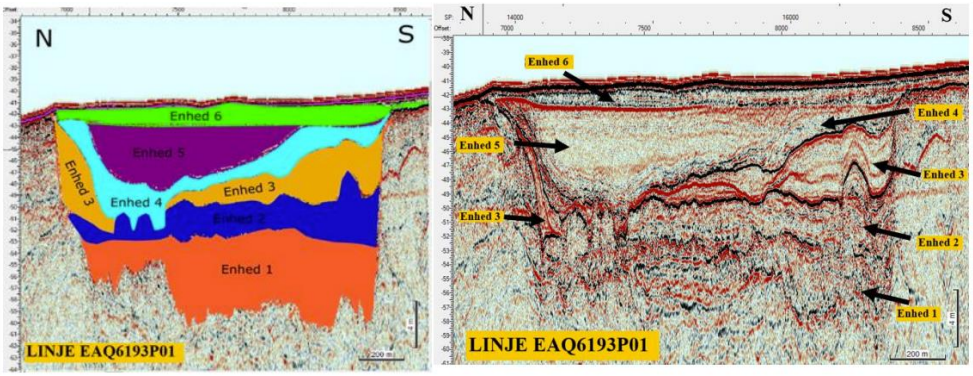

Figure 9-22: Example of more detailed interpretation of the same channel as mapped by Unit 21 and Unit 22 (Ref. /31/).

9.8.3 Weichselian (Unit 23 to Unit 35)

The chronostratigraphic group Weichselian include layers which seem to have been deposited primarily in a wide extramarginal meltwater valley. The different units indicate a gradual development in the depositional environment from glaciofluvial on a wide outwash plain (Unit 35) to glaciolacustrine environment (Unit 25). The change of the of the depositional environment is interpreted to be linked to the advance of Fennoscandic and British ice sheets and finally blocking of the northern opening to the Atlantic. This barrier is interpreted to have caused the water level in the valley to rise and form an ice-dammed lake.

Part of the area, which the units cover has been impacted by glaciotectonic deformation by the subsequent glacial advance of the Last Glacial Maximum. The impact can be seen most evident in the clayey deposits which easily deform when affected by glacial movement. Unit 23 represent the deformed layers and consists primarily of clay.

The relatively low geotechnical strength of the clay layers indicates that the thickness the Weichselian ice sheet covering the northern part of the site was too small to perform significant over-consolidation of the underlying deposits.

Unit 23

Unit 23 (see Figure 9-23) is present mainly in the north-western part of the site and consists of Weichselian glaciolacustrine deposits and to a minor degree glaciofluvial deposits which has been deformed by the main glacial advance in Late Weichselian. The deposits are dominated by silt/clay but sandier parts have also been identified. In some areas sandy parties may also be present. The unit is highly related to Unit 24 and Unit 25 which are the undeformed equivalent to Unit 23. In some areas the deformation reaches deeper and has entrained deeper parts which has previously been Unit 30.

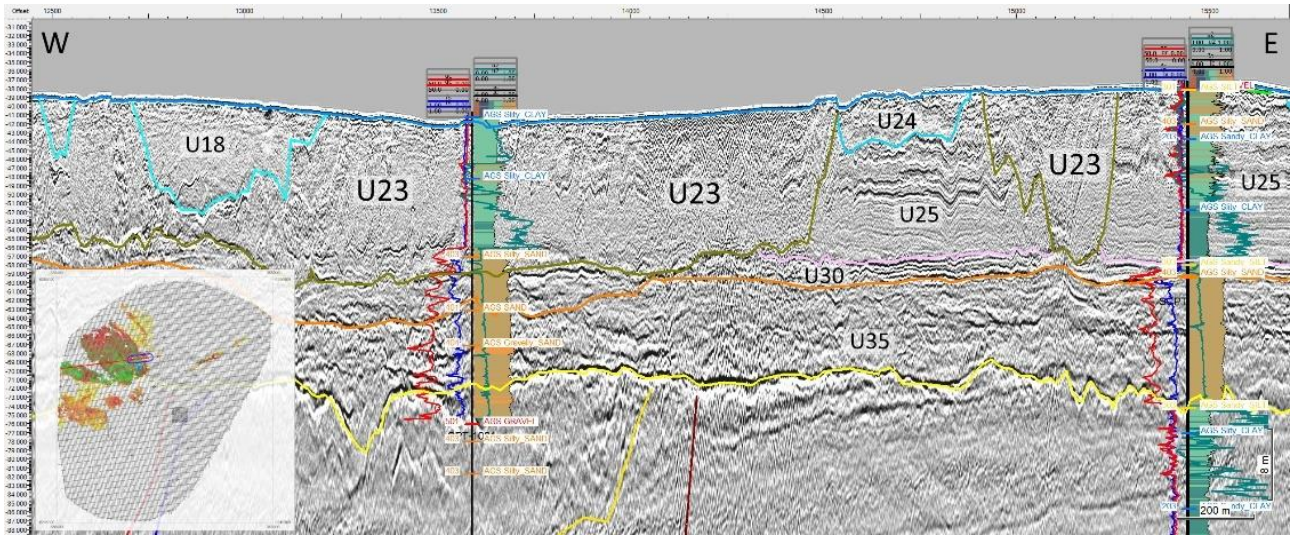

Figure 9-23: Unit 23 (U23) as interpreted in section EAX2297P01 (Fugro) with geotechnical logs from LOC-1031.

Enclosure 3.14 shows the depth below seabed of the top of Unit 23 and enclosure 4.14 shows the thickness (isochore) of Unit 23.

Unit 24

Unit 24 (see Figure 9-24) is present in a large area mainly in the central and south-eastern part of the site and consists of Weichselian glaciofluvial deposits. The deposits consist mainly of sand. Unit 24 is highly related to the underlying glaciolacustrine Unit 25. There is a gradual and fluctuating transition between the facies of Unit 25 and Unit 24 so boundary between the two had to be placed pragmatically where the seismic signature change from been dominated by Unit 25 facies to be dominated by Unit 24 facies. The fluctuation of the facies is interpreted to reflect a variable water level – submerged when the lacustrine Unit 25 is deposited and low water level and maybe partly subaerial when fluvial Unit 24 is deposited.

Enclosure 3.15 shows the depth below seabed of the top of Unit 24 and enclosure 4.15 shows the thickness (isochore) of Unit 24.

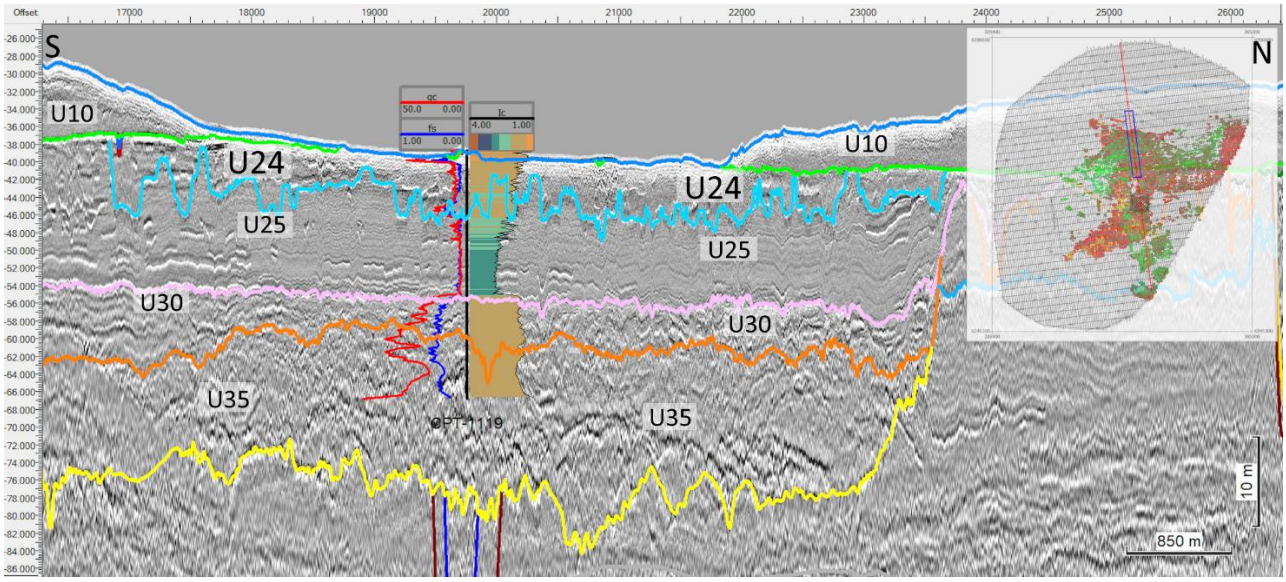

Figure 9-24: Unit 24 (U24) as interpreted in section BM2_OWF_E_2D_04410 (MMT) with geotechnical logs from LOC-1119.

Unit 25

Unit 25 (see Figure 9-25) is present in a large area mainly in the central and south-eastern part of the site and consists of Weichselian glaciolacustrine deposits. The deposits consist mainly of clay and silt becoming slightly sandier towards the top where it transitions into Unit 24.

The lacustrine deposits of Unit 25 are interpreted to be deposited in a moraine- and/or ice-dammed lake confined by the ice sheet advancing from north, blocking the connection to the North Atlantic during the largest advance in Weichselian and eventually overriding part of the area in Late Weichselian.

Internal wide and shallow channel-like features are visible in almost the entire Unit 25. They become gradually more frequent towards the top where they also resemble actual channels – the channels that make Unit 24. The deeper parts of the channel features located in the interior of Unit 25 are interpreted to be deposits from sediment gravity flows like turbidity currents.

Enclosure 3.16 shows the depth below seabed of the top of Unit 25 and enclosure 4.16 shows the thickness (isochore) of Unit 25.

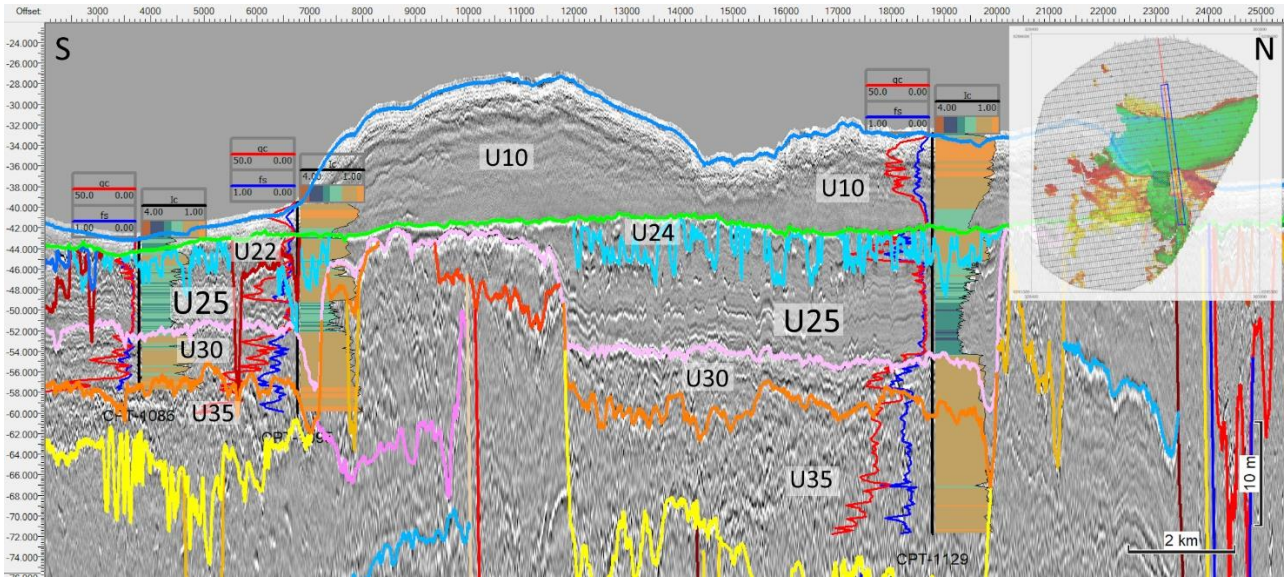

Figure 9-25: Unit 25 (U25) as interpreted in section BM3_OWF_E_2D_06720 (MMT) with geotechnical logs from LOC-1086, LOC-1095, and LOC-1129.

Unit 30

Unit 30 (see Figure 9-26) is present in a large area in mainly the central and south-eastern part of the site and consists of Weichselian glaciofluvial to - lacustrine deposits. The deposits consist mainly of sand becoming slightly siltier towards the top where the deposits shift to Unit 25. Geotechnically there is typically a clear shift between Unit 30 and Unit 25. This shift is not as significant in the seismic data, however, still identifiable.

Unit 30 are deposited in a wide extramarginal river valley leading meltwater from the front of the ice sheet located further to the east towards the Atlantic through the northern opening of the North Sea area. At a later stage the opening was blocked by the ice sheet connection between Norway and UK. Unit 30 is interpreted to represent the final stage before the ice sheets more or less closed the northern connection to the Atlantic. Unit 30 also represents the transition phase from entirely fluvial in the underlying Unit 35 to lacustrine in Unit 25 above. Unlike the below Unit 35 the deposits of Unit 30 are not restricted to the channel but because of the rising water level it covers extensive parts of the surrounding areas.

Enclosure 3.17 shows the depth below seabed of the top of Unit 30 and enclosure 4.17 shows the thickness (isochore) of Unit 30.

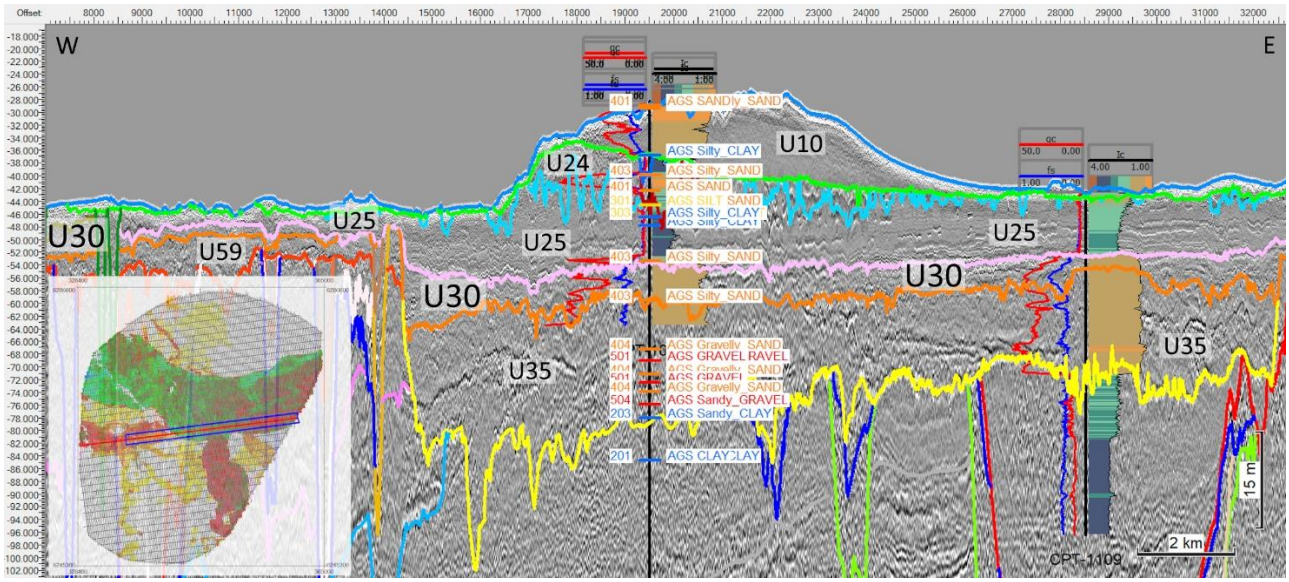

Figure 9-26: Unit 30 (U30) as interpreted in section BX3_OWF_2D_Baseline_2 (MMT) with geotechnical logs from LOC-1023 and LOC-1109.

Unit 35

Unit 35 (see Figure 9-27) is present in a large area in mainly the central and south-eastern part of the site and consists of Weichselian glaciofluvial deposits of mainly sand.

Unit 35 are deposited in a wide extramarginal river valley formed by meltwater erosion and subsequently filled by meltwater transported sediments in a glaciofluvial outwash plain environment. The valley led meltwater from the front of the ice sheet located further to the east towards the Atlantic through the northern opening of the North Sea area.

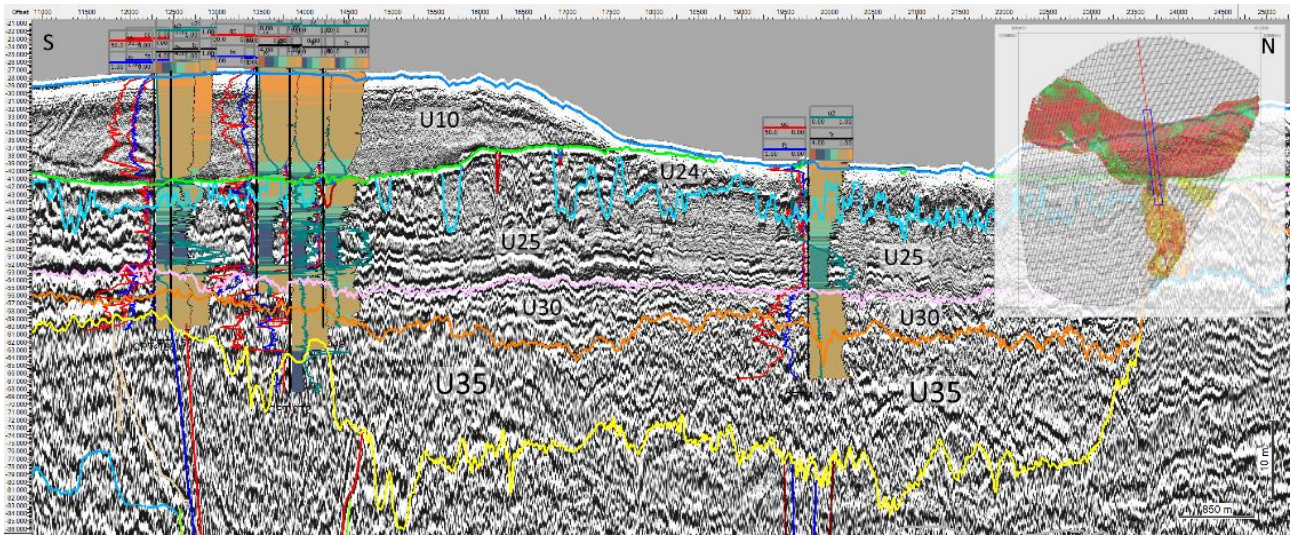

Figure 9-27: Unit 35 (U35) as interpreted in section BM2_OWF_E_2D_04410 (MMT) with geotechnical logs from LOC-0165, LOC-0153, LOC-0014, LOC-0118, LOC-0095, LOC-0072, LOC-0049, LOC-0025, and LOC-1119.

Enclosure 3.18 shows the depth below seabed of the top of Unit 35 and enclosure 4.18 shows the thickness (isochore) of Unit 35.

9.8.4 Saalian (Unit 37 to Unit 59)

The chronostratigraphic group Saalian consists both of units deposited before the glacial advance reached the area, during and after the ice sheet had melted away from the area. Unit 56 to Unit 59 generally represents periglacial fluvial and lacustrine layers deposited prior to the Saalian ice sheet overriding. Unit 40 to Unit 50 represent infill deposits in buried tunnel valleys deposited during and after the ice sheet overriding. Unit 37 and Unit 38 represent periglacial fluvial and lacustrine layers deposited subsequent to the ice sheet overriding that formed the tunnel valleys.

Unit 37

Unit 37 (see Figure 9-28) is present in the north-eastern corner of the site and is interpreted to represent Saalian glaciolacustrine deposits. The deposits consist mainly of clay. From the seismic data alone, it is difficult to determine if the unit has been subjected to glacial compaction by the Saalian ice sheet, however, geotechnical data indicate over-consolidation of this layer indicating glacial compaction.

Deep subsidence which at least can be traced to the base of the underlying Unit 38 has visible effect on Unit 37 in the area around LOC-1051 where it becomes deeper and significantly thicker than seen elsewhere. Potentially, the subsidence could be driven by melting of a buried ice (glacier ice or frozen meltwater) below Unit 38. Unit 37 appears to be thicker within the area of subsidence than elsewhere which indicates that the subsidence event started during or slightly prior to deposition of Unit 37 and continued in the time after. The underlying Unit 38 is also impacted by the subsidence but does not have a significantly different thickness in the area. An alternative explanation to the subsidence could be salt tectonics at great depth. However, it is difficult to see if the Miocene layers below Unit 38 have experienced the same subsidence since these already appear chaotic because of glaciotectonic deformation.

It is possible that Unit 37 could instead be interglacial or interstadial, but there is no information available to separate this unit clearly from the underlying glacial deposits.

Enclosure 3.19 shows the depth below seabed of the top of Unit 37 and enclosure 4.19 shows the thickness (isochore) of Unit 37.

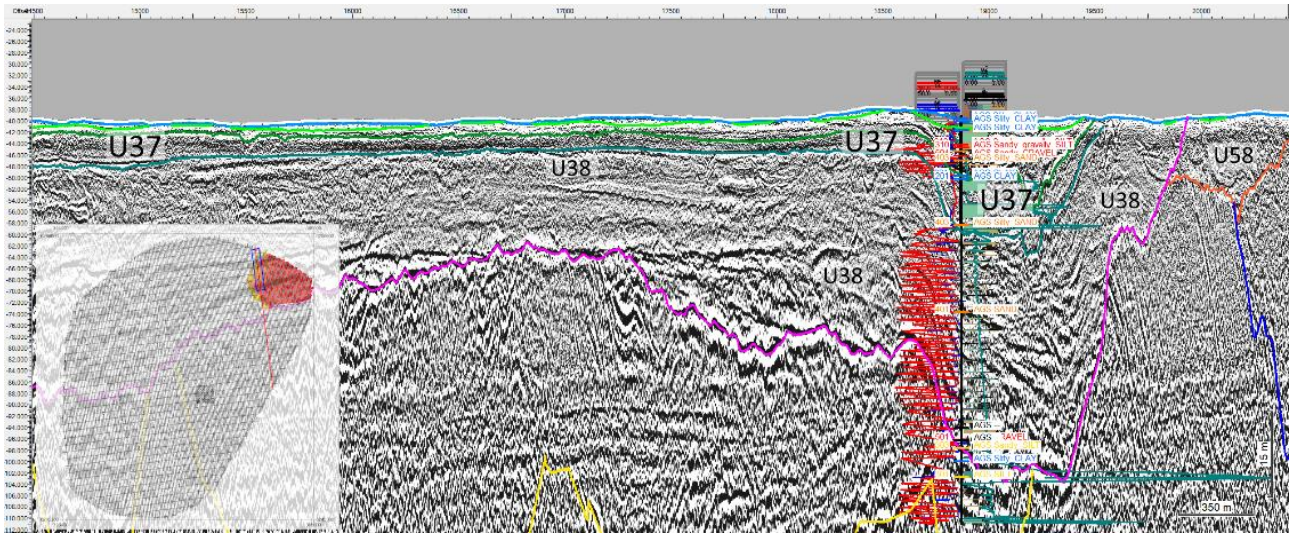

Figure 9-28: Unit 37 (U37) as interpreted in section BM5_OWF_E_2D_14280 (MMT) with geotechnical logs from LOC-1051.

Unit 38

Unit 38 (see Figure 9-29) is present in north-eastern corner of the site and is interpreted to represent Saalian extramarginal glaciofluvial deposits. The deposits consist mainly of sand and with gravel in a thin layer at the base. Unit 38 includes a deeper channel feature along the western extent of the layer. Remarkable about the unit is some large internal structures that constitute downlapping clinoforms specially developed in the deeper part in the depression in the west.

The channel depression could have been formed by subglacial meltwater erosion. However, the infill deposits interpreted to have been deposited in a periglacial fluvial environment like an outwash plain. In an area around LOC-1051 the impact of subsidence is seen. The subsidence is interpreted to have been driven by melting of stagnant ice. The stagnant ice may have been left as frozen meltwater in the many subglacial meltwater tunnels, which over time has formed the depression.

Unit 38 appear similar to Unit 58 located to the west and might share depositional environment. However, the two units are separated by Unit 40 (a buried valley unit) which cuts into Unit 58 and is eroded by Unit 38. The two units do not belong to the same event and is interpreted to be time-wise separated by Saalian glacial overriding. There is also clear erosional contact between Unit 38 and Unit 58.

Enclosure 3.20 shows the depth below seabed of the top of Unit 38 and enclosure 4.20 shows the thickness (isochore) of Unit 38.

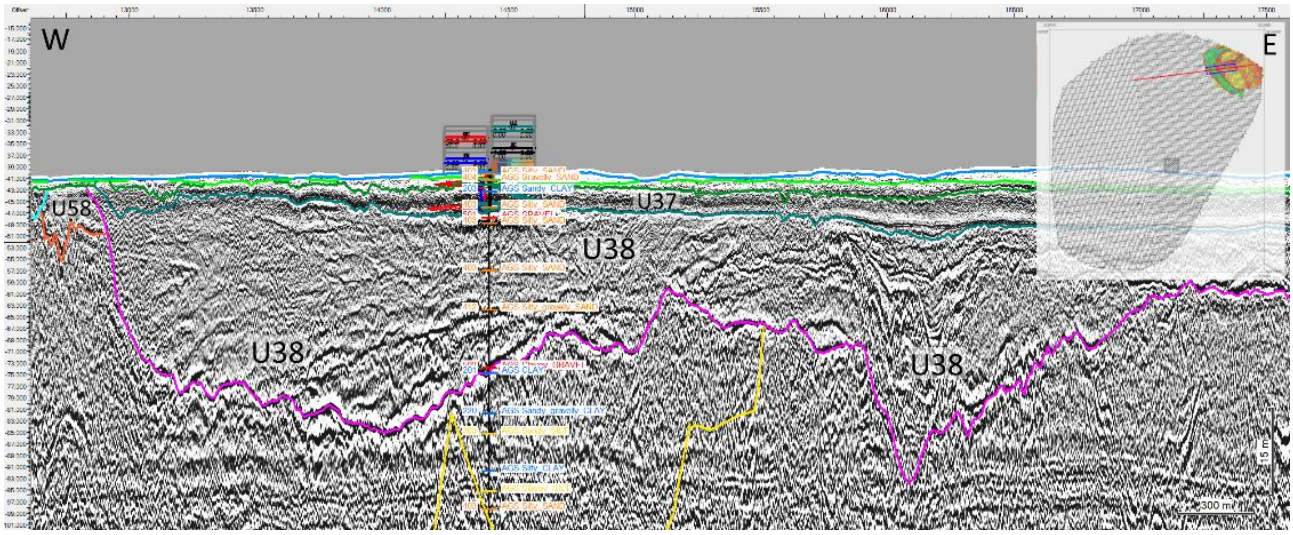

Figure 9-29: Unit 38 (U38) as interpreted in section BX1_OWF_E_XL_07000 (MMT) with geotechnical logs from LOC-1044.

Unit 40

Unit 40 (see extend of the unit in Figure 9-30) is present in buried valleys spread over the site and is interpreted to represent Saalian mainly glaciofluvial to -lacustrine deposits. The valleys in which Unit 40 is deposited are formed by subglacial meltwater erosion. Some of the deeper deposits are interpreted to be glaciofluvial deposits from the subglacial environment, whereas the shallower deposits are mainly glaciolacustrine from the periglacial environment. It is difficult to assess if all the channels have been formed and filled at the same time. The processes, however, seem similar for the different valleys.

The southern valley system branches out into several smaller valleys in WNW direction. Further to the west, the channels seem to become smaller and discontinuous. The smaller valleys are interpreted to indicate upstream channels in subglacial meltwater system, so that transport was towards an ice sheet margin in ESE direction.

The northern valley system also seems to branch out around midway in its crossing of the site and the branches becomes very shallow before they connect again and form a big valley.

The Valley system is interpreted to have had a primary meltwater transport direction towards SE, and the shallow branching midway may be caused by some local conditions in the substratum, which have not been possible to clarify.

Unit 40 has three subunits: Subunit 40-01 (see Figure 9-31) represents the latest periglacial lacustrine deposits consisting of clay that spreads out across a wider area than the underlying valley. Subunit 40-01 is only present in a relatively small area in the east. Subunit 40-02 (see Figure 9-31 and Figure 9-32) represents the upper undisturbed glaciolacustrine deposits both consisting of sand and clay and is present in the top of the valley fill along limited sections of the valleys.

Subunit 40-03 (see Figure 9-31 and Figure 9-32) constitutes the majority of Unit 40 and consists of both the deep glaciofluvial deposits and the overlying thick glaciolacustrine layers. The deposits belonging to Subunit 40-03 generally appear more chaotic than the above lying subunits. Subunit 40-03 contains clay, silt and sand.

Irregular subsidence is attributed to melting of stagnant ice, which might have been placed together with the glaciofluvial sediments.

Enclosure 3.21 shows the depth below seabed of the top of Unit 40 and enclosure 4.21 shows the thickness (isochore) of Unit 40.

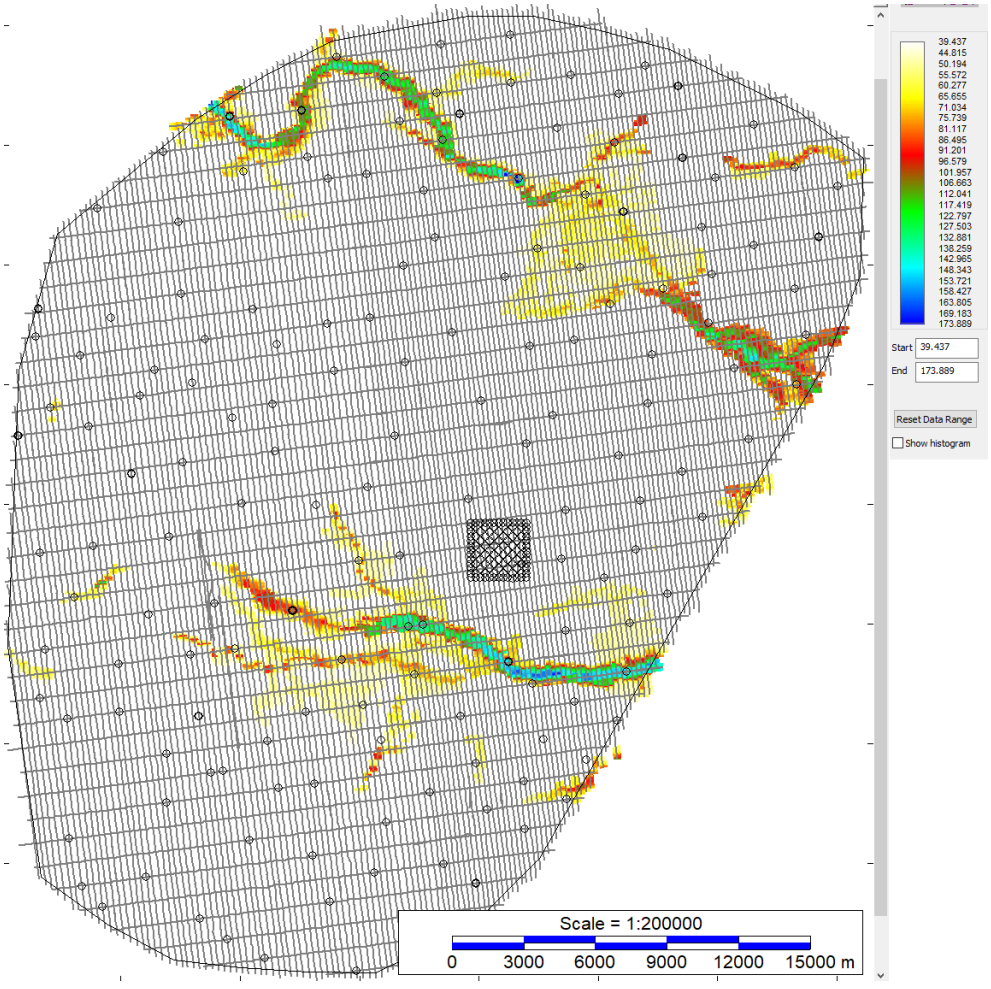

Figure 9-30: Depth map of the base horizon of Unit 40.

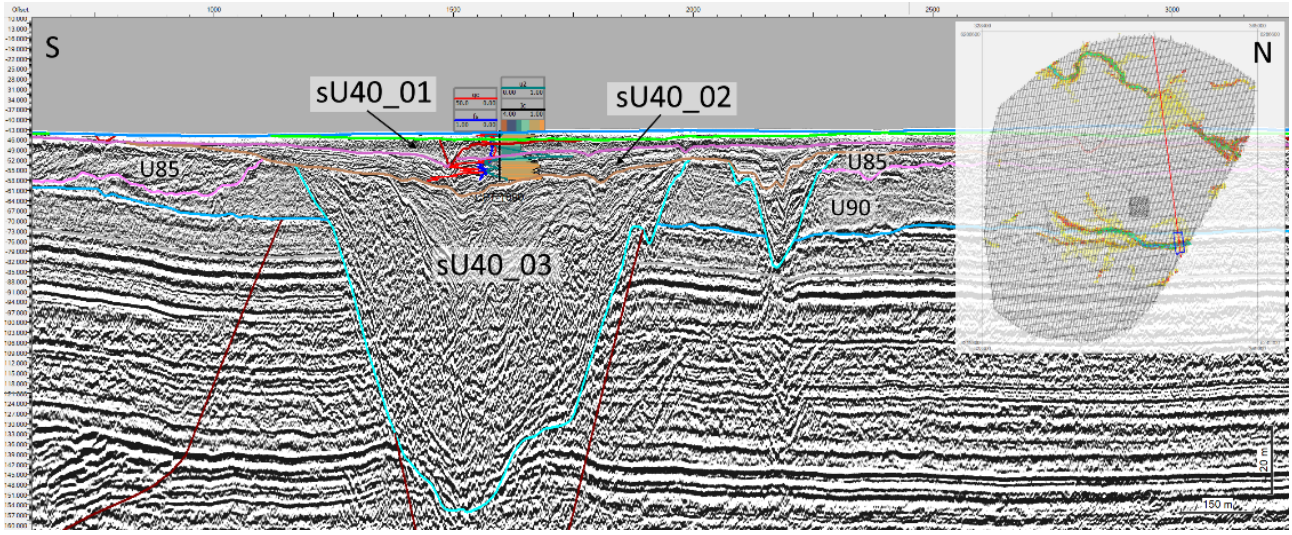

Figure 9-31: Subunit 40-01 (sU40_01), Subunit 40-02 (sU40_02) and Subunit 40-03 (sU40_03) as interpreted in section BM4_OWF_E_2D_09030 (MMT) with geotechnical logs from LOC-1090.

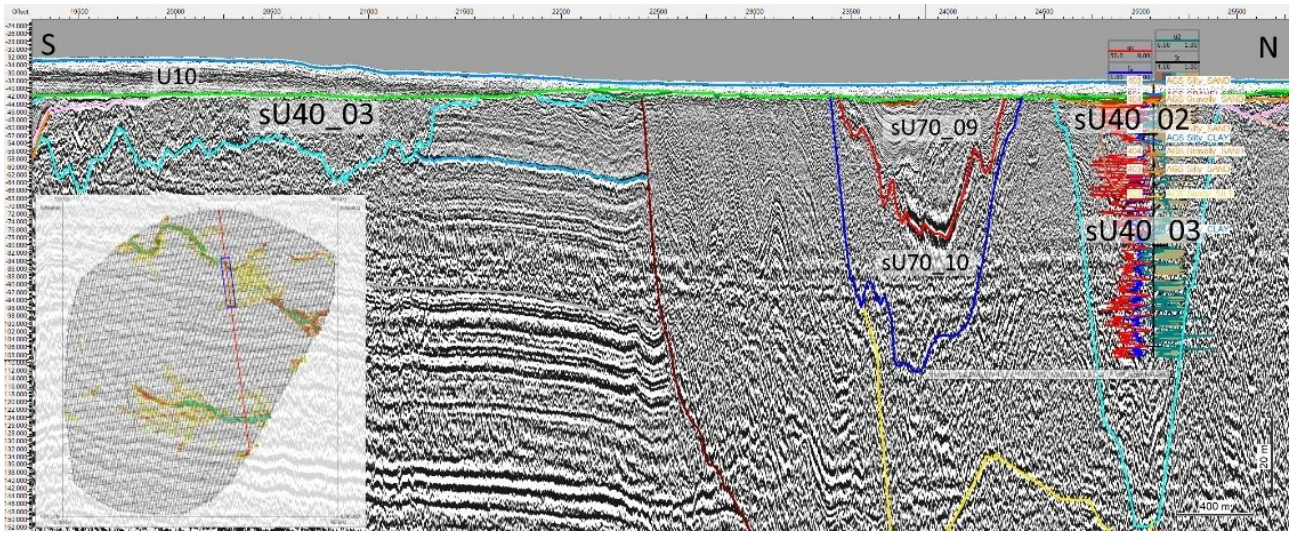

Figure 9-32: Subunit 40-02 (sU40_02) and Subunit 40-03 (sU40_03) as interpreted in section BM4_OWF_E_2D_07140 (MMT) with geotechnical logs from LOC-1042.

Unit 41

Unit 41, 42, 45 and 50 are all interpreted to represent fill deposits in buried valley systems that are located in the southern part of the site with orientation ranging from W-E to SW-NE. Since they do not overlap with the valleys in Unit 40 it is not possible to determine if they are contemporaneous or which is the youngest. The valleys of Unit 42, 45 and 50 are all formed by subglacial meltwater erosion and has a similar path and cuts into each other and in some sections the younger overtakes the place of an older buried valley.

Unit 41 (see Figure 9-33) represents the latest unit in the system and is found at the top of the valleys of Unit 42 and Unit 45. Unit 41 represents a layer of laminated periglacial lacustrine clay deposits.

Enclosure 3.22 shows the depth below seabed of the top of Unit 41 and enclosure 4.22 shows the thickness (isochore) of Unit 41.

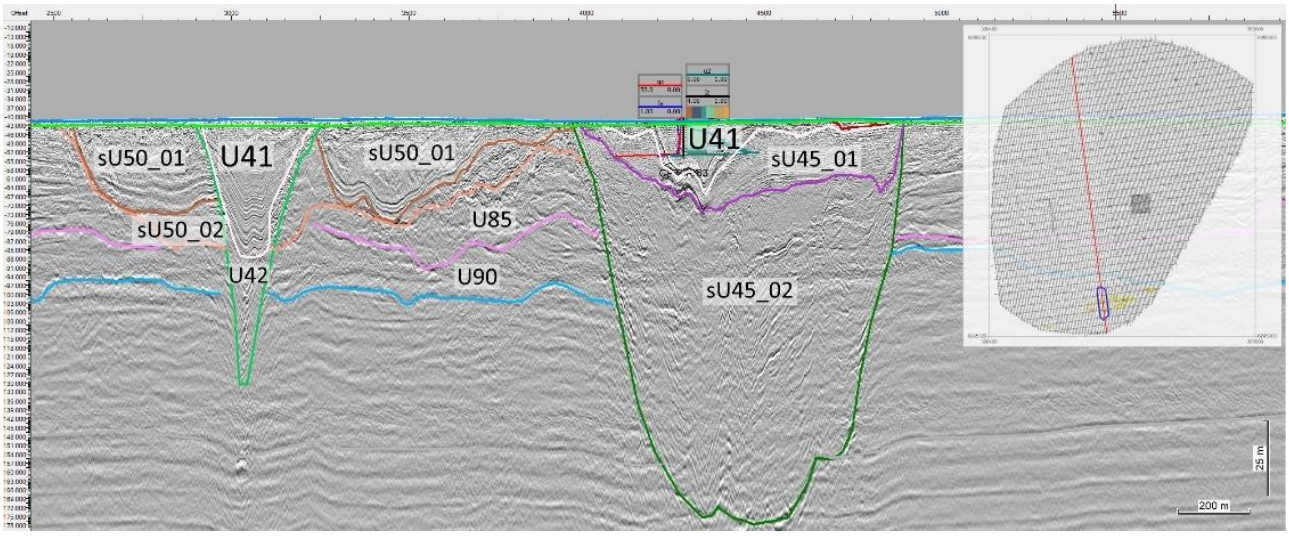

Figure 9-33: Unit 41 (U41) as interpreted in section EAT2225P01 (Fugro) with geotechnical logs from LOC-1063.

Unit 42

Unit 42 (see Figure 9-34), the youngest of the three underlying valleys is deep and narrow with a distinct V-shape. In Figure 9-14, the valley of Unit 42 (including Unit 41) is approximately 110 m deep and 400 m wide. The content of Unit 42 ranges from silty clay to gravelly sand and is interpreted to be partly deposited in a subglacial fluvial environment and partly in a proglacial or periglacial fluvial and lacustrine environment. In some sections, irregular subsidence structures are attributed to melting of stagnant ice.

Enclosure 3.23 shows the depth below seabed of the top of Unit 42 and enclosure 4.23 shows the thickness (isochore) of Unit 42.

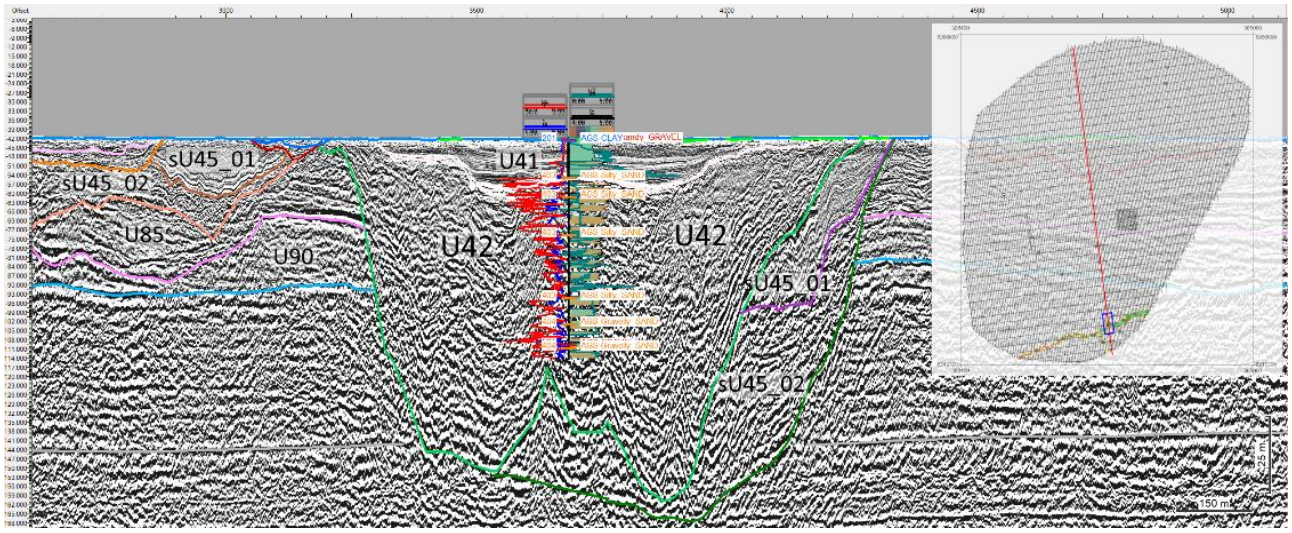

Figure 9-34: Unit 42 (U42) as interpreted in section BM1_OWF_E_2D_00420 (MMT) with geotechnical logs from LOC-1004.

Unit 45

Unit 45 represents a valley which is approximately parallel to but wider and deeper than Unit 42. In a section, the valley of Unit 42 is located inside the valley of Unit 45. In Figure 9-15 the valley is approximately 140 m deep, approximately 1 km wide at the same location and has a more distinct U-shape. The fill deposits in the valley are divided into Subunit 45-01 and Subunit 45-02 (see Figure 9-35) where Subunit 45-01 represents the latest fill sequence before the overlying Unit 41. Primarily a laminated and undisturbed subunit which is interpreted to be dominated by silt and clay deposited in periglacial lacustrine environment.

The depression that both Subunit 45-01 and Subunit 45-02 fills up is a result of irregular subsidence initiated deeply in Subunit 45-02 – interpreted to be melting of embedded ice. The subsidence has continued during deposition of Subunit 45-01.

Subunit 45-02 represents most of the deposits in the valley and consists of gravelly to silty sand interpreted to be deposited in subglacial and proglacial fluvial to proglacial lacustrine environments.

Enclosure 3.24 shows the depth below seabed of the top of Unit 45 and enclosure 4.24 shows the thickness (isochore) of Unit 45.

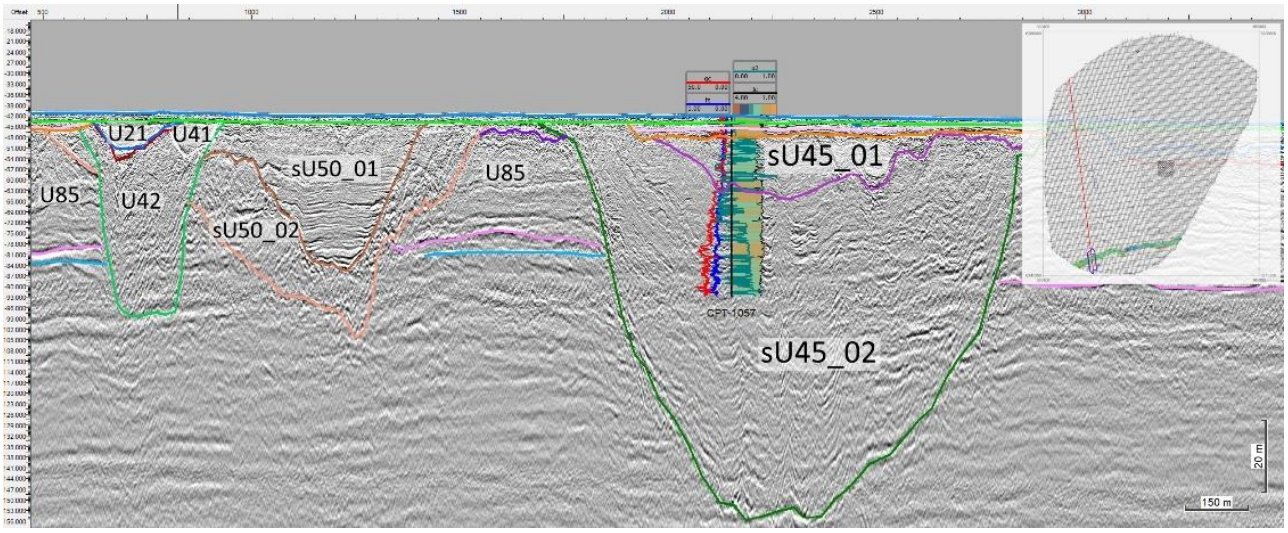

Figure 9-35: Subunit 45-01 (sU45_01) and Subunit 45-02 (sU45_02) as interpreted in section EAH2105P01 (Fugro) with geotechnical logs from LOC-1057.

Unit 50

Unit 50 represents the deepest of the three buried valleys with similar position and orientation. Similar to the two above lying valleys Unit 50 has a deeper more chaotic part which is interpreted to be subglacial and proglacial glaciofluvial deposits and a shallower part which is interpreted to be proglacial to periglacial glaciolacustrine deposits. Unit 50 is divided into two subunits (see Figure 9-36) – where Subunit 50-01 is the shallow part and Subunit 50-02 is the deeper part.

Subunit 50-01 is interpreted to be dominated by clay. However, in part the subunit, clear impact from glacial deformation can be interpreted, which makes it likely that the subunit is mixed in some areas.

Subunit 50-02 is interpreted to mainly consist of sand form the subglaclal fluvial environment. Only one CPT location samples Unit 50.

In the western part Unit 50 appears to separate into two branches that both turn towards SW. The valley of Unit 50 is generally shallower and wider than the two younger valleys. However, in sections the valley of Unit 45 seems to have eroded Unit 50 completely away though the width of Unit 50 is generally larger than Unit 45. Further, Unit 42 cuts into Unit 50 and runs inside it in sections.

Enclosure 3.25 shows the depth below seabed of the top of Unit 50 and enclosure 4.25 shows the thickness (isochore) of Unit 50.

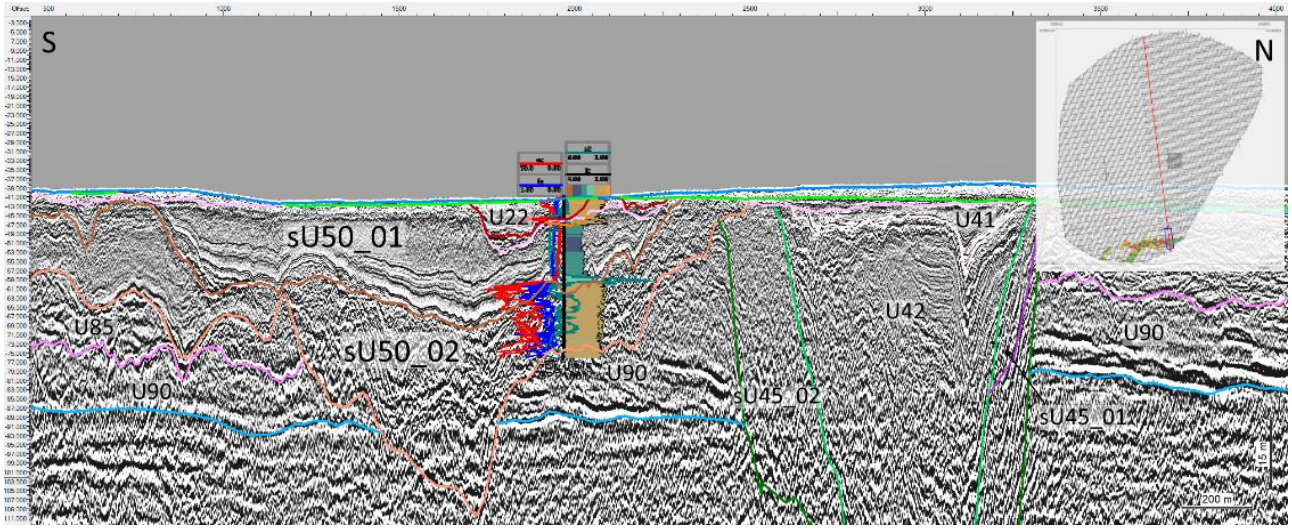

Figure 9-36: Subunit 50-01 (sU50_01) and Subunit 50-02 (sU50_02) as interpreted in section BM1_OWF_E_2D_01680 (MMT) with geotechnical logs from LOC-1061.

Unit 56

Unit 56 (see Figure 9-37) is present in the northernmost part of the site in a generally tabular layer intersected by several of the younger buried valleys especially Unit 40. In some areas the unit appears laminated and in other areas it appears cross-bedded to chaotic. The unit consists of both sand and clay deposits.

The unit is interpreted to have been deposited in a periglacial lacustrine to -fluvial environment and some impact of glaciotectonic deformation can be seen. The origin of this layer is uncertain, and a shallow marine environment cannot be ruled out. It could be interglacial or interstadial, but there is no information available to separate this unit clearly from the underlying glacial deposits.

Enclosure 3.26 shows the depth below seabed of the top of Unit 56 and enclosure 4.26 shows the thickness (isochore) of Unit 56.

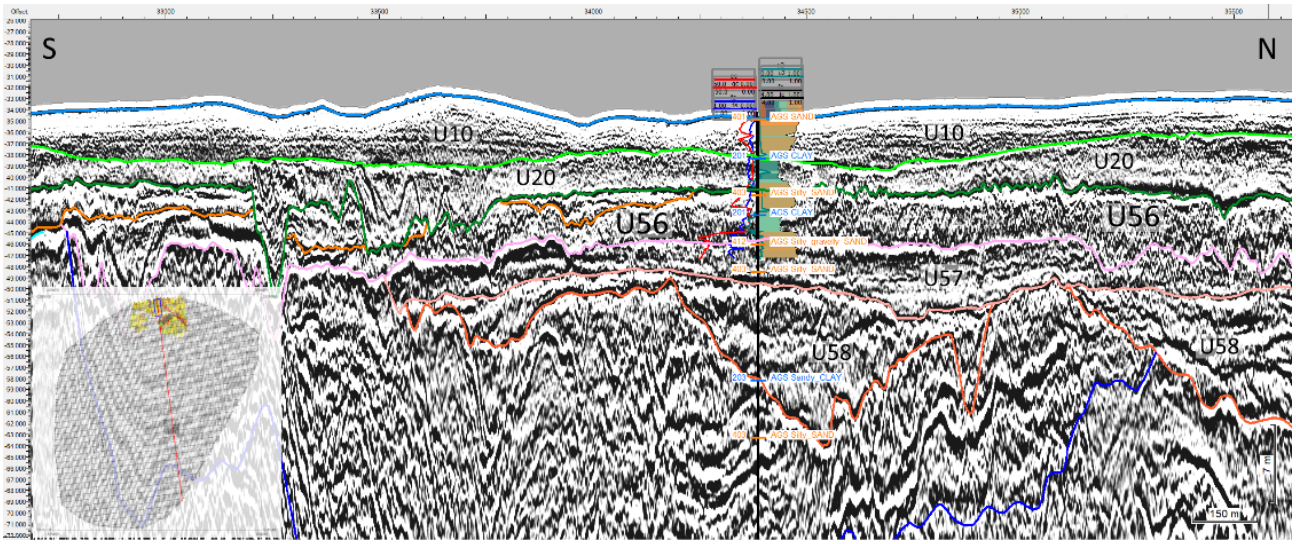

Figure 9-37: Unit 56 (U56) as interpreted in section BM2_OWF_E_2D_04620_01 (MMT) with geotechnical logs from LOC-1053.

Unit 57

Unit 57 (see Figure 9-38) is present in the northernmost part of the site as a relatively thin layer intersected by younger buried valleys. The unit generally appears cross-bedded to chaotic. The unit is interpreted to have been deposited in a periglacial fluvial or fluvial environment. The origin of this layer is uncertain, and a coastal marine environment cannot be ruled out.

The unit consists of sand. Like the above lying Unit 56 it could be interglacial or interstadial, but there is no information available to separate this unit clearly from the underlying glacial deposits.

Enclosure 3.27 shows the depth below seabed of the top of Unit 57 and enclosure 4.27 shows the thickness (isochore) of Unit 57.

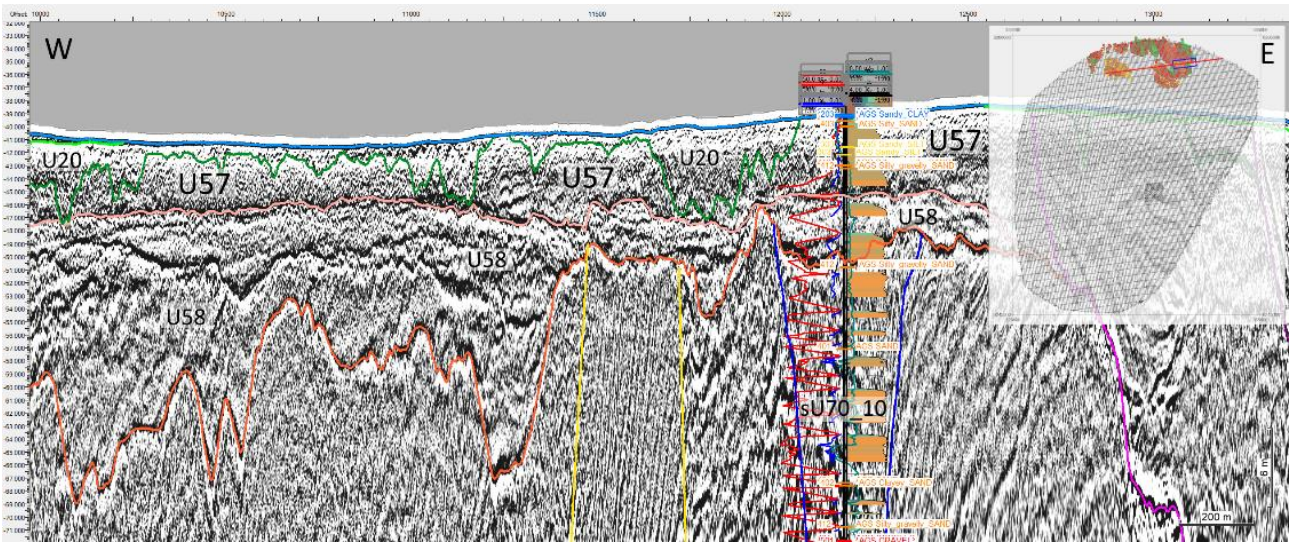

Figure 9-38: Unit 57 (U57) as interpreted in section BX1_OWF_E_XL_04000 (MMT) with geotechnical logs from LOC-1050.

Unit 58

Unit 58 (see Figure 9-39) is present in the northernmost part of the site and consists mainly of sand. Like Unit 38, Unit 58 has large internal structures that constitute downlapping clinoforms. The clinoforms may represent large scale point bar deposits, an interpretation which is supported by their orientation towards the channel-like depressions at the base of the unit indicating the SW migrating thalweg path. Unit 58 is interpreted to represent a periglacial fluvial deposit.

Enclosure 3.28 shows the depth below seabed of the top of Unit 58 and enclosure 4.28 shows the thickness (isochore) of Unit 58.

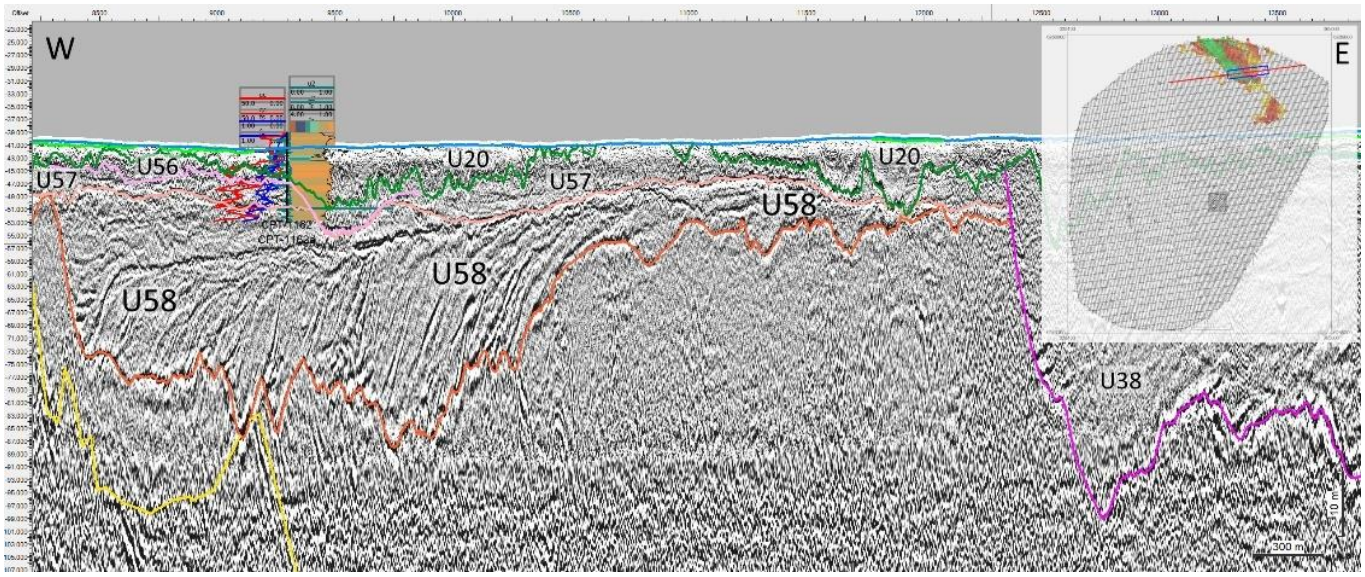

Figure 9-39: Unit 58 (U58) as interpreted in section BX1_OWF_E_XL_05000 (MMT) with geotechnical logs from LOC-1162.

Unit 59

Unit 59 (see Figure 9-40) is present in the central part of the site and consists mainly of sand and interpreted to represent periglacial fluvial deposits on an outwash plain. The unit is intersected by buried valleys of Unit 40 and the wide Unit 35 valley.

Enclosure 3.29 shows the depth below seabed of the top of Unit 59 and enclosure 4.29 shows the thickness (isochore) of Unit 59.

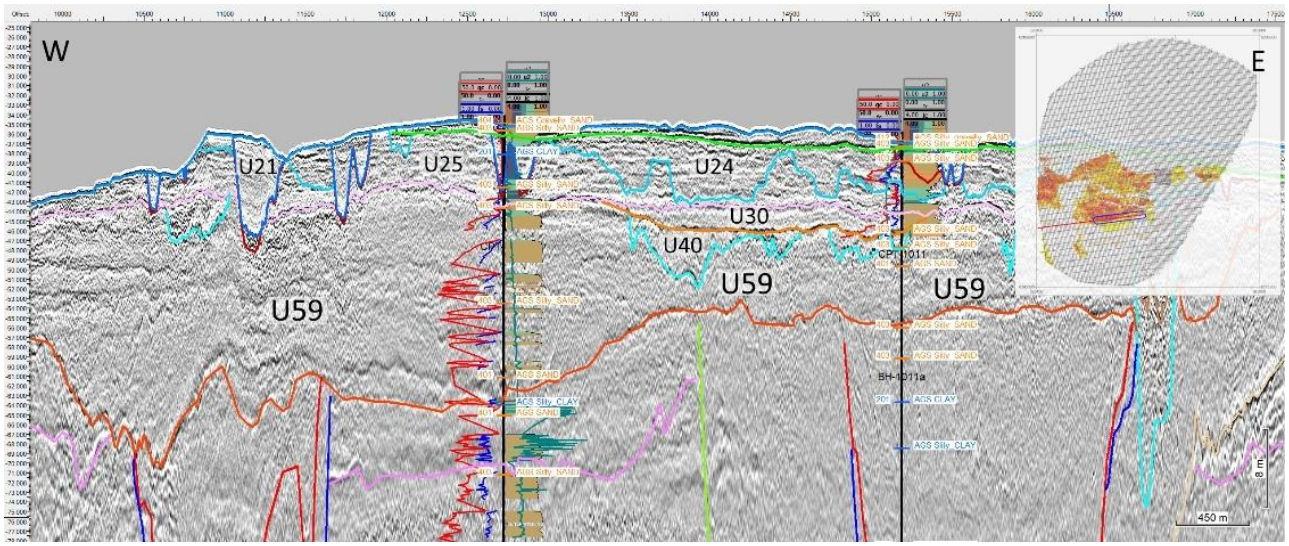

Figure 9-40: Unit 59 (U59) as interpreted in section EAX2281P01 (Fugro) with geotechnical logs from LOC-1010 and LOC-1011.

9.8.5 Elsterian (Unit 65 to Unit 73)

The term Elsterian used for this chronostratigraphic group is an interpretation indicating that tunnel valleys within this group are older than the layers (including tunnel valleys) assigned to the Saalian group. It is difficult to rule out that the tunnel valley within this group could have been formed by an earlier glacial advance within the Saalian Glaciation or an older glacial advance within the Cromerian Complex.

The Elsterian group consists of three units: Unit 65 a buried valley partly overlying the extensive buried valley complex of Unit 70 and deep deformation structures reaching deeply into the Miocene deposits where Quaternary deposits are mixed with Miocene deposits in Unit 73. Unit 70 is subdivided into 12 subunits representing different infilling events.

Unit 65

Unit 65 (see Figure 9-41) is present in the southern part of the site as a buried valley which cut into the top of the Unit 70 buried valley complex. The buried valley of Unit 65 is interpreted to have been formed by subglacial meltwater erosion and filled by outwash deposits in the same process. Deposits consist of sand.

Enclosure 3.30 shows the depth below seabed of the top of Unit 65 and enclosure 4.30 shows the thickness (isochore) of Unit 65.

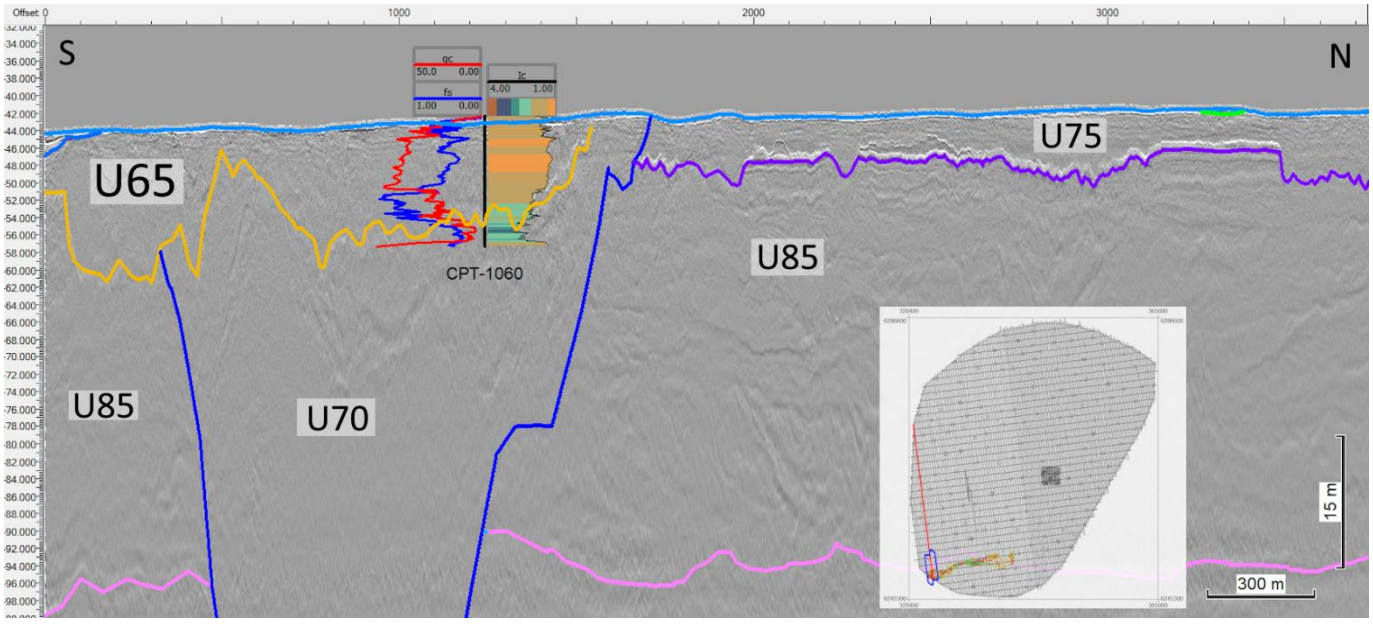

Figure 9-41: Unit 65 (U65) as interpreted in section EAC2029P01 (Fugro) with geotechnical logs from LOC-1060.

Unit 70

Unit 70 represents infill deposits to a complex system of deep buried valleys across the site and covers a large part of the site with an overall trending orientation of NE to SW.

Unit 70 consists mainly of two major valley systems which may not have been formed at the exact same time, but stratigraphically they are placed in the same position. To the NNW Unit 70 consists of a complex many-branched valley with several connection points. To the SE Unit 70 consists of a less complex valley with a distinct U-shape. Unit 70 is subdivided into 12 subunits (see Figure 9-42 and Figure 9-43). Generally, many of the different subunits represent different infilling sequences.

Subunit 70-01 and Subunit 70-02 represent shallow layers of limited extent in the NNW valley system. Subunit 70-01 is a layer of glaciolacustrine deposits consisting of clay. Subunit 70-02 is also a clay layer, but with very different appearance most likely due to glaciotectonic deformation.

Subunit 70-03 to Subunit 70-07 represents several infill sequences visible in the southeastern part of the NNW valley system. The individual layers represented by each subunit extend into several branches of the valley system, which indicates that the different branches have been infilled in same process. The valley branches have most likely been formed by subglacial meltwater currents with shifting paths during the same glacial event. The subsequent infilling process is interpreted to have taken place in the proglacial lacustrine environment. Some of the infilling sequences have a distinct chaotic signature indicating glaciotectonic deformation from a glacial readvance.

Subunit 70-03 and Subunit 70-04 represents laminated deposits. Subunit 70-03 contains silty clay and Subunit 70-04 contains deposits ranging from clay to sand.

Subunit 70-05 is a clay layer with a distinct chaotic signature which is interpreted to indicate that a glacial readvance has overridden the layer.

Subunit 70-06 is primarily a laminated deposit expected to consist of silt or clay, however no CPTs or boreholes sample this layer.

Subunit 70-07 represents deposits ranging from low to high amplitude in the seismic section and often chaotic reflections. The layer is interpreted to represent both proglacial fluvial and lacustrine deposits which have been glacially overridden. A single CPT sampling this layer indicates sand, however, the layer is expected to contain mixed lithologies.

Subunit 70-08 represents the upper part of Unit 70 in the northern part of the NNW located valley. Subunit 70-08 is a thick layer of proglacial lacustrine deposits consisting of silty clay and clay. The layer is separated from the underlying similar Subunit 70-09 by the impact of glaciotectonic deformation, which can be seen in top of Subunit 70-09, while laminae of Subunit 70-08 seem unaffected. However, later glacial events also do impact Subunit 70-08 in some areas.

Subunit 70-09 is present in most of the major valleys of Unit 70 and constitutes an often thick layer of mainly glaciolacustrine deposits.

In some areas the layer has been affected by glacial readvances seen as internal layer boundaries of glaciotectonic deformation. A minor part of the layer also represents subglacial deposits – both till and glaciofluvial sand and gravel. Otherwise, most of Subunit 70-09 is considered to consist of clay and silty clay.

Subunit 70-10 is the most extensively mapped subunit of Unit 70. The reflection pattern is often chaotic with varying amplitudes. Generally, Subunit 70-10 consists of subglacial fluvial deposits, till and glaciotectonically deformed proglacial fluvial and -lacustrine deposits.

In the major valleys Subunit 70-10 is often a relatively thin layer at great depth but is also present as the only unit in many valleys. From CPT and borehole samples, Subunit 70-10 is expected to be dominated by sandy deposits.

Subunit 70-11 is present only in the large valley in SE part of the site. Subglacial fluvial to proglacial lacustrine deposits are interpreted to dominate Subunit 70-11 but sub- and proglacial fluvial deposits are also interpreted to be part of the layer. The reflection pattern shows laminated to chaotic layers generally with high amplitudes. The deposits are dominated by sand.

Subunit 70-12 is the deepest subunit in the large valley in the SE part of the site and generally represents chaotic deposits interpreted to primarily be subglacial fluvial deposits and till. The reflection pattern is chaotic and generally with high amplitudes. The deposits are dominated by mixed lithologies (sand-silt-clay mixtures) or coarse deposits (sand and gravel).

Enclosure 3.31 shows the depth below seabed of the top of Unit 71 and enclosure 4.31 shows the thickness (isochore) of Unit 70.

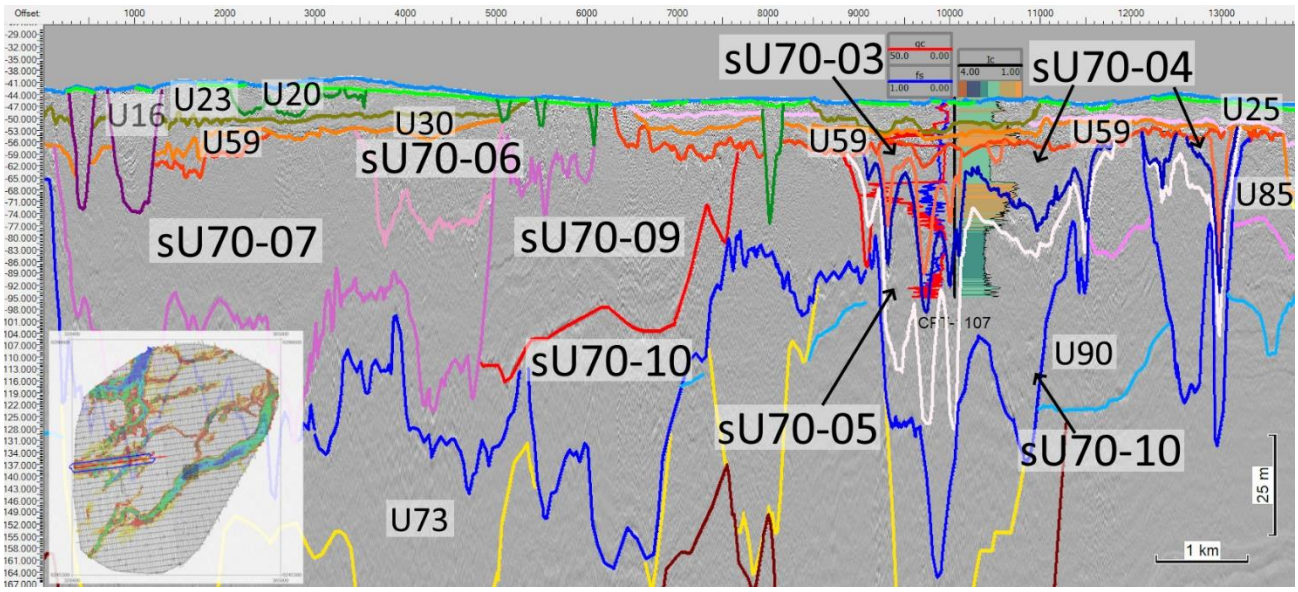

Figure 9-42: Subunits of Unit 70 (U70) as interpreted in section EAX2290P01 (Fugro) with geotechnical logs from LOC-1107.

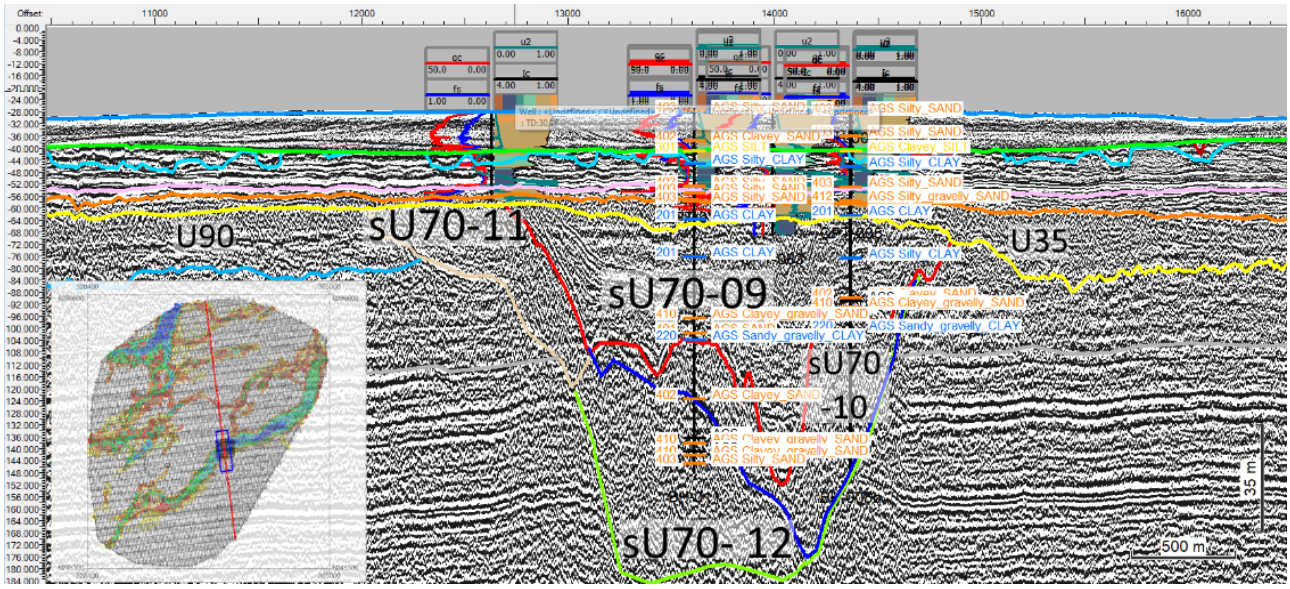

Figure 9-43: Subunits of Unit 70 (U70) as interpreted in section BM2_OWF_E_2D_04200 (MMT) with geotechnical logs from LOC-0164, LOC-0011, and LOC-0005.

Unit 73

Unit 73 (see Figure 9-44) is a unit which represents deep glaciotectonic deformation and mixing with underlying Miocene deposits. Within this unit it can be difficult to separate the Pleistocene deposits and the Miocene deposits. Boreholes within the area all indicate deposits that are interpreted to be of glacial origin.

Enclosure 3.32 shows the depth below seabed of the top of Unit 73 and enclosure 4.32 shows the thickness (isochore) of Unit 73.

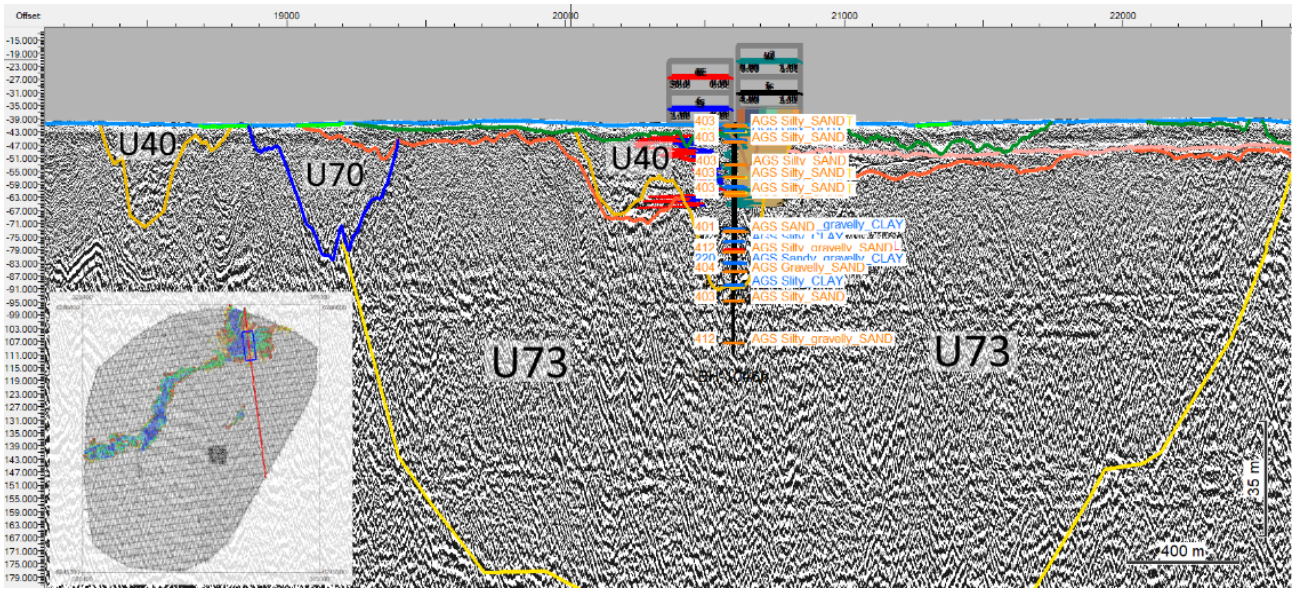

Figure 9-44: Unit 73 (U73) as interpreted in section BM4_OWF_E_2D_11340 (MMT) with geotechnical logs from LOC-1046.

9.8.6 Elsterian or older (Unit 75 to Unit 85)

The chronostratigraphic group Elsterian or older include layers which are interpreted to be older than the units in the Elsterian chronostratigraphic group. Some of the layers within this group is expected to predate the first glacial advance in Pleistocene. The ages of the deposits within this group are uncertain and could potentially include ages between Elsterian and Pliocene (Pre-Quaternary).

Unit 75

Unit 75 (see Figure 9-45) is present primary in the western part of the site and represent mainly sandy deposits interpreted to belong to periglacial or interglacial fluvial to lacustrine depositional environments. Layers of peat has been found within the unit.

Enclosure 3.33 shows the depth below seabed of the top of Unit 75 and enclosure 4.33 shows the thickness (isochore) of Unit 75.

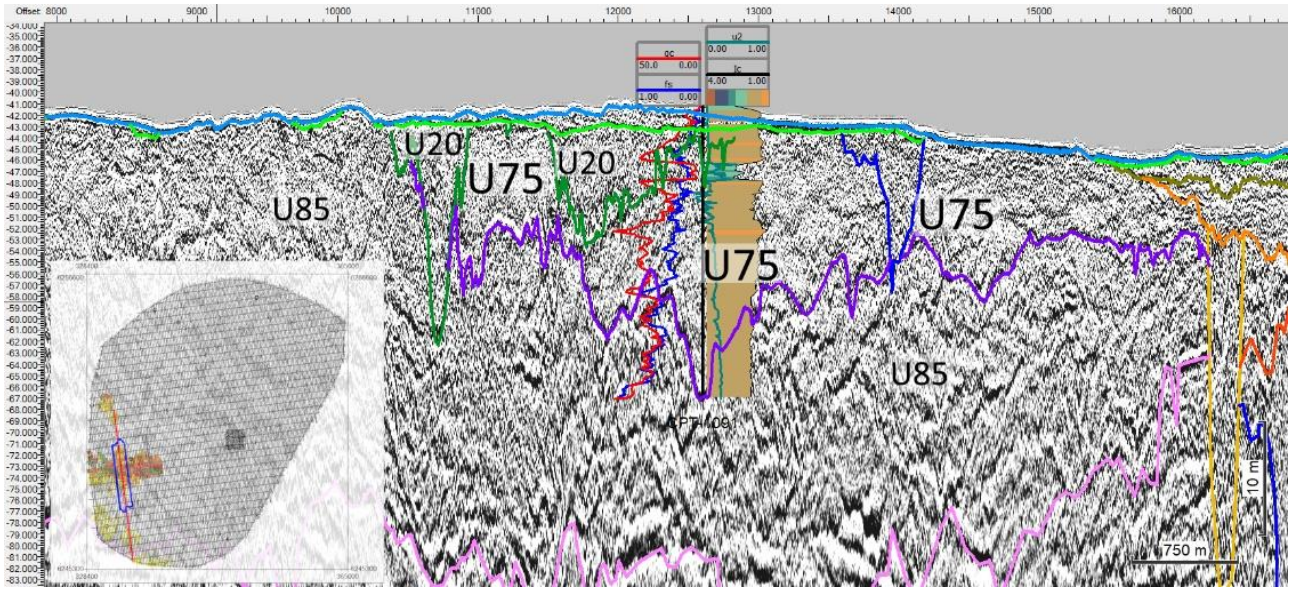

Figure 9-45: Unit 75 (U75) as interpreted in section EAF6073P01 (Fugro) with geotechnical logs from LOC-1091.

Unit 85

Unit 85 (see Figure 9-46) is present primary in the central, southern and western part of the site and represent mainly sandy deposits interpreted to belong to both subglacial fluvial, periglacial fluvial and pre-glacial fluvial environments.

It is difficult to determine the age of the unit more specifically. It is interpreted to be mixed – partly glacial Pleistocene, but also pre-glacial Pleistocene and possibly partly Pliocene deposits from the Eridanos river system (see section 7.1) (if the early Pleistocene and Pliocene deposits have been preserved in the area and not completely eroded away by the glaciations in Mid and Late Pleistocene).

Layers of peat have been found within the unit and is interpreted to originate from the fluvial system.

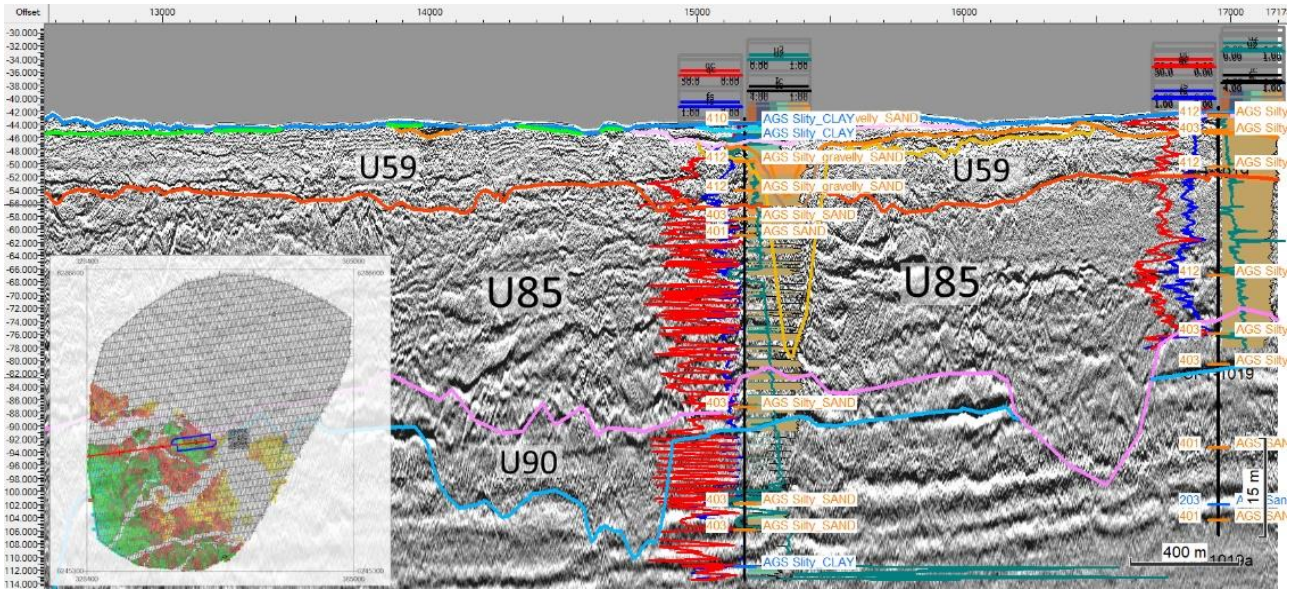

Figure 9-46: Unit 85 (U85) as interpreted in section EAX2287P01 (Fugro) with geotechnical logs from LOC-1017 and LOC-1019.

Since the layer primarily comprises sand, it has geotechnically been considered less important to subdivide the layer further.

Enclosure 3.34 shows the depth below seabed of the top of Unit 85 and enclosure 4.34 shows the thickness (isochore) of Unit 85.

9.8.7 Miocene (Unit 89 to Unit 96)

The Miocene chronostratigraphic group consists of four mainly marine units. Unit 89 consists of glaciotectonically deformed Miocene layers. Unit 90 is interpreted to consist of prodelta to fluvial deposit and Unit 95 and Unit 96 consist of laminated marine deposits.

Unit 89

Unit 89 (see Figure 9-47) consists of glaciotectonically deformed primarily Miocene marine deposits. The originally planar layers have been riddled with thrust faults and folds.

The décollement (gliding plane, basis of deformation) is in many places located deeper than the seismic sections, which reach approximately 190 m below MSL. The deformed deposits are considered primarily to be clay dominated parts of Miocene marine layers. Chronostratigraphically these deposits are expected to correlate mostly with Unit 96 but also Unit 95 in some areas.

In Figure 9-47 some of thrust fault lines are inclined in the opposite direction that primary trend (push from north-west) could indicate that some of the thrust blocks have been turned or folded. It could also just indicate that the direction of

the deformation has not be uniform the through the different ice sheet advances which have driven the deformation.

Unit 89 is not considered the line up with a paleo ice margin. The reason why the deformation has not continued further to the south is that the overlying sand layers (U75, U85, U90, upper part of U95) are considered too coarse grained for pore pressure to build up in the sediments below the ice margin to drive the deformation.

On a single location on the site, the Miocene layers are deformed by normal faults. This location is interpreted to have experienced local subsidence. The subsidence is interpreted to be caused by salt tectonics. Only the Miocene layers seem to have been affected by this deformation and the overlying deposits show no impact of the subsidence. This indicates that the subsidence took place before the overlying Quaternary layers were deposited.

According to Figure 7-1 the area covered by Unit 89 to some extent coincides with areas affected by salt-tectonics. However, the extensive thrust fault structures make it difficult to identify the impact of the salt-tectonics in the area.

Enclosure 3.35 shows the depth below seabed of the top of Unit 89 and enclosure 4.35 shows the thickness (isochore) of Unit 89.

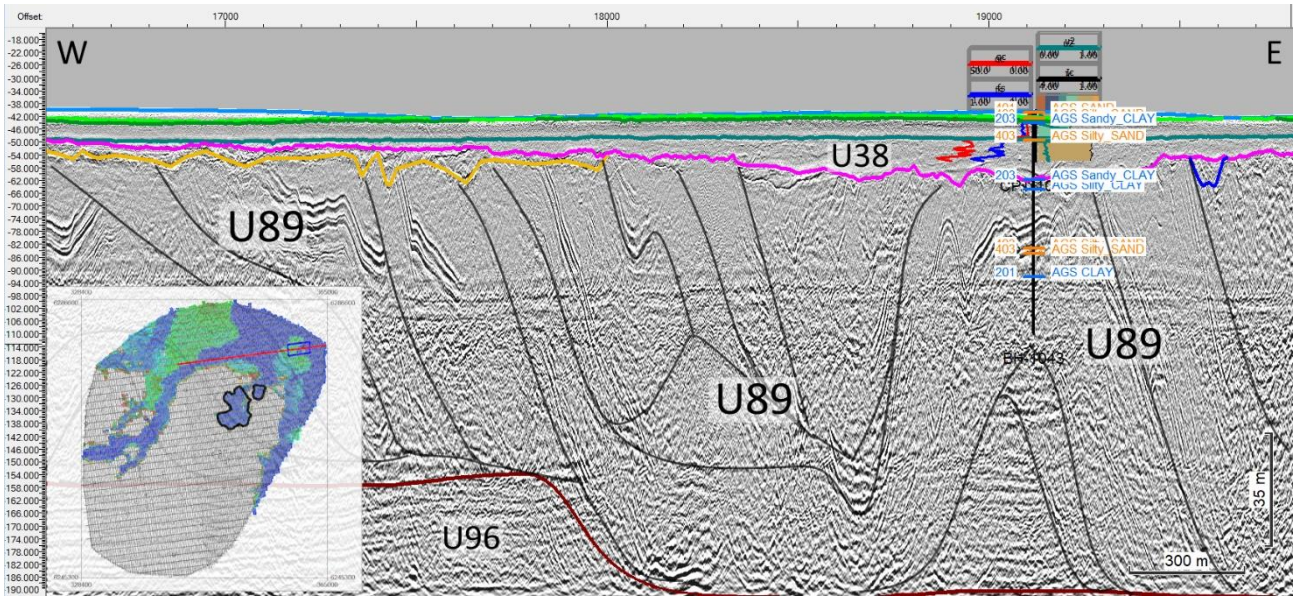

Figure 9-47: Unit 89 (U89) as interpreted in section BM2_OWF_E_XL_08000 (MMT) with geotechnical logs from LOC-1043. The black line polygons outline the area visibly influenced by subsidence interpreted to be caused by salt tectonics. Grey lines in the sections some of the thrust faults within Unit 89.

Unit 90

Unit 90 (see Figure 9-48) is interpreted to indicate fluvial to deltaic and pro-deltaic sand deposits which are interpreted to belong to Miocene (alternatively Pliocene).

Unit 90 could be related to the Marbæk Fm or the Luna Fm, but this correlation is uncertain. The base of Unit 90 has possibly been interpreted too shallow in the western part and the sand may extend deeper than the horizon indicates. The internal structure of Unit 90 ranges from large scale downlapping clinoforms most pronounced in the eastern part of its extent to transparent and slightly chaotic reflections with some sub-horizontal extensive internal reflectors.

Enclosure 3.36 shows the depth below seabed of the top of Unit 90 and enclosure 4.36 shows the thickness (isochore) of Unit 90.

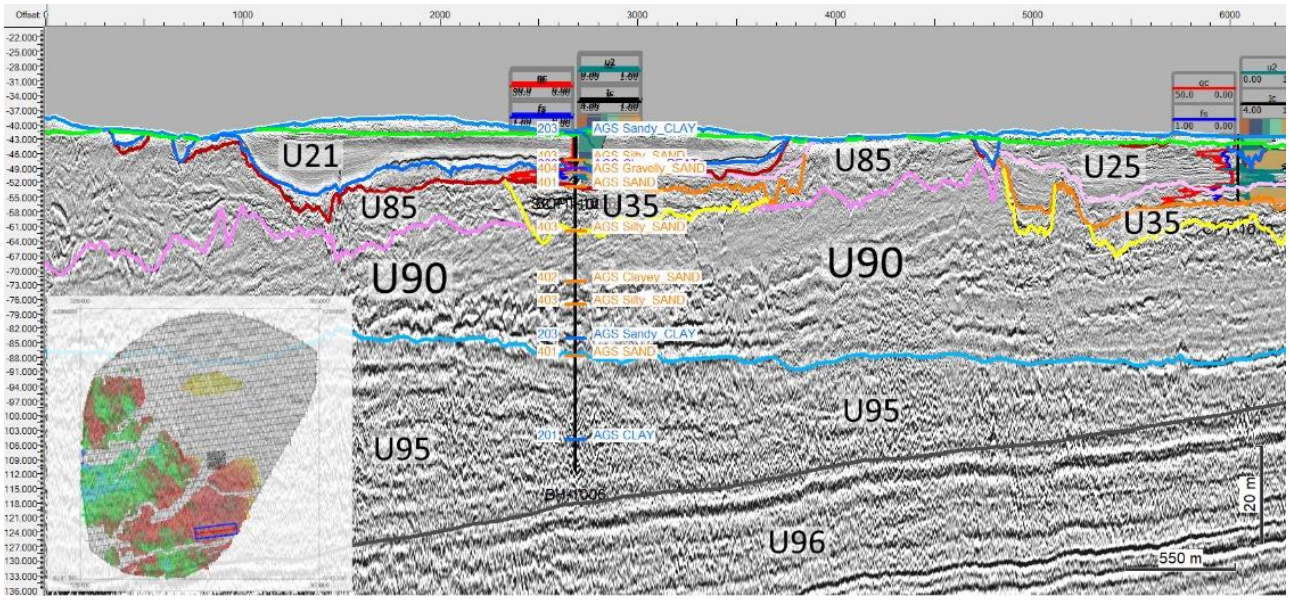

Figure 9-48: Unit 90 (U90) as interpreted in section BX4_OWF_E_XL_33000 (MMT) with geotechnical logs from LOC-1006.

Units 95 and 96

Unit 95 and Unit 96 (see Figure 9-49) consist primarily of laminated clay deposits. These could primarily be correlated to the Gram Fm. However, it is uncertain if internal sand layers could be correlated to the Marbæk Fm. The interpreted boundary between Unit 95 and Unit 96 was an attempt to divide a sandier upper unit from deeper more consistent clay unit. However, the boundary doesn't seem to match this trend everywhere – sand extends deeper in some areas and stops at shallower depths in other areas. The boundary has mostly been kept to provide an understanding and illustration of the dipping trend of the bedding planes of Unit 95 and Unit 96 towards southwest.

Even though the mapped boundary doesn't match a shift in trend completely (shift from sand and clay interlayering to consistent clay), the trend can be seen in samples and CPT responses across the OWF area.

Enclosure 3.37 shows the depth below seabed of the top of Unit 95 and enclosure 4.37 shows the thickness (isochore) of Unit 95. Enclosure 3.38 shows the depth below seabed of the top of Unit 96.

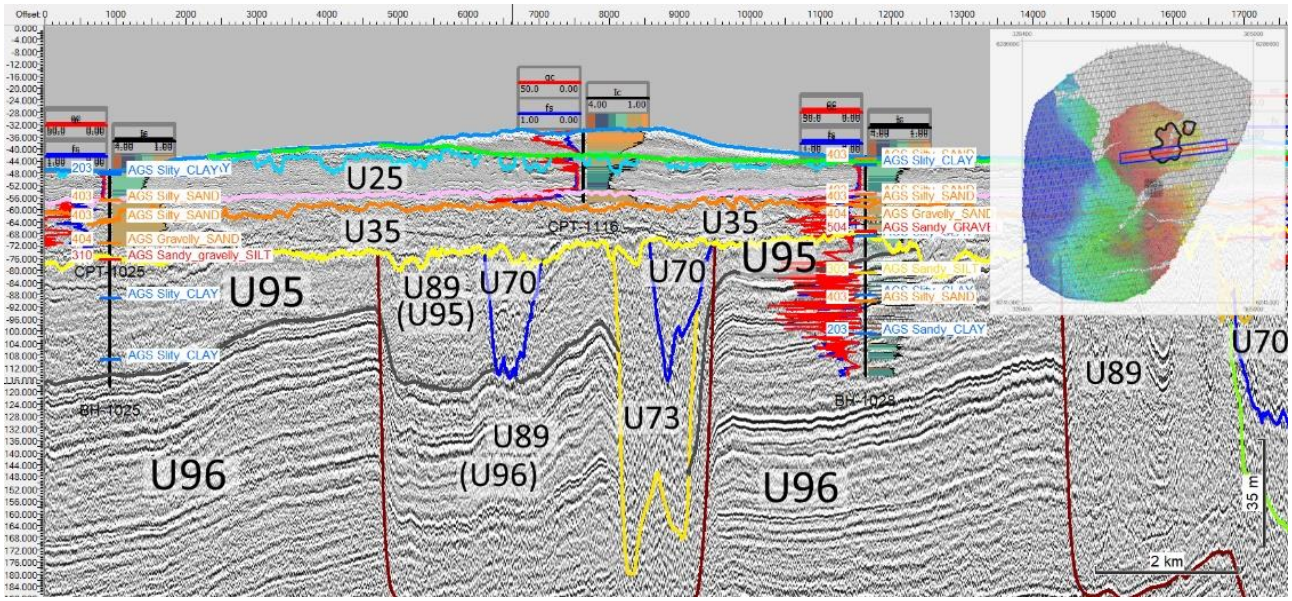

Figure 9-49: Unit 95 (U95) and Unit 96 (U96) as interpreted in section BX3_OWF_E_XL_17000 (MMT) with geotechnical logs from LOC-1025, LOC-1116, and LOC-1028. In the section between 4500 m and 9500 m U89 is interpreted to represent subsidence structures resulting from salt tectonics. The black line polygons outline the area visibly influenced by the subsidence.

10 Geotechnical zonation and representative soil profiles

Based on the geotechnical and geophysical data, and the interpreted model a soil zonation has been made. The soil zonation provides the basis for clustering the main geological deposits and structures relevant for the wind turbine foundations.

The soil zonation is further simplified into one single map dividing the entire site into seven (7) different geotechnical zones. The simplification is made by selecting the most significant parameters in relation to foundation conditions.

The purpose of the geotechnical zonation map is to provide a geological overview of the OWF project site with regards to foundation conditions. The map should ideally divide the OWF project site into a limited number of provinces with similar foundation conditions.

The workflow of the process is presented in Figure 10-1.

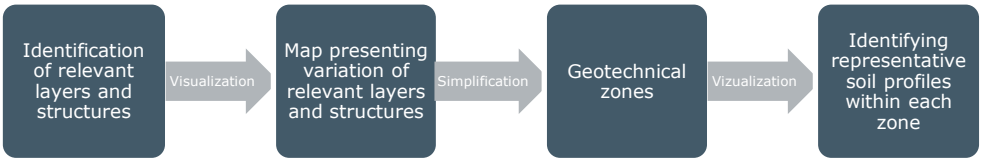

Figure 10-1 Workflow for dividing the area into geotechnical zones.

10.1.1 Identification of relevant layers and structures

For the geotechnical zonation of the OWF project site, relevant layers and structures have been identified. For the identification of these relevant layers and structures, focus have been on the following:

- Soils present at depths less than 50 m below seabed, as this depth range is considered relevant for wind turbine foundations.
- Mapping extent of weaker soil layers.

Regarding weaker soil layers, it is noted that the OWF project site generally consist of good soil conditions in regard to foundation installation and design. Some weaker geotechnical units which are normally consolidated to slightly over-consolidated are present. However, these geotechnical units generally have limited thickness (except for Geotechnical zone VII, cf. section 10.4.7) and hence their presence does generally not hinder foundation design, but they have some effect on foundation dimensions.

The ground conditions at the OWF project site consists of a large number of coarse-grained materials.

The coarse-grained material generally contains a high relative density (and hence also a high strength and stiffness) for both younger and older sediments. Some increase in relative density is however observed from the deposits in integrated model unit U30 to the deposits in integrated model unit U35. Hence, the depth to top of U35 (and deeper integrated model units) is considered a relevant boundary for zonation as a shallow depth below seabed to this boundary indicates competent ground conditions for WTG foundation design.

Within the Holocene, Late Weichselian and Weichselian chronostratigraphic groups, the clay deposits encountered are typically normally consolidated to slightly over-consolidated, whilst older clay deposits are generally over-consolidated to highly over-consolidated. Hence, the strength and stiffness of the clay deposits within Holocene, Late Weichselian and Weichselian are generally low, and the thickness of these clay deposits has a significant effect on the wind turbine foundations, with increasing thickness resulting in increased size of WTG foundations. The clays in integrated model units U13, U15 and U21 are generally slightly softer than the clays in integrated model units U17, U18, U23 and U25. Hence, for the geotechnical zonation the combined thickness of U13, U15 and U21, as well as the combined thickness of U13, U15, U17, U18, U21, U23 and U25 are relevant for the geotechnical zonation.

The material from the Elsterian and older chronostratigraphic groups show slightly higher over-consolidation compared to the material from Saalian chronostratigraphic group. Hence, the depth to top of integrated model unit U65 (and deeper units) is relevant for the geotechnical zonation as a shallow depth below seabed to this boundary indicates very competent ground conditions for WTG foundation design.

Given the above considerations four maps have been prepared. These maps are considered to provide valuable input for the geotechnical zonation. The presented maps are as follows:

- Figure 10-2 presents a map showing the combined thickness of U13, U15 and U21. The map hence shows the combined thickness of the softer clay layers within Holocene, Late Weichselian and Weichselian.

- Figure 10-3 presents a map showing the combined thickness of U13, U15, U17, U18, U21, U23 and U25. The map hence shows the combined thickness of clay layers within Holocene, Late Weichselian and Weichselian.

- Figure 10-4 presents a map showing the depth below seabed to top of U35 and deeper units. The map hence shows the depth to the high relative density material present in U35 and deeper and competent integrated model units.

- Figure 10-5 presents a map showing the depth below seabed to top of U65 and deeper integrated model units. The map hence shows the depth to the Elsterian and older chronostratigraphic groups which exhibit high over-consolidation ratio.

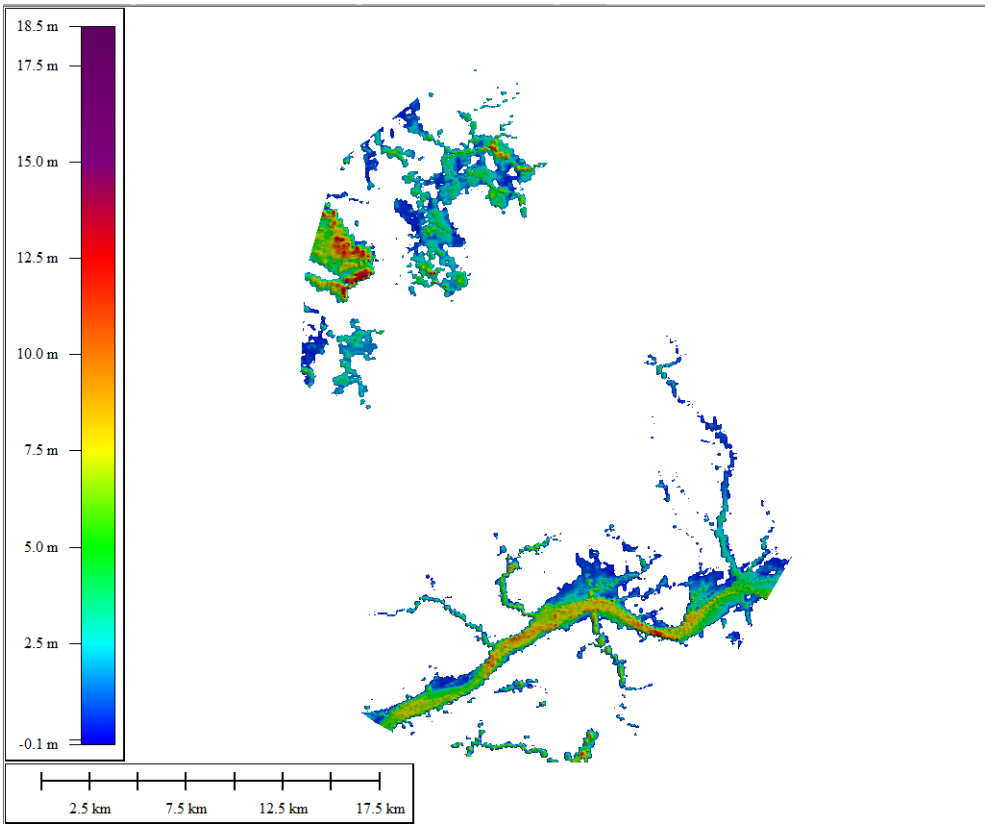

Figure 10-2 Combined thickness of U13, U15, and U21.

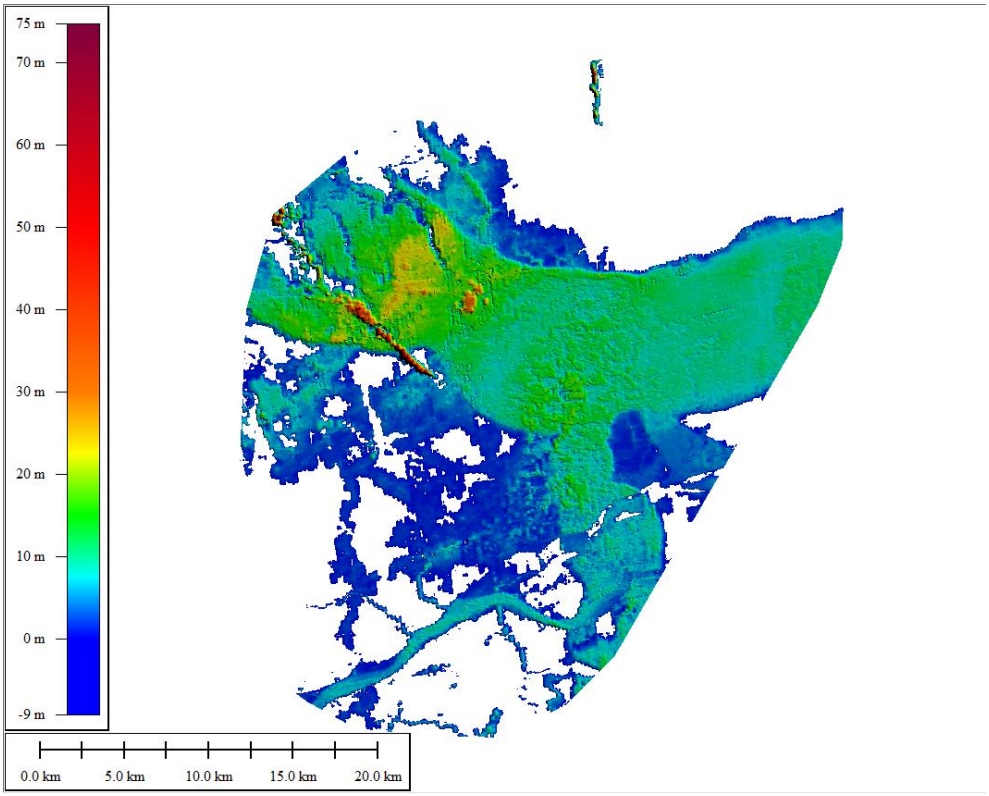

Figure 10-3 Combined thickness of U13, U15, U17, U18, U21, U23, and U25.

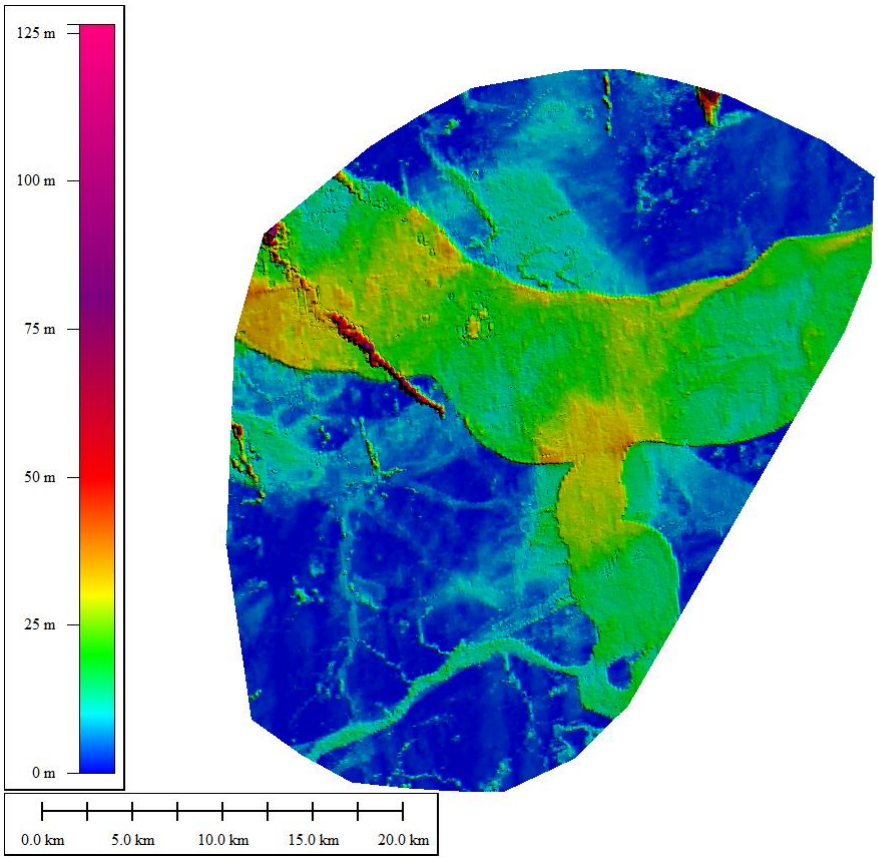

Figure 10-4 Depth below seabed to top of U35 and deeper units.

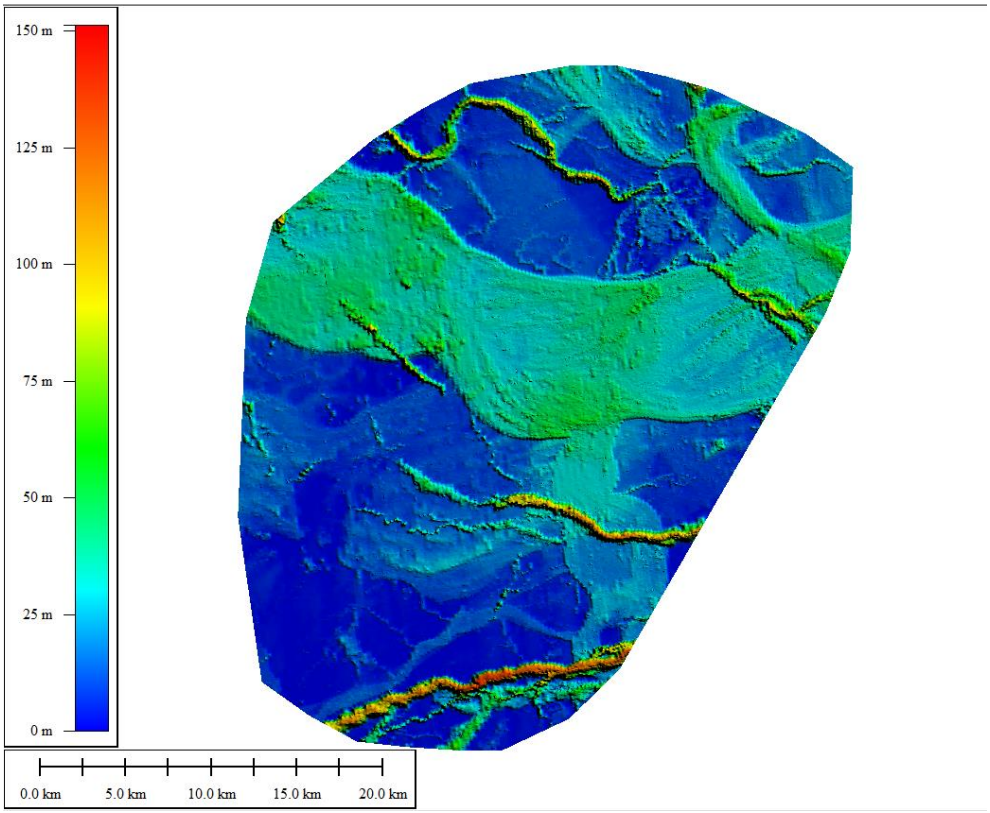

Figure 10-5 Depth below seabed to top of U65 and deeper units.

10.2 Variation of relevant layers and structures

Based on Figure 10-2 to Figure 10-5, the following relevant criteria have been defined for the combined thickness of U13, U15 and U21, for the combined thickness of U13, U15, U17, U18, U21, U23 and U25, for the depth to top of U35 and deeper units, and for the depth to top of U65 and deeper units. These criteria are as follows:

- Combined thickness of U13, U15, and U21 between 4 m and 8 m (See enclosure 1.06).
- Combined thickness of U13, U15, and U21 greater than 8 m (See enclosure 1.06).
- Combined thickness of U13, U15, U17, U18, U21, U23, and U25 between 4 m and 8 m (See enclosure 1.07).
- Combined thickness of U13, U15, U17, U18, U21, U23, and U25 greater than 8 m (See enclosure 1.07).
- Depth below seabed to top of U35 and deeper units greater than 12 m (See enclosure 1.08).
- Depth below seabed to top of U65 and deeper units greater than 25 m (See enclosure 1.09).

The above-mentioned criteria are in Figure 10-6 plotted on a map of the OWF project site. This map is also provided by Enclosure 1.05.

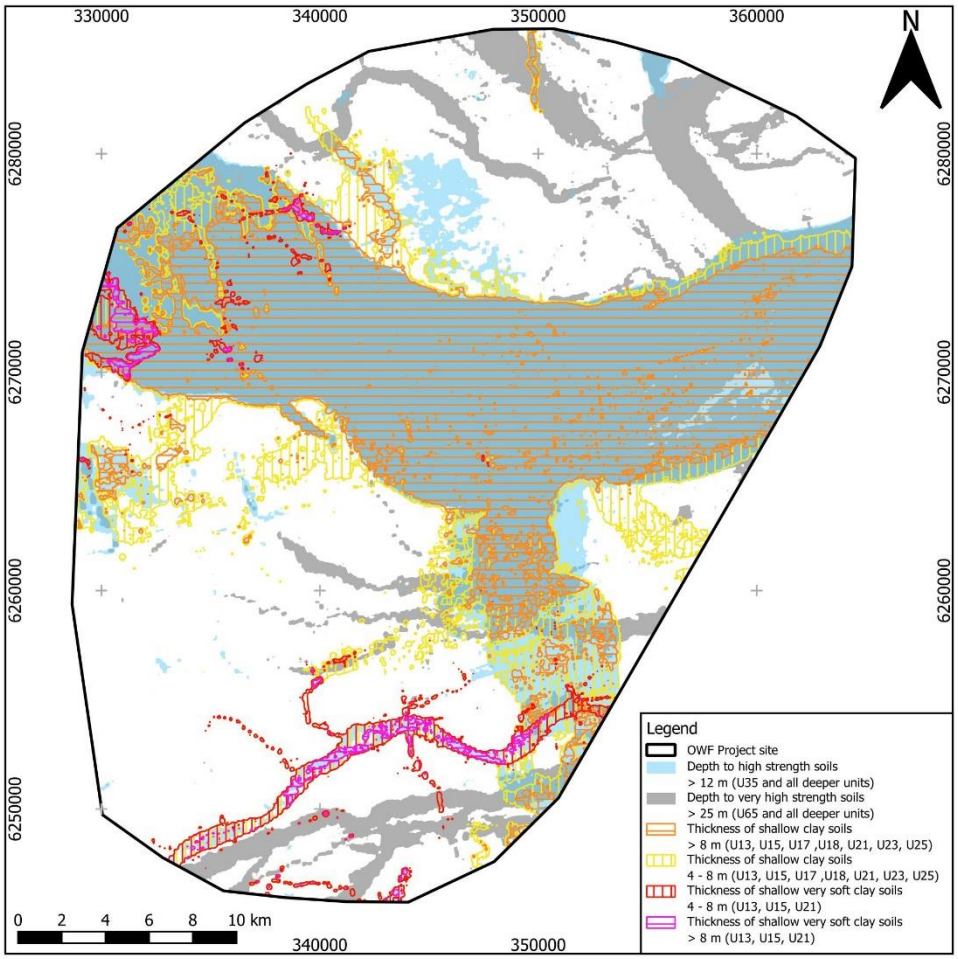

Figure 10-6 Map showing extent/variation across site of relevant layers and structures.

In addition to the above-mentioned criteria, it is noted that in one valley very thick deposits of soft clay is encountered. This valley can be seen on Figure 10-3, where the total thickness of U13, U15, U17, U18, U21, U23 and U25 in a small area reaches up to 70 m. This valley is not presented on Figure 10-6 as the valley overlaps several of the other areas and hence would reduce the readability of the figure. However, the valley is considered for the geotechnical zonation as part of geotechnical zone VII (see section 10.4.7).

10.3 Geotechnical zones

Geotechnical zones have been established based on the content of Figure 10-6. The geotechnical zones represent a simplification of Figure 10-6 aiming to have a limited number of geotechnical zones. For the simplification the following has been considered:

- The combined thickness of U13, U15 and U21 has been considered higher importance than the other criteria. Hence, in areas with large thickness of this material, sub-zones due to other criteria are not considered.

- The combined thickness of U13, U15, U17, U18, U21, U23 and U25 is considered higher importance than the depth to top of U35 and deeper units, and the depth to top of U65 and deeper units. Hence, for areas with large, combined thickness of U13, U15, U17, U18, U21, U23 and U25 also sub-zones due to these other criteria are not considered.

- The depth to top of U35 and deeper units is considered more important than the depth to top of U65 and deeper units. Hence, for areas with large depth to top of U35 and deeper units, sub-zones for the depth to U65 and deeper units are not considered.

Based on the above considerations seven (7) geotechnical zones as presented in Figure 10-7 have been defined. The geotechnical zonation map is also added as Enclosure 1.04. The characteristics of the geotechnical zones are described in detail in section 10.4. Geotechnical zone I to VI generally show good ground conditions for WTG foundation design and installation, with the conditions generally being most competent for Geotechnical zone I. For Geotechnical zone VII thick deposits of soft clay are anticipated and hence in this zone heavy WTG foundations are expected to be required.

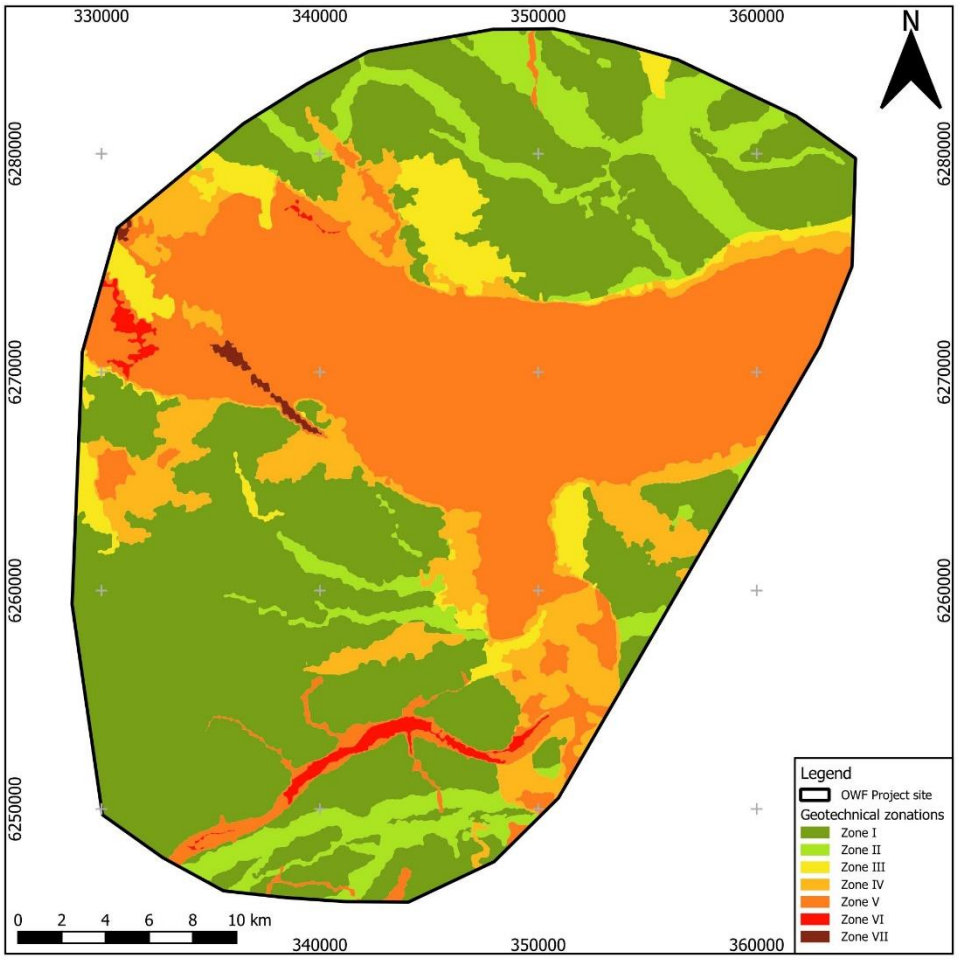

Figure 10-7 Geotechnical zonation.

10.4 Representative soil profile for each geotechnical zone

The seven (7) geotechnical zones are described in the following subsections, and further representative soil profiles are also presented. The representative profiles are selected based on geotechnical location tests present within each zone. For zones where a high number of tests are available, the representative profiles are selected from considering locations providing information to depths deeper than 50 m below seabed (Geotechnical zone I, II, IV and V) or 30 m below seabed (Geotechnical zone III). A summary of the following sections are found in section 10.4.8.

10.4.1 Geotechnical zone I

This zone is characterised by having limited depth to over-consolidated soil materials from Elsterian and older age. Also, the zone is characterised to comprise of no to very limited extent of soft clay. The soil material in this zone is therefore in general of high strength and high stiffness. Two representative profiles are selected for this zone due to the zone is covering a large area and the variation of soil stratigraphy across the zone. The two selected profiles are LOC-1008, where the CPT profile is presented in Figure 10-8 and the stratigraphy in table format is presented in Table 10-1, and LOC-1164, where the CPT profile is presented in Figure 10-9 and the stratigraphy in table format is presented in Table 10-2. The soil profile at LOC-1008 represents a sand dominated position, whilst LOC-1164 represent a clay dominated position.

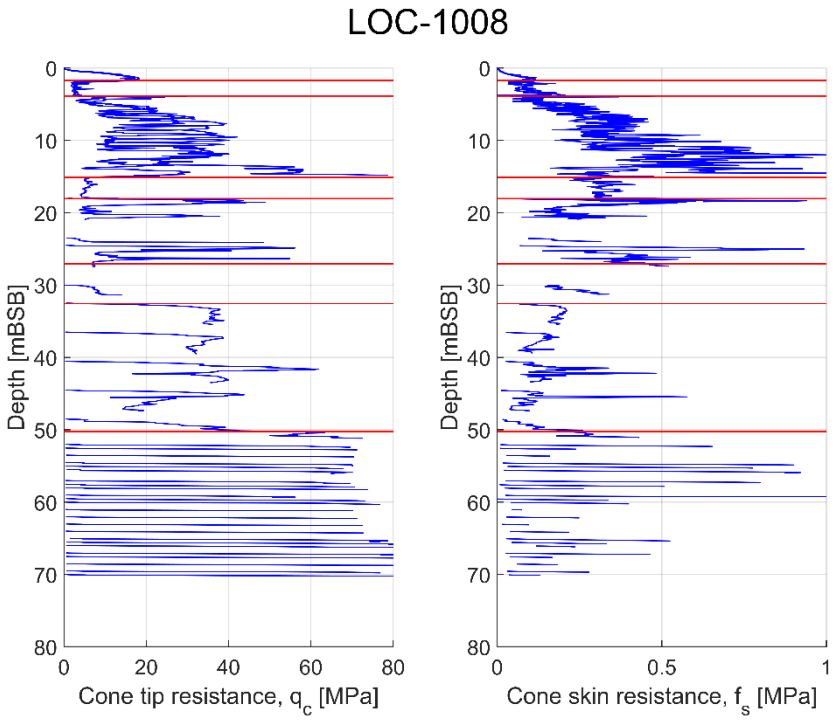

Figure 10-8 *q_c and f_s from CPT measurements for LOC-1008 found as representative for zone I. More information about the location can be found in Appendix A.*

Table 10-1 Soil stratigraphy for LOC-1008 found as representative for zone I.

Layer	Top [m]	Bottom [m]	Integrated model unit	Geotechnical unit
1	0	1.7	U10	Holocene Sand
2	1.7	3.9	U25	Weichselian Mix
3	3.9	15.1	U70-09	Elsterian Sand
4	15.1	18.0	U70-12	Elsterian Clay
5	18.0	27.1	U70-12	Elsterian Mix
6	27.1	32.6	U70-12	Elsterian Clay
7	32.6	50.3	U70-12	Elsterian Sand
8	50.3	70.2	U95	Miocene Sand

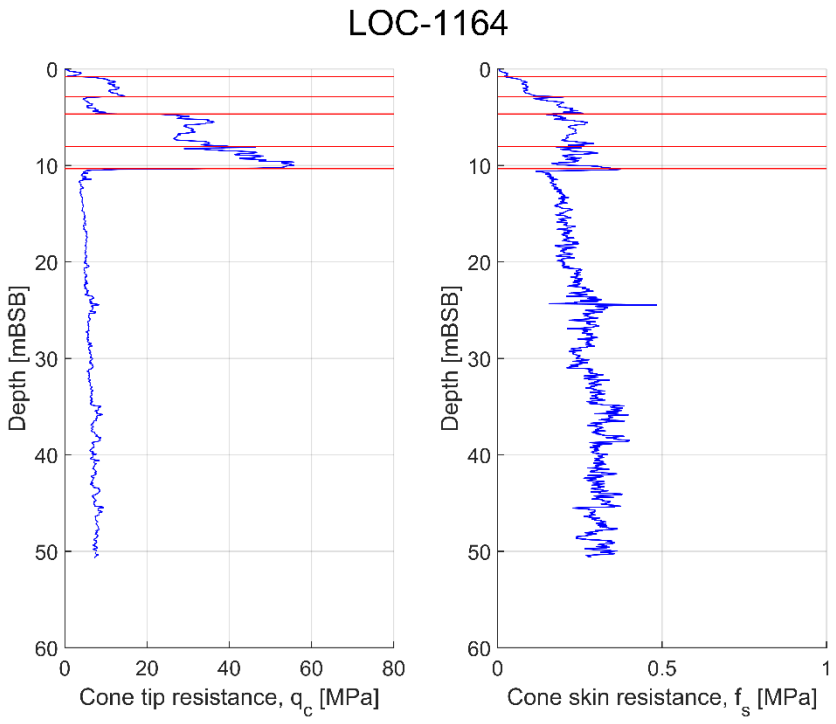

Figure 10-9 q_c and f_s from CPT measurements for LOC-1164 found as representative for zone I. More information about the location can be found in Appendix A.

Table 10-2 Soil stratigraphy for LOC-1164 found as representative for zone I.

Layer	Top [m]	Bottom [m]	Integrated model unit	Geotechnical unit
1	0	0.8	U10	Holocene Sand
2	0.8	2.9	U10	Holocene Sand
3	2.9	4.7	U20	Late Weichselian Sand
4	4.7	8.0	U30	Weichselian Sand
5	8.0	10.3	U57	Saalian Sand
6	10.3	50.7	U89	Miocene Clay

10.4.2 Geotechnical zone II

This zone is characterised by having presence of deposits from Saalian followed by older material. The zone is characterised to comprise of no to very limited extent of soft clay, and the soil material in this zone is generally over-consolidated and has high strength and high stiffness. Two representative profiles are selected for this zone due to the zone is covering a large area and the variation of soil stratigraphy across the zone. The two selected profiles are LOC-1047, where the CPT profile is presented in Figure 10-10 and the stratigraphy in table format is presented in Table 10-3, and LOC-1057, where the CPT profile is presented in Figure 10-10 and the stratigraphy in table format is presented in Table 10-3. The soil profile at LOC-1047 represents a position with very dense sand to 34.1 m depth underlain by layers of clay and mix material. The soil profile at LOC-1057 represents a position dominated by sand and mixed material.

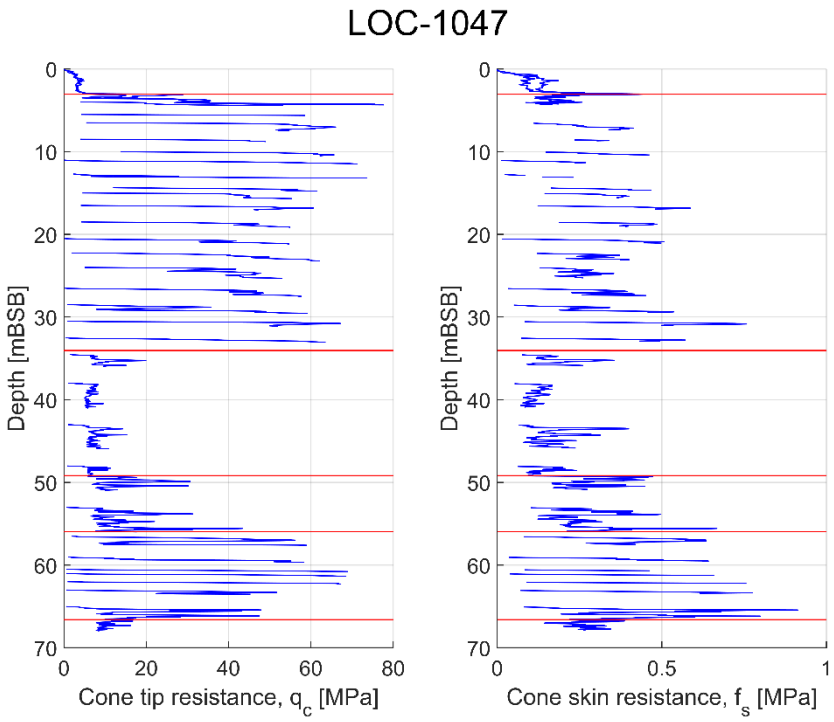

Figure 10-10 *q_c and f_s from CPT measurements for LOC-1047 found as representative for zone II. More information about the location can be found in Appendix A.*

Table 10-3 *Soil stratigraphy for LOC-1047 found as representative for zone II.*

Layer	Top [m]	Bottom [m]	Integrated model unit	Geotechnical unit
1	0	3.1	U13	Holocene Mix
2	3.1	34.1	U40-03	Saalian Sand
3	34.1	49.2	U40-03	Saalian Clay
4	49.2	55.9	U40-03	Saalian Mix
5	55.9	66.6	U40-03	Saalian Mix
6	66.6	67.9	U40-03	Saalian Clay

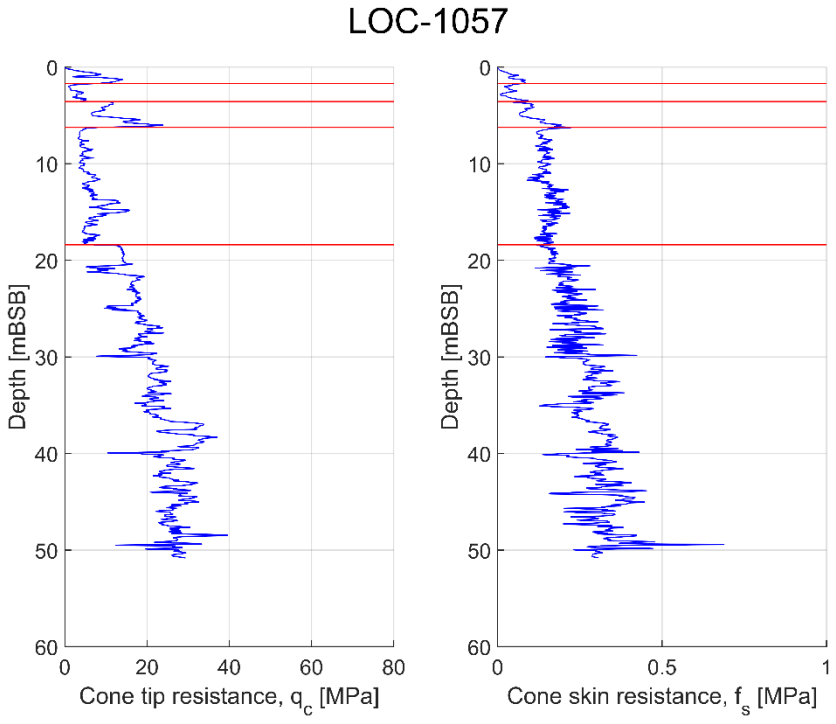

Figure 10-11 *q_c and f_s from CPT measurements for LOC-1057 found as representative for zone II. More information about the location can be found in Appendix A.*

Table 10-4 *Soil stratigraphy for LOC-1057 found as representative for zone II.*

Layer	Top [m]	Bottom [m]	Integrated model unit	Geotechnical unit
1	0	1.7	U10	Holocene Sand
2	1.7	3.6	U25	Weichselian Mix
3	3.6	6.3	U30	Weichselian Sand
4	6.3	18.4	U45-01	Saalian Mix
5	18.4	50.9	U45-02	Saalian Sand

10.4.3 Geotechnical zone III

This zone is characterised by having presence of more than 12 m of younger deposits showing limited over-consolidation. However, the younger deposits consist mainly of granular materials and hence with limited presence of soft clay. The representative profile for this zone is selected as LOC-1169 where the CPT profile is presented in Figure 10-12 and the stratigraphy in table format is presented in Table 10-5.

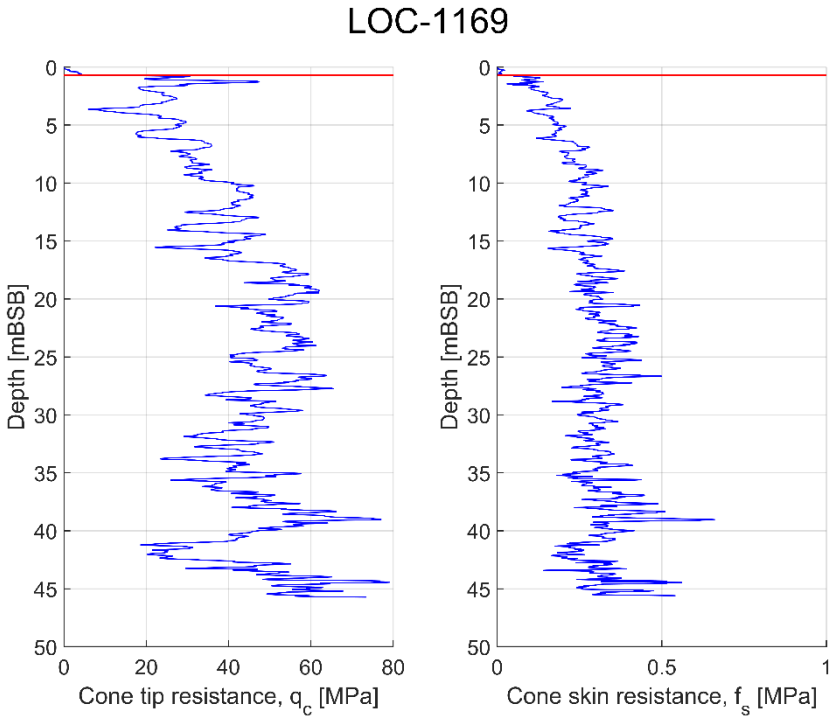

Figure 10-12 *q_c and f_s from CPT measurements for LOC-1169 found as representative for zone III. More information about the location can be found in Appendix A.*

Table 10-5 *Soil stratigraphy for LOC-1169 found as representative for zone III.*

Layer	Top [m]	Bottom [m]	Integrated model unit	Geotechnical unit
1	0	0.7	U10	Holocene Sand
2	0.7	45.7	U16	Late Weichselian Sand

10.4.4 Geotechnical zone IV

This zone is characterised by having between 4 m and 8 m total thickness of U13, U15, U17, U18, U21, U23 and U25, all mainly comprising slightly over-consolidated soft clay. The representative profile for this zone is selected as LOC-1152 where the CPT profile is presented in Figure 10-13 and the stratigraphy in table format is presented in Table 10-6.

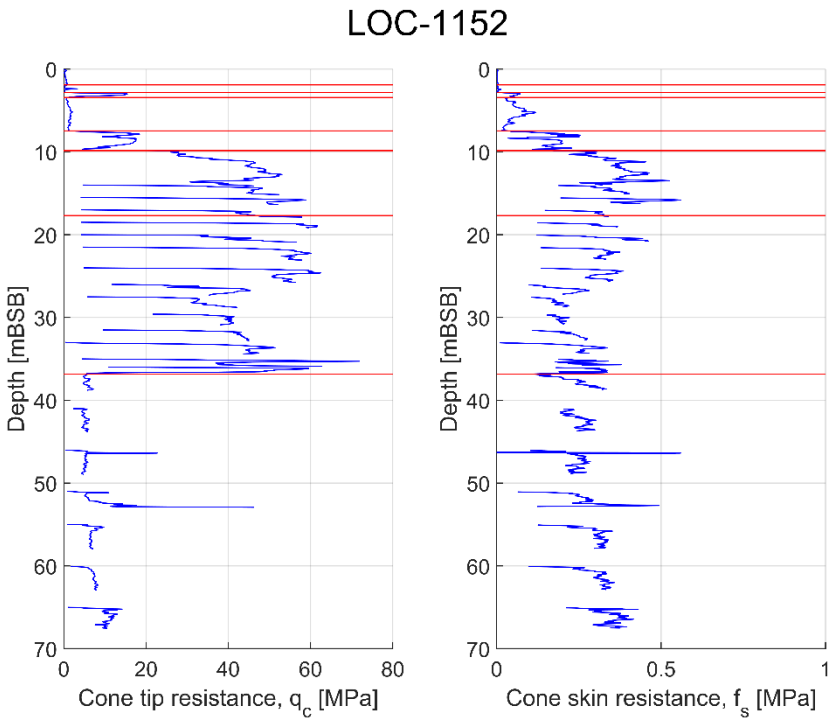

Figure 10-13 *q_c and f_s from CPT measurements for LOC-1152 found as representative for zone IV. More information about the location can be found in Appendix A.*

Table 10-6 *Soil stratigraphy for LOC-1152 found as representative for zone IV.*

Layer	Top [m]	Bottom [m]	Integrated model unit	Geotechnical unit
1	0	1.9	U10	Holocene Sand
2	1.9	2.8	U12	Holocene Clay
3	2.8	3.4	U13	Holocene Sand
4	3.4	7.5	U18	Late Weichselian Clay
5	7.5	9.8	U19	Late Weichselian Sand
6	9.8	17.7	U30	Weichselian Sand
7	17.7	36.9	U35	Weichselian Sand
8	36.9	67.6	U70-09	Elsterian Clay

10.4.5 Geotechnical zone V

This zone is characterised by having between 4 m and 8 m total thickness of U13, U15, and U21 (all mainly comprising normally consolidated soft clay) or more than 8 m total thickness of U13, U15, U17, U18, U21, U23, and U25 (comprising normally consolidated to slightly over-consolidated soft clay).

Large parts of the zone also show large depth to Saalian and older chronostratigraphical groups. The representative profile for this zone is selected as LOC-1150 where the CPT profile is presented in Figure 10-14 and the stratigraphy is table format is presented in Table 10-7.

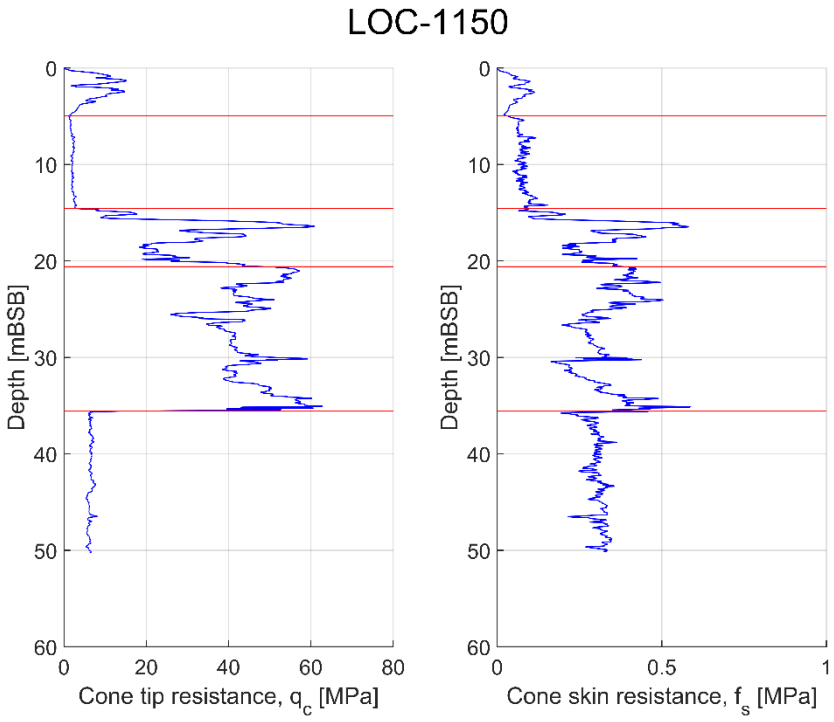

Figure 10-14 *q_c and f_s from CPT measurements for LOC-1150 found as representative for zone V. More information about the location can be found in Appendix A.*

Table 10-7 *Soil stratigraphy for LOC-1150 found as representative for zone V.*

Layer	Top [m]	Bottom [m]	Integrated model unit	Geotechnical unit
1	0	5.0	U10	Holocene Sand
2	5.0	14.6	U23	Weichselian Clay
3	14.6	20.6	U30	Weichselian Sand
4	20.6	35.6	U35	Weichselian Sand
5	35.6	50.3	U70-09	Elsterian Clay

10.4.6 Geotechnical zone VI

This zone is characterised by having more than 8 m total thickness of U13, U15, U21, all mainly comprising normally consolidated soft clay. The zone generally also shows large depth to Saalian and older chronostratigraphic groups.

The representative geotechnical profile is selected among two test locations being present within the zone. The location LOC-1127 is selected as the other position LOC-1065 is only available down to a depth of approximately 10 m below seabed. The CPT profile for the representative location (LOC-1127) is presented in Figure 10-15 and the stratigraphy is presented in Table 10-8.

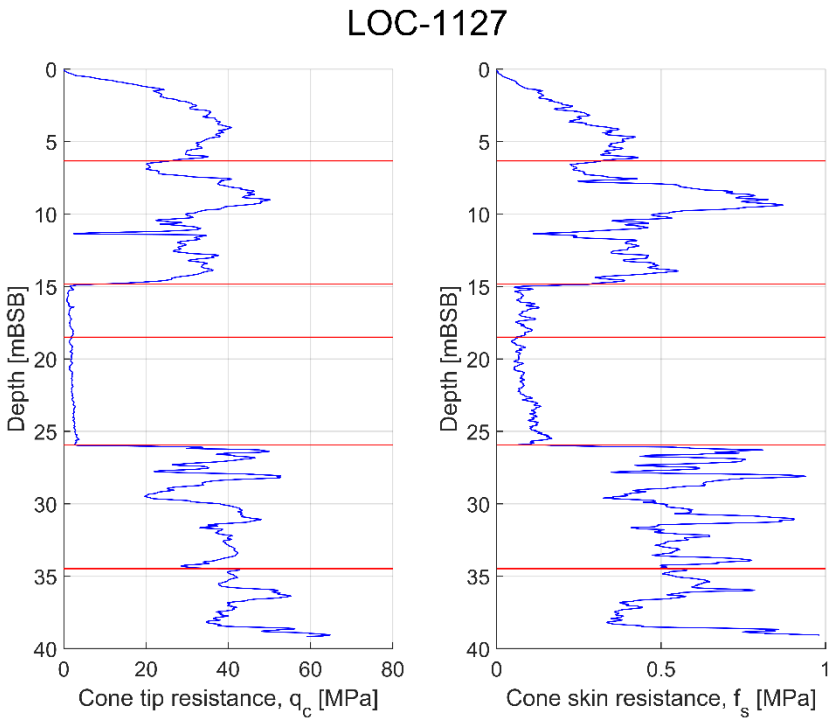

Figure 10-15 *q_c and f_s from CPT measurement for LOC-1127 found as representative for zone VI. More information about the location can be found in Appendix A.*

Table 10-8 *Soil stratigraphy for LOC-1127 found as representative for zone VI.*

Layer	Top [m]	Bottom [m]	Integrated model unit	Geotechnical unit
1	0	6.3	U10	Holocene Sand
2	6.3	14.8	U12	Holocene Sand
3	14.8	18.5	U15	Holocene Clay
4	18.5	26.0	U23	Weichselian Clay
5	26.0	34.5	U30	Weichselian Sand
6	34.5	39.2	U35	Weichselian Sand

10.4.7 Geotechnical zone VII

This zone is characterised by having very large total thickness of U13, U15, U17, U18, U21, U23 and U25 (up to 70 m total thickness), which generally consist of soft normally to slightly over-consolidated clay material. LOC-1122 is selected as the representative geotechnical profile as this is the only test location within the zone. The CPT profile is presented in Figure 10-16 together with the stratigraphy in Table 10-9.

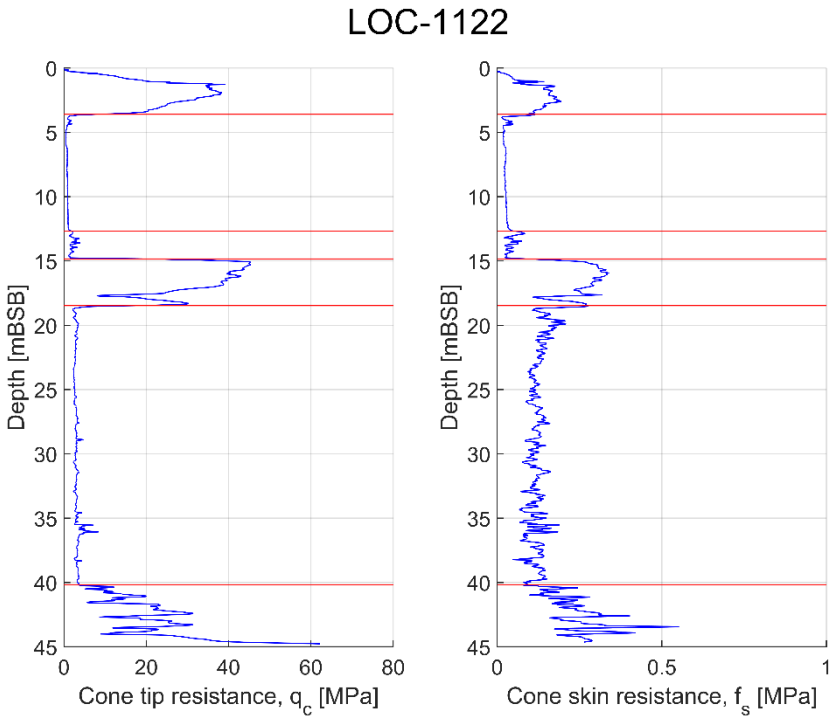

Figure 10-16 *q_c and f_s from CPT measurements for LOC-1122 found as representative for zone VII. More information about the location can be found in Appendix A.*

Table 10-9 *Soil stratigraphy for LOC-1122 found as representative for zone VII.*

Layer	Top [m]	Bottom [m]	Integrated model unit	Geotechnical unit
1	0	3.6	U11	Holocene Sand
2	3.6	12.7	U13	Holocene Clay
3	12.7	14.8	U14	Holocene Mix
4	14.8	18.5	U14	Holocene Sand
5	18.5	40.2	U17	Late Weichselian Clay
6	40.2	44.8	U19	Late Weichselian Mix

10.4.8 Summary

Based on the previous sections per geotechnical zone, a summary for the geotechnical zonation can be found in Table 10-10.

Table 10-10 Summary of geotechnical zonation.

Geotechnical zone	Representative location	Description
I	LOC-1008 & LOC-1164	Limited depth to over-consolidated geotechnical units from Elsterian and older age and no to very limited extent of soft clay. The soil material is in general of high strength and high stiffness. The two soil profiles represent a profile with mainly sand and a profile with mainly clay, respectively.
II	LOC-1047 & LOC-1057	Deposits from Saalian followed by older material and no to very limited extent of soft clay. Soil material is generally over-consolidated and has high strength and high stiffness. The two soil profiles represent a profile with mainly clay and mix material and a profile with mainly sand and mix material, respectively.
III	LOC-1169	More than 12 m of younger deposits showing limited over-consolidation. However, the younger deposits consist mainly of granular materials and hence with limited presence of soft clay.
IV	LOC-1152	Characterised by having between 4 m and 8 m total thickness of U13, U15, U17, U18, U21, U23 and U25, all mainly comprising slightly over-consolidated soft clay.
V	LOC-1150	Characterised by having between 4 m and 8 m total thickness of U13, U15, and U21 (all mainly comprising normally consolidated soft clay) or more than 8 m total thickness of U13, U15, U17, U18, U21, U23, and U25 (comprising normally consolidated to slightly over-consolidated soft clay). Large parts of the zone show large depth to Saalian and older chronostratigraphical groups.
VI	LOC-1127	Characterised by having more than 8 m total thickness of U13, U15, U21, all mainly comprising normally consolidated soft clay. Generally, shows large depth to Saalian and older chronostratigraphical groups.
VII	LOC-1122	This zone is characterised by having very large total thickness of U13, U15, U17, U18, U21, U23 and U25 (up to 70 m total thickness).

11 Leg penetration analysis

This section describes a high-level leg penetration risk assessment. The assessment is performed to provide an indication of potential geotechnical risks associated with jack-up operations at the OWF project site.

The assessment is intended to provide an overview of the potential behaviour of two selected generic vessel configurations, which can inform on potential jack-up risks during the next project phases and provide a basic understanding of how the risks vary from different vessel configurations.

In general, a leg penetration analysis performed at an offshore wind farm site, can help in:

- determining whether a jack-up is suitable for operating at a site or not,
- knowing what leg penetration behaviour and risks to anticipate,
- identifying and being able to mitigate possible geotechnical hazards.

Furthermore, leg penetration analysis is part of site-specific assessment that needs to be performed for all offshore wind farm sites once the project has matured further.

11.1 Selection of vessels

To provide a range of possibilities in terms of leg penetration behaviour and a good basic understanding of jack-up operations at the OWF project site, two different vessel configurations have been selected for the current study.

To select the appropriate vessel configurations, experience from previous leg penetration analyses (performed by COWI) has been used as database. The specifications of the vessels considered are confidential, however the selected vessels are characterized by the following:

- The vessels must be operational (recently) in Danish waters,
- The selected vessels shall give insight into the possible range of penetration behaviours, where the limits of the range roughly correspond to a generic installation vessel and a generic operation and maintenance (O&M) vessel. The range of penetration behaviour was deduced from several leg penetration analyses for representative soil conditions at the OWF project site.

The first vessel (further denoted Generic Installation Vessel) is a six-legged vessel, equipped with a large spudcan and a maximum preload of 84 MN, whereas the second vessel (further denoted Generic O&M Vessel) is a four-legged vessel, equipped with a smaller spudcan and a maximum preload of 7 MN.

The foundation pressure applied to the seabed is dependent on the spudcan area and geometry, which is confidential. The ratio of foundation pressure between the Generic Installation Vessel and the Generic O&M Vessel is around a factor 2.

The final decision on the type of vessel to be adopted for the OWF project site is based on several factors, such as:

- vessel suppliers tendering for the installation/maintenance work,
- type of foundation solution,
- crane capacity, incl. lifting height and (horizontal) reach,
- deck size and capacity with regard to planned operations, e.g., how many installation units can be stored at once,
- amount and complexity of structural adjustments to be made to adopt vessel to planned operations,
- speed, capacity, and size of the vessel,
- distance to the port,
- installation method, etc.

These are only a few of the factors that should be considered when selecting a certain jack-up vessel for installation works. All of them contribute to the final cost (and required duration) of the installation and should therefore be given special attention.

11.2 Geotechnical risks during jack-up

The main geotechnical risks that can be encountered during jack-up operations at an offshore wind site will be elaborated in the following subsections, cf. Ref. /35/. These are intended to give a high-level understanding of the spudcan behaviour and potential effects on the operations and how these effects may generally be handled or mitigated. During operations it is the responsibility of the owners, operators and crew on jack-ups to exercise sound judgement based on their education, training and experience, while taking into account leg penetration assessments provided, including related recommendations.

The term "preloading" should be well understood before discussing the risks. Preloading can be looked upon as a full-scale test, which eliminates some of the uncertainties related to soil behaviour. The initial soil displacement/compression obtained during preloading, which results in the leg penetration, will reduce/eliminate further leg penetrations during later operations under working loads. In general preloading shall be carried out corresponding to at least 1.5 times the actual maximum load during operations.

It is to be noted that the terms that describe the risk types used in this report might differ from the terms presented in various literature, therefore the description of the risks, failure mechanisms and particularities are more important than the actual terms. To highlight the most important characteristics of each of the risks, these have been gathered in Table 11-1.

Table 11-1 Overview of main characteristics of the geotechnical risks during jack-up.

Risk	Description	Circumstance	Effect	Observation	Consequence
Leg scour	Formation of local scour hole around spudcan	Cohesionless soil at seabed	Loss/reduction of soil bearing capacity	To be monitored continuously	Small [1)]
Squeezing	Thin and soft soil layer is squeezed horizontally	Thin, soft layer in between strong/stiff layers	Controllable leg settlements during initial preloading operations	Controllable penetration rate	Small
Fast leg penetration	Leg footing penetrates rapidly through strong layer and down to a soft layer	Thicker, soft layer below a strong/stiff layer	Structural damage, stability issues, personnel safety	Occurs during preloading before reaching maximum preload	Medium
Punch through	Leg footing penetrates rapidly through strong layer and down to a soft layer	Thicker, soft layer below a strong/stiff layer	Structural damage, significant stability issues, personnel safety	Occurs during operations after reaching maximum preload	High
Deep penetration	Leg has insufficient length to reach a stable penetration level	Penetration depth larger than available leg length	Non-operational, Lack of stability, risk for adjacent structures	To be mitigated before operations start	High
Difficulties during leg extraction	High resistance when attempting to extract legs after operations	Large suction below spudcan and large weight of soil above spudcan (can be caused by deep penetration in soft soils)	Operational downtime, structural damage, soil alteration at the location due to mitigation measures	To be mitigated before operations start	High

1) *Consequence is generally small when (initial phase of) operations consider scour adequately but can be large when scour occurs (very) fast or when their circumstance exists in combination with a soil stratigraphy where scour can result in a later risk of punch through, and insufficient attention should have been paid to the (possible) existence of these circumstances. Scour is dependent on the current velocity (at seabed), and this could consequently be larger at a later moment in time than during the preloading phase.*

11.2.1 Leg scour

Under certain flow and seabed conditions, seabed erosion may occur when temporarily introducing spudcans and/or jack-up legs. The presence of a spudcan/leg will cause the water flow in its vicinity to change. This local change in the flow will cause an increase in the sediment transport capacity on the seabed close to the structure, which can lead to the formation of a local scour hole.

When scour occurs the maximum bearing capacity of the soil beneath the spudcan will decrease due to loss of supporting soil. If the bearing capacity drops to a level below the footing load, additional penetration will occur.

Furthermore, scour may cause the spudcan to be loaded eccentrically and exert a corresponding load and bending moment on the spudcan and leg.

Relevant scour typically occurs when one or more of the situations below are encountered:

- Shallow water depths at jack-up locations,
- (Very) shallow spudcan penetrations into seabed,
- Cohesionless soil at seabed level.

Some of the most common mitigation measures are:

- If possible, planning of operations for periods when current velocities are lowest and during benign weather,
- Monitor scour during operations and take actions in accordance to observations,
- For operations with long durations, scour protection such as gravel beds, prefabricated mattresses and front mats can be used,
- Excavation to obtain larger initial penetration.

11.2.2 Squeezing

The potential for squeezing is present when a relative thin and soft layer is sandwiched between the leg footing and a harder layer or when the thin, soft layer is present between two stronger layers. The thin soil layer can in such cases squeeze laterally between the hard layers, when the vertical stress on this layer is large enough and occurs over sufficiently large finite area.

Ref. /32/ presents two criteria to be used in order to make an initial check for a possible risk of squeezing, see equations and figure below. If both geometrical criteria are satisfied, there is a potential risk of squeezing.

$$B > 3.45\,T$$

$$\frac{D}{B} \leq 2.5$$

B is the width of the spudcan

T is the thickness of the soft layer

D is the thickness of the soil above the soft layer

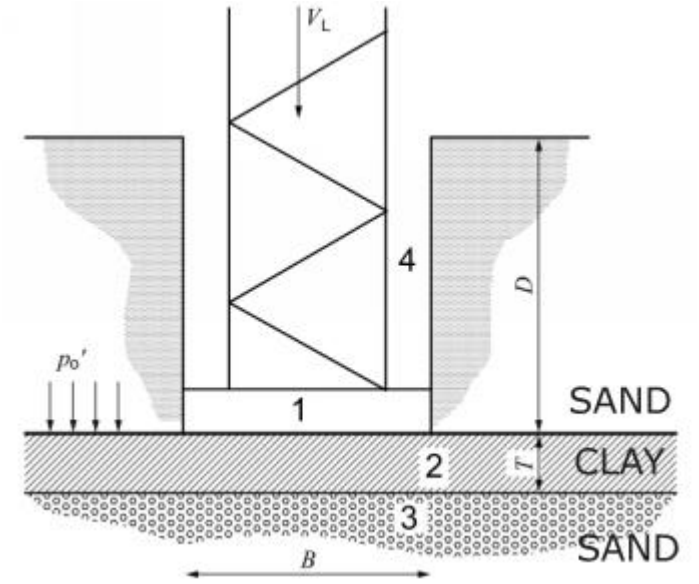

Figure 11-1 Sketch illustrating relevant parameters regarding squeezing, Ref. /32/.

It is important to note, however, that an actual risk of squeezing will only be present if the strength of the soft layer is insufficient relative to the vertical stress to be imposed on it. The difference in strength of the two materials (strong vs soft) should therefore be considered on top of the criteria shown above, which only relate to the geometry of the spudcan and soil situation.

The risk of squeezing generally leads to controllable leg settlements occurring during initial preloading operations. Therefore, most of the times no measures are taken to mitigate it.

11.2.3 Fast leg penetration

Fast leg penetration occurs in circumstances where a leg footing is temporarily supported by a stronger layer of soil that overlies a weaker layer and where the vertical footing load, as it is increased up to the preload, subsequently exceeds the bearing capacity of the soil, allowing the leg to penetrate rapidly through the stronger upper layer into the layer below.

In principle this is a punch through, see section 11.2.4, but as it occurs at a load level below the preload, the situation can be managed and is thus generally only referred to as fast (or rapid) leg penetration.

In such circumstances the upper soil layer may for instance be sand or stiff clay overlying soft clay. This type of failure is different to a squeezing failure described in section 11.2.2, as in this case the soil mass fails through large continuous soil failure surfaces rather than by many small internal soil shear failures within the weaker layer, which (only) cause the soil of the weaker layer to displace laterally. The penetration rates for squeezing are usually more controllable than penetration rates for fast leg penetration.

As the risk of fast leg penetration is defined to occur during preloading, it is important to make sure close and continuous monitoring is performed according to standards and the preloading is performed without jacking up completely out of the water (with zero air gap), such that in case a leg experiences fast/larger penetration than the others, the situation can be handled and the vessel will not tilt more than the allowable limit.

11.2.4 Punch through

The failure mechanism of punch through is the same as described above for fast leg penetration and occurs in circumstances where a leg footing has become temporarily supported by a stronger layer of soil that overlies a weaker layer, and where the vertical footing load, as it is increased, subsequently exceeds the foundation bearing capacity allowing the footing to penetrate rapidly through the upper layer into the layer below.

The main difference between fast leg penetration and punch through is that the former is defined as occurring before reaching the maximum preload, therefore occurring during close and continuous monitoring and with zero air gap, whereas the latter describes the potential occurrence of the same phenomenon, but after preloading (when the jack-up has an air gap), this making it (more/very) dangerous for the operations, possibly resulting in significant tilting of the jack-up with all related consequences. Because they are described by the same failure mechanism, sometimes both types of risk are referred to as “rapid penetration”.

Depending on the local soil conditions in terms of stratigraphy and strength of materials, it is sometimes difficult to predict which of the two types of risks (fast leg penetration and punch through) is expected at a certain location. Conducting a leg penetration analysis using a range of parameters usually helps in identifying the expected risk, provided that the soil data is reliable.

The quality of soil data is therefore one of the most important factors in estimating the penetration behaviour that will occur during jack-up operations.

When the soil conditions show a significant reduction in soil strength with penetration depth, then there is a potential for punch through to occur. However, Ref. /34/ suggests several procedures to mitigate punch through:

- carry out a detailed soil survey at the OWF project site,
- if spudcan data from previous penetrations at the location is available, use this to back analyse and confirm the prediction methods for bearing capacity,
- ensure procedures for reducing the spudcan loads during the potential punch through phases, including the use of buoyancy (preload in water) and zero air gap (prevent vertical displacement using buoyancy of the hull) and preloading of one leg at a time,
- consider the use of jetting system (if available) to penetrate the harder soils.

To conclude, an important observation provided in Ref. /34/ states that "*Whereas mitigation techniques exist to allow for the possibility of punch-through during the installation phase, there is none for the in-service condition. It is vital, therefore, that soil data is assessed carefully, and that actual penetration behaviour is used to verify predicted behaviour.*"

Therefore, reliable soil data is the most important factor in estimation and mitigation of potential risk of punch through.

11.2.5 Deep penetration

The risk of deep penetration exists when the leg penetration is larger than the available leg length of the jack up vessel.

Deep penetration occurs when the soil conditions are so soft, that they do not provide sufficient bearing capacity to reach the maximum preloading. This means that there is no available leg length left, but the leg has not reached a stable penetration level.

It is important to highlight situations in which the leg length of the vessel to be used may not be sufficient, as there will then generally be the need to employ a different vessel at the specific location/site. However, in some cases the selection of another vessel can be avoided. This is the case when there is the possibility to operate at a given location with smaller operational loads than considered for the initial assessment and these loads, and the related preloads, lead to less and feasible leg penetrations.

Deep penetrations may also pose a potential risk for adjacent structures.

11.2.6 Difficulties during leg extraction

The process of extracting the legs after operations at a certain location might sometime prove to be difficult and it is important to include this in the risk overview, such that the right measures are taken beforehand.

When extracting a leg and spudcan from a deep penetration in clay, the weight of the leg and the soil above the spudcan is to be overcome, together with the mobilised friction in the soil above the spudcan, and the suction below the spudcan. When the spudcan is in low permeable clay, the water cannot run freely to the bottom of the spudcan during extraction.

This implies that no equalising water pressure can develop below the spudcan during spudcan extraction. Thus, a resulting suction is developed below the spudcan, acting downwards, counteracting the retraction process.

According to Ref. /32/, leg extraction difficulties can be caused by conditions including the following:

- deeply penetrated spudcan in soft clay or loose silt,
- skirted or caisson-type spudcan where uplift resistance can be greater than the installation reaction,
- sites where the soil exhibits increased strength with time (this of course depends on the duration of the operations).

Ref. /32/ suggests jetting and/or excavation of the surface soils as mitigation measures against difficulties during leg extraction. A remark is added regarding soil alteration at the location due to these mitigation measures, which can affect future emplacement of jack-ups at the specific site.

11.3 Risk categories across the OWF project site

At the OWF project site, 269 unique soil investigation locations have been grouped into three different categories. For each of the categories, the primary geotechnical risks are defined and a graphical representation of all the locations and their corresponding category is presented in Enclosure 2.02 and 2.03.

It is important to acknowledge that the assessment presented here, and the associated evaluation of the geotechnical risk is based on local soil data, and that the outcome only applies to conditions that can be represented by the considered CPT profile and/or borehole. As such, lateral interpolation of risk between soil investigation locations is not possible and should be avoided.

When estimating the risk(s) at each location during this categorisation process, the CPT results and borehole logs have been considered, together with the soil strength of the layers, derived based on CPT results, as outlined in section 5 and 6.

The strength of sand layers is characterized by friction angle and the strength of clay and mixed soil conditions by the undrained shear strength.

To categorize the locations, the following factors have been considered:

- Stratigraphy at each location, based on CPT results. For categorization purposes, only the first 25 meters starting from the seabed have been considered, as the influence on the penetration behaviour for larger depths is considered negligible in relation to the currently assumed vessel configurations and spudcan geometries.

- The strength properties used for the assessment requires a constant value per layer. For estimating this, the required strength parameters for sand and clay are determined from the average of the value when disregarding the lowest and highest 10% of the data within the considered layer for removing small outliers. Mixed soil conditions are considered undrained for this assessment and the undrained strength is determined disregarding the lowest 10% and the highest 70% of the data. This has been done as the mixed soil conditions have larger variations within the layer, and the lower CPT measurements generally provide information on the clay part of the layer. The derived strength profiles considered for the assessment are presented in Appendix G.

- Penetration risk analysis was performed following ISO guidelines, as per Ref. /33/.

In Table 11-2 below, a summary of the three categories across the OWF project site when considering operations with both vessels, including their description and corresponding risks is presented.

Considering operations at the offshore wind site are performed with either one of the vessels selected in the study, the outcome of the analyses and the final categorisation is shown in Enclosure 2.02 and 2.03. Comparison of the results of the leg penetration analysis shown on

Enclosures 2.02 and 2.03 with the zonation presented in Figure 10-7 (and Enclosure 1.04) shows that the higher leg penetration risk mainly occurs in the geotechnical zones with thick layers of normally consolidated clays, which is also expected based on the considered criteria for the leg penetration analyses and the descriptions for the geotechnical zones defined from the zonation.

Table 11-2 Summary table presenting categories and corresponding potential risks.

Category	Description	Potential risk(s)
1	› Category 1 comprises locations where in the first 25 meters below the seabed only sand and/or very competent silt/clay layers are encountered. › If sand is encountered at seabed level, there might be a risk of scour.	› Leg scour
2	› Category 2 comprises locations where in the first 25 meters below the seabed only sand is encountered, except for an interbedded thin clay layer, which presents the potential for squeezing. › If sand is encountered at seabed level, there might be a risk of scour. › According to Ref. /32/ and considering the spudcan geometry of both vessels, the following criteria has been applied in order to select locations within Category 2: › Thickness of clay layer to be: › < 2.8 m (Generic Installation Vessel), › < 1.0 m (Generic O&M Vessel). › Top of clay layer to be: › ≤ 24.4 m depth (Generic Installation Vessel), › ≤ 8.7 m depth (Generic O&M Vessel). › The formula given in Ref. /32/ is not dependent on the strength of clay layer. In the current assessment it was however considered relevant to consider that only a clay layer with a corresponding conservative c_u as per below has the potential of squeezing: › < 300 kPa (Generic Installation Vessel) › < 200 kPa (Generic O&M Vessel)	› Leg scour › Squeezing
3	› Category 3 comprises locations where in the first 25 meters below the seabed sand is encountered and overlies a thick clay layer, which presents potential for rapid penetration, i.e., the risk of fast leg penetration (if rapid penetration occurs during preloading) or punch through (if rapid penetration occurs during operations). › If sand is encountered at seabed level, there might be a risk of scour. › To select locations within Category 3, the following criteria has been applied: › Thickness of clay layer to be (in order not to consider squeezing): › > 2.8 m (Generic Installation Vessel), › > 1.0 m (Generic O&M Vessel). › Strength of clay layer c_u › < 150 kPa (Generic Installation Vessel), › < 100 kPa (Generic O&M Vessel). › In the event of fast leg penetration or punch through occurring, the spudcan can penetrate deep into clay layer, thus leading to potential retraction difficulties, due to suction below spudcan and weight of soil above spudcan.	› Leg scour › Fast leg penetration › Punch through › Difficulties during leg extraction

12 List of deliverables

Below is a complete list of appendixes and enclosures delivered with this report.

Appendixes	
Number	Title
Appendix A	Interpreted stratigraphy at CPT locations
Appendix B	CPT for geotechnical units
Appendix C	Calculated soil properties per CPT location
Appendix D	CPT plots per geotechnical unit including properties from laboratory testing
Appendix E	Range of soil properties per geotechnical unit
Appendix F	Conceptual geological model
Appendix G	Soil profiles for LPA assessment
Appendix H	Units in superseded models
Appendix I	Units in updated integrated geological model

Enclosures	
Number	Title
1.01	Overview map Bathymetry
1.02	Overview map Survey lines - SBP
1.03	Overview map Survey lines - 2D UHRS
1.04	Geotechnical zonation
1.05	Variation of relevant geotechnical layers
1.06	Shallow, very weak clay soils (U13, U15, U21) Thickness (isochore)
1.07	Shallow, very weak to weak clay soils (U13, U15, U17, U18, U21, U23, U25) Thickness (isochore)
1.08	Depth to high strength soils (U35 and all deeper units)
1.09	Depth to very high strength soils (U65 and all deeper units)
2.01	Geotechnical test locations
2.02	Leg penetration analysis - Generic Installation Vessel
2.03	Leg penetration analysis - Generic O&M Vessel
3.01	Top of model layer Unit 10 Depth below seabed
3.02	Top of model layer Unit 11 Depth below seabed
3.03	Top of model layer Unit 12 Depth below seabed
3.04	Top of model layer Unit 13 Depth below seabed
3.05	Top of model layer Unit 14 Depth below seabed
3.06	Top of model layer Unit 15 Depth below seabed
3.07	Top of model layer Unit 16 Depth below seabed
3.08	Top of model layer Unit 17 Depth below seabed
3.09	Top of model layer Unit 18 Depth below seabed
3.10	Top of model layer Unit 19 Depth below seabed
3.11	Top of model layer Unit 20 Depth below seabed
3.12	Top of model layer Unit 21 Depth below seabed
3.13	Top of model layer Unit 22 Depth below seabed
3.14	Top of model layer Unit 23 Depth below seabed
3.15	Top of model layer Unit 24 Depth below seabed
3.16	Top of model layer Unit 25 Depth below seabed
3.17	Top of model layer Unit 30 Depth below seabed
3.18	Top of model layer Unit 35 Depth below seabed
3.19	Top of model layer Unit 37 Depth below seabed
3.20	Top of model layer Unit 38 Depth below seabed
3.21	Top of model layer Unit 40 Depth below seabed
3.22	Top of model layer Unit 41 Depth below seabed
3.23	Top of model layer Unit 42 Depth below seabed
3.24	Top of model layer Unit 45 Depth below seabed
3.25	Top of model layer Unit 50 Depth below seabed
3.26	Top of model layer Unit 56 Depth below seabed

Enclosures	
Number	Title
3.27	Top of model layer Unit 57 Depth below seabed
3.28	Top of model layer Unit 58 Depth below seabed
3.29	Top of model layer Unit 59 Depth below seabed
3.30	Top of model layer Unit 65 Depth below seabed
3.31	Top of model layer Unit 70 Depth below seabed
3.32	Top of model layer Unit 73 Depth below seabed
3.33	Top of model layer Unit 75 Depth below seabed
3.34	Top of model layer Unit 85 Depth below seabed
3.35	Top of model layer Unit 89 Depth below seabed
3.36	Top of model layer Unit 90 Depth below seabed
3.37	Top of model layer Unit 95 Depth below seabed
3.38	Top of model layer Unit 96 Depth below seabed
4.01	Layer Unit 10 Thickness (isochore)
4.02	Layer Unit 11 Thickness (isochore)
4.03	Layer Unit 12 Thickness (isochore)
4.04	Layer Unit 13 Thickness (isochore)
4.05	Layer Unit 14 Thickness (isochore)
4.06	Layer Unit 15 Thickness (isochore)
4.07	Layer Unit 16 Thickness (isochore)
4.08	Layer Unit 17 Thickness (isochore)
4.09	Layer Unit 18 Thickness (isochore)
4.10	Layer Unit 19 Thickness (isochore)
4.11	Layer Unit 20 Thickness (isochore)
4.12	Layer Unit 21 Thickness (isochore)
4.13	Layer Unit 22 Thickness (isochore)
4.14	Layer Unit 23 Thickness (isochore)
4.15	Layer Unit 24 Thickness (isochore)
4.16	Layer Unit 25 Thickness (isochore)
4.17	Layer Unit 30 Thickness (isochore)
4.18	Layer Unit 35 Thickness (isochore)
4.19	Layer Unit 37 Thickness (isochore)
4.20	Layer Unit 38 Thickness (isochore)
4.21	Layer Unit 40 Thickness (isochore)
4.22	Layer Unit 41 Thickness (isochore)
4.23	Layer Unit 42 Thickness (isochore)
4.24	Layer Unit 45 Thickness (isochore)
4.25	Layer Unit 50 Thickness (isochore)
4.26	Layer Unit 56 Thickness (isochore)
4.27	Layer Unit 57 Thickness (isochore)
4.28	Layer Unit 58 Thickness (isochore)
4.29	Layer Unit 59 Thickness (isochore)
4.30	Layer Unit 65 Thickness (isochore)
4.31	Layer Unit 70 Thickness (isochore)
4.32	Layer Unit 73 Thickness (isochore)
4.33	Layer Unit 75 Thickness (isochore)
4.34	Layer Unit 85 Thickness (isochore)
4.35	Layer Unit 89 Thickness (isochore)
4.36	Layer Unit 90 Thickness (isochore)
4.37	Layer Unit 95 Thickness (isochore)
5.01	Cross section BM2_OWF_E_2D_04200
5.02	Cross section BM3_OWF_E_2D_06720
5.03	Cross section BM4_OWF_E_2D_09030
5.04	Cross section BM5_OWF_E_2D_12600
5.05	Cross section BM5_OWF_E_2D_15330
5.06	Cross section BM6_OWF_E_2D_19320
5.07	Cross section BX2_OWF_2D_Baseline_1
5.08	Cross section BX3_OWF_2D_Baseline_2
5.09	Cross section EAD6049P01

Enclosures	
Number	Title
5.10	Cross section EAH6097P01
5.11	Cross section EAM6145P01 and EAM6145P02
5.12	Cross section EAQ6193P01
5.13	Cross section EAU6241P01
5.14	Cross section EAX2273P01 and BX4_OWF_E_XL_36000
5.15	Cross section EAX2282P01 and BX4_OWF_E_XL_27000
5.16	Cross section EAX2306P01 and BX1_OWF_E_XL_03000

Digital deliverables *)	
Item	Format
Kingdom Suite Project (version 2022) including spatial geological model	Kingdom project
Geotechnical Appendix G data	Excel file
Bathymetry/ Bathymetry Depth below MSL [m]	GeoTIFF
Boreholes/ Boreholes, Boreholes_island	ESRI Shapefile
Boreholes/ Boreholes_island	ESRI Shapefile
General/ OWF project site	ESRI Shapefile
General/ Danmark_outline_region	ESRI Shapefile
General/ EEZ_external_DK	ESRI Shapefile
General/ Eu_countires	ESRI Shapefile
General/ OWF Zone East	ESRI Shapefile
General/ OWF Zone West	ESRI Shapefile
General/ Island area	ESRI Shapefile
General/ Site area	ESRI Shapefile
LPA/ Leg penetration analysis	ESRI Shapefile
LPA/ Leg penetration analysis_island	ESRI Shapefile
Model layers/ Top of model layers, depth below seabed (grids)	ASCII and GeoTIFF
Model layers/ Isopach grids (vertical layer thickness)	ASCII and GeoTIFF
Geotechnical zones	ESRI Shapefile

13 Conclusions

A 3D integrated geological model has been made for the entire OWF project site for the Energy Island project. The new model comprises a merged, updated, and revised version of the existing geophysical models and is based on the newly gathered geotechnical and seismic data.

With respect to the purpose of the integrated geological model a new and better basis can now be provided for developers to evaluate the ground conditions in relation to foundation assessment and positioning of offshore wind turbines.

The integrated geological model contains 38 integrated model units. Thus, the existing geophysical model has been revised with respect to both the number of layers as well as to the spatial distribution of the layers. The model comprises layers of Holocene, Pleistocene, and Miocene deposits.

Together with the new model, updated geological descriptions of the geological layers in the model are provided. The descriptions include stratigraphical, lithological, and geotechnical characteristics.

The integrated geological model is delivered as a digital 3D model in a Kingdom suite project. Enclosures provided with the digital model present the new layers with respect to depth below seabed, thickness, and lateral extent. The enclosures are also supporting the geotechnical zonation where thickness and depth of grouped units of importance from the geological model are presented.

Sixteen (16) cross sections distributed over the entire OWF-project site show the layering in the model. The cross sections follow the seismic survey lines and display CPT logs (q_c, f_s, u_2, and I_c) and geological descriptions from boreholes at top of layers from boreholes located on the seismic survey lines.

A geotechnical zonation has been made from the geological model with focus on the low and high strength deposits and geological structures assessed to be important for the foundation design and installation works. The soil zonation maps have been simplified into a single map showing seven (7) selected geotechnical zones which provides a geological overview of the entire site relevant for foundation conditions. One of these geotechnical zones (VII) shows presence of soft clay to large depth below seabed. The other geotechnical zones generally comprise competent geotechnical deposits, however, some of the geotechnical zones (IV to VI) have presence of soft clay at shallow depths.

The leg penetration risk has been assessed for each of the geotechnical survey locations, and for two generic vessels a risk category has been assigned for each survey location.

14 References

Ref. /1/ Fugro. "*Geophysical Results Report. North Sea OWF Zone West (Lot 2) Geophysical Survey"*. F176286-REP-GEOP-001 04. Final. 07.06.2022

Ref. /2/ MMT. (2022). Geophysical Survey Report - Energy Islands - North Sea East. 103783-ENN-MMT-SUR-REP-SURVWPA. 10.08.2022

Ref. /3/ FUGRO. "*Energy Islands – North Sea Artificial Island, Investigation Results, Geotechnics*". Project no. F191074, Rev 04 Final (revised), date 21.02.2023.

Ref. /4/ FUGRO. "*Energy Islands – North Sea Offshore Wind Farm Area, Investigation Results, Geotechnics*". Project no. F191074, Rev 03 Final, date 15.06.2023.

Ref. /5/ DNV-RP-C207, Statistical representation of soil data, September 2021.

Ref. /6/ Robertson and Cabal, 2015: Guide to Cone Penetration Testing, 6th Edition.

Ref. /7/ Lunne, T., Robertson, P. K., and Powell, J. J. M., 1997: Cone Penetration Testing in Geotechnical Practice, 1st edition.

Ref. /8/ Mayne, P. W & Sharp, J. 2019 - CPT Approach to Evaluating Flow Liquefaction Using Yield Stress Ratio.

Ref. /9/ Jamiolkowski, M., Lo Presti, D. C. F. & Manassero, M. 2003 - Evaluation of Relative Density and Shear Strength of Sands from CPT and DMT.

Ref. /10/ Rix, G. J. & Stokoe, K. H. 1991 - Correlation of initial tangent modulus and cone penetration resistance. In International Symposium on Calibration Chamber Testing, pages 351–362.

Ref. /11/ Surlyk, F. D. 2006 - Stevns Klint, Denmark: Uppermost Maastrichtian chalk, Cretaceous-Tertiary boundary, and lower Danian bryozoan mound complex. Bulletin of the Geological Society of Denmark 54, 1-48.

Ref. /12/ Pharaoh, T. D. 2010 - Petroleum Geological Atlas of the Southern Permian Basin Area. EAGE puplications b.v. (Houten), 25-33.

Ref. /13/ Stampfli, G. M. 2013 - The formation of Pangea. Tectonophysics, 1-19.

Ref. /14/ Cameron, T. D. 1992 - The geology of the southern North Sea. London, HMSO: United Kingdom Offshore.

Ref. /15/ Ziegler, P. A. 1992 - North Sea rift system. Tectonophysics, 55-75.

Ref. /16/ Sorgenfrei, T. &. Buch, A. 1964 - Deep Tests in Denmark 1935/1959. Geological Survey of Denmark, III. Series 36.

Ref. /17/ Vejbæk, O. B. 2007 - Chalk depth structure map Central to East North Sea, Denmark. GEUS. Geological Survey of Denmark and Greenland Bulletin 13, 9-12.

Ref. /18/ Nielsen, T. M.-A. 2008 - Base Quaternary in the Danish part of the North Sea and Skagerrak. Geological Survey of Denmark and Greenland Bulletin 15, 37-40.

Ref. /19/ Gibbard, P. A., Lewin, J. 2016 - Filling the North Sea Basin: Cenozoic sediment sources and river styles. Geologica Belgica 19 (3-4), 201-217.

Ref. /20/ Jepsen, P. 2000 - Fra Kridthav til Vesterhav. Nordsøbassinets udvikling vurderet ud fra seismiske hastigheder. Geologisk tidsskrift, hæfte 2, 1-36.

Ref. /21/ Huuse, M. L. A. 2000 - Overdeepened Quaternary valleys in the eastern Danish North Sea: morphology and origin. *Quaternary Science Reviews, 19*, 1233-1253.

Ref. /22/ Larsen, B. A. 2005 - Late Quaternary stratigraphy and morphogenesis in the Danish eastern North Sea and its relation to onshore geology. Netherlands Journal of Geosciences 84-2, 113-128.

Ref. /23/ Ramboll. "*Energy Island; Danish North Sea, Geoarchaeological and Geological Desk Study*", Project No. 1100046209, date 18.05.2021.

Ref. /24/ Nicolaisen, J. F. 2010 - Marin råstof- og naturtypekortlægning i Nordsøen. Naturstyrelsen.

Ref. /25/ Leth, J. 1996 - Late Quaternary geological development of the Jutland Bank and the initiation of the Jutland Current , NE North Sea. 25-34: Nor. Geol. Unders. Bull. 430.

Ref. /26/ Bennike, O. J. 1998 - Late- and postglacial shore level changes in the southwestern Baltic Sea. Bulletin of the Geological Society of Denmark, Vol. 45, 27-38.

Ref. /27/ Novak, B., Pedersen, G. K. 2000 - Sedimentology, seismic facies and stratigraphy of a Holocene spit– platform complex interpreted from high-resolution shallow seismics, Lysegrund, southern Kattegat, Denmark. Marine Geology 162, 317–335.

Ref. /28/ Novak, B. Björck, S. 2002 - Late Pleistocene–early Holocene fluvial facies and depositional processes in the Fehmarn Belt, between Germany and Denmark, revealed by high-resolution seismic and lithofacies analysis. Sedimentolog, 49, 451–465.

Ref. /29/ Houmark-Nielsen, M. K. 2005 - De seneste 150.000 år i Danmark. Istidslandskabet og naturens udvikling. Geoviden, geologi og geografi nr. 2.

Ref. /30/ GEUS. *"A desk study of the geological succession below a proposed energy island, Danish North Sea*". 2022

Ref. /31/ Nwosu, L. B. 2023 – Integreret tolkning og 3D geomodellering af geofysiske, geotekniske data fra kanalsystem i den sydlige del af Energi-ø Nordsø-området.

Ref. /32/ European Standard EN ISO 19905-1, Petroleum and natural gas industries – Site-specific assessment of mobile offshore units – Part 1: Jack-ups, February 2016.

Ref. /33/ ISO 19905-1:2016: Petroleum and natural gas industries, Site-specific assessment of mobile offshore units, Part 1: Jack-ups.

Ref. /34/ MSL Engineering Ltd., 2004, Guidelines for jack-up rigs with particular reference to foundation integrity (HSE Research Report 289).

Ref. /35/ LOC, January 2013, Geotechnical engineering for jack-ups, Ref no. LOC/CM/MANUAL/2013/R0.1-4.